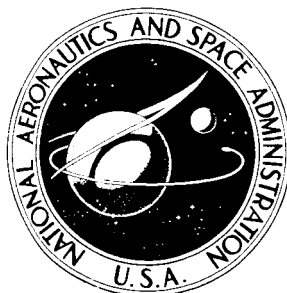


**NASA CONTRACTOR
REPORT**



NASA CR-1080

NASA CR-1080

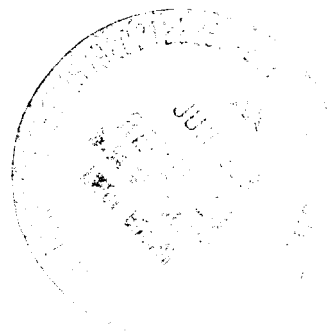
GPO PRICE \$ _____

CFSTI PRICE(S) \$ _____

Hard copy (HC) 300

Microfiche (MF) 6.5

ff. 653 and 655



**INVESTIGATION OF ELECTROCALORIC
EFFECTS IN FERROELECTRIC SUBSTANCES**

by Gordon G. Wiseman

Prepared by
UNIVERSITY OF KANSAS
Lawrence, Kans.
for

FACILITY FORM 602

972
[ACCESSION NUMBER]

(THRU)

[PAGES]

(CODE)

[NASA CR OR TMX OR AD NUMBER]

CATEGORY

INVESTIGATION OF ELECTROCALORIC EFFECTS
IN FERROELECTRIC SUBSTANCES

By Gordon G. Wiseman

Distribution of this report is provided in the interest of information exchange. Responsibility for the contents resides in the author or organization that prepared it.

Prepared under Grant No. NsG-575 by
UNIVERSITY OF KANSAS
Lawrence, Kans.

for

NATIONAL AERONAUTICS AND SPACE ADMINISTRATION

PRECEDING PAGE BLANK NOT FILMED.

TABLE OF CONTENTS

NASA RESEARCH GRANT Nsg-575
March 1, 1964 to July 1, 1967
Final Report

DEFINITION OF TERMS AND SYMBOLS

LIST OF EQUATIONS

INTRODUCTION

THERMODYNAMICS OF THE ELECTROCALORIC EFFECT

The Paraelectric State

The Inner Field Equations for the Ferroelectric State

Phenomenological Description of Ferroelectricity

The Pyroelectric Effect

APPARATUS AND TECHNIQUES

Crystalline Samples

Temperature Regulation of the Sample Chamber

Measurements of Electrocaloric Temperature Changes

Measurements of Electrical Polarization

Procedure of Measurement

DISCUSSION OF RESULTS

Potassium Dihydrogen Phosphate, KH_2PO_4

KH_2PO_4 in the Paraelectric Phase

KH_2PO_4 in the Ferroelectric Phase

The Pyroelectric Coefficient for KH_2PO_4

Triglycine Sulfate, $(\text{NH}_2\text{CH}_2\text{COOH})_3 \cdot \text{H}_2\text{SO}_4$

TGS in the Paraelectric Phase

TGS in the Ferroelectric Phase

The Pyroelectric Coefficient for TGS

Potassium Dihydrogen Arsenate, KH_2AsO_4
 KH_2AsO_4 in the Paraelectric Phase
 KH_2AsO_4 in the Ferroelectric Phase
The Order of Transition in KH_2AsO_4
The Pyroelectric Coefficient for KH_2AsO_4

Tartaric Acid, $\text{C}_4\text{H}_6\text{O}_6$
The Intrinsic Polarization of Tartaric Acid
The Coefficient for Tartaric Acid
The Electrocaloric Effect in Tartaric Acid

CONCLUSIONS

LIST OF REFERENCES

PERSONNEL

Project Supervisor: Gordon G. Wiseman
Graduate Student Assistants: Richard J. Brincks, Joe A. Hostetter,
Joe L. Luthey, Michael L. Nicholas, Jack E. Smith, Robert G. Spahn
NSF Undergraduate Trainees who assisted: Robert W. Manweiler,
Michael C. Rasmussen, and David Woodall.

DEFINITION OF TERMS AND SYMBOLS

Rationalized MKS units are used throughout. Thermodynamic formulas such as $dU = TdS + Xdx + EdP$ are written for a unit volume of material. This procedure is not exactly proper because the thermodynamic system (the experimental crystal) changes its volume slightly, but only inappreciable errors result.

C = Curie constant. Curie-Weiss Law is $K \approx \chi = C/(T - T_p)$.

c_E = Specific heat at constant field (and zero stress).

c_p = Specific heat at constant polarization (and zero stress).

D = Electric displacement. $D = \epsilon_0 E + P$.

E = Applied electric field.

G_1 = Elastic Gibbs function. $G_1 = U - TS - xX$.

G_{10} = G_1 at some (arbitrary) reference temperature.

K = Dielectric constant.

p = Electric dipole moment.

P = Electric polarization per volume. P_s = Spontaneous electric polarization per volume.

p^E = Pyroelectric coefficient at constant field (and stress).

S = Entropy per volume.

S' = That part of the entropy which is associated with P .

T = Temperature in degrees Kelvin.

T_c = Critical Temperature. Loosely speaking, either T_f or T_p for a ferroelectric substance. The temperature at which P_s approaches zero in a pyroelectric substance.

T_f = Ferroelectric Curie temperature = the temperature at which P_s disappears when the substance is heated.

T_p = Paraelectric Curie temperature as defined by the Curie-Weiss Law,
 $\chi = C/(T - T_p)$.

U = Internal energy per volume.

X = Applied stress. (Tensile stress has a positive sign.)

x = Strain. (Elongation has a positive sign.)

Δ = A measureable incremental change in a quantity such as ΔT or ΔP .

ϵ_0 = Electric permittivity of vacuum = $8.85 \times 10^{-12} \text{ coul}^2/\text{n m}^2$.

- ζ = Devonshire's sixth-order coefficient (of P^6) in G-expansion.
 ξ = Devonshire's fourth-order coefficient (of P^4) in G-expansion.
 ρ = Mass density.
 χ = Electric susceptibility. $dP = \epsilon_0 \chi dE$. The symbol χ may carry subscripts as p (paraelectric), or superscripts such as T (constant temperature), X (constant stress), etc.
 ω = Devonshire's second-order coefficient (of P^2) in G-expansion.

LIST OF EQUATIONS

A list of the more important equations is given below. They are numbered consecutively as they appear in this report. The first law of thermodynamics has been written as $dQ = dU + dW$ where a positive value of dW represents mechanical and/or electrical work done on the system. The equations as written are valid only if all directional quantities are parallel or antiparallel to each other. Complete specification of stress, strain, field, and polarization would require appropriate tensor, matrix, or vector subscripts; they can be inserted later as needed when multidirectional effects occur.

$$dU = TdS + Xdx + EdP \quad (1)$$

$$(\partial T/\partial P)_S = (T/\rho c_p)(\partial E/\partial T)_P \quad (2)$$

$$(\Delta T/\Delta P)_S = (T/\rho c_p)(\partial E/\partial T)_P \quad (2a)$$

$$G_2 = U - TS - XX - EP \quad (3)$$

$$(\partial T/\partial E)_S = -(T/\rho c_E)(\partial P/\partial T)_E \quad (4)$$

$$(\Delta T/\Delta E)_S = -(T/\rho c_E)(\partial P/\partial T)_E \quad (4a)$$

$$(\partial T/\partial E)_S = \epsilon_0 CTE/\rho c_E (T - T_p)^2 \quad (5)$$

$$\Delta T = \epsilon_0 CTE^2/2\rho c_E (T - T_p)^2 \quad (6)$$

$$\Delta T = T\Delta P^2/2\epsilon_0 C\rho c_p \quad (7)$$

$$P = f(a) = f[p(E + \gamma P)/kT] \quad (8)$$

$$dT = (\gamma/\rho c_p)PdP \quad (9)$$

$$dG_1 = -SdT - xdx + EdP \quad (10)$$

$$G_1 = G_{10} = \omega P^2/2 + \xi P^4/4 + \zeta P^6/6 + \quad (11)$$

$$(\partial G_1/\partial P)_{X,T} = E = \omega(T)P + \xi P^3 + \zeta P^5 \quad (12)$$

$$(\Delta T/\Delta P^2) = (T/2\rho c_p)(\partial \omega/\partial T)_P \quad (13)$$

$$\omega(T > T_c) = (\partial E/\partial P)_T = 1/\epsilon_0 \chi_p \quad (14)$$

$$P_s^2 = -\omega/\xi \quad (15)$$

$$\omega(T < T_c) = -1/2\epsilon_0 \chi_f \quad (16)$$

$$(c_E - c_p) = TdS'/\rho dT \quad (17)$$

$$(c_E - c_p) = -(T/\rho)(\partial \omega/\partial T)_P dP^2/dT \quad (18)$$

$$(c_E - c_p) = -(T/2\epsilon_0 C)(dP_s^2/dT) \quad (19)$$

$$(c_E - c_p) = -(\gamma/2\rho)dP^2/dT \quad (20)$$

$$\omega(T_c) = 3\xi^2/16\zeta \quad (21)$$

$$P_s^2(T_c) = -3\xi^2/4\zeta \quad (22)$$

$$dP = (\partial P/\partial X)_{E,T}dX + (\partial P/\partial E)_{X,T}dE + (\partial P/\partial T)_{X,E}dT \quad (23)$$

$$dP = p^{X,E}dT \quad (24)$$

$$dP = [(\partial P/\partial x)_{E,T} + (\partial x/\partial T)_{X,E} + (\partial P/\partial T)_{X,E}]dT \quad (25)$$

$$p^{X,E} - p^{X,E} = e^{E,T} \alpha_{X,E} \quad (26)$$

$$p^{X,E} - p^{X,E} = d^{E,T} \alpha_{X,E} E,T \quad (27)$$

$$dE = - (1/\epsilon_0 X^{X,T}) (\partial P/\partial T)_{X,E} dT = - (1/\epsilon_0 X^{X,T}) p^{X,E} dT \quad (28)$$

$$p^E = - (\rho c_E/T) (\Delta T/\Delta E) \quad (29)$$

$$i = A dP/dt = A (\partial P/\partial T) (\partial T/\partial t) \quad (30)$$

$$P(T) = BE + A(T_c - T)^{1/2} \quad (31)$$

$$G_1 = G_{10} - (A/B)(T_c - T)^{1/2} p + p^2/2B \quad (32)$$

$$\Delta T = (AT/\rho c_E)(T_c - T)^{-1/2} \Delta E \quad (33)$$

INTRODUCTION

The electrocaloric effect is the change in temperature that is produced in a dielectric by an adiabatic change in the applied electric field. From a strictly thermodynamic point of view, the electrocaloric effect is analagous to the magnetocaloric effect ("adiabatic demagnetization") which has been so useful both as a means to study the nature of magnetism¹ and as a technique for obtaining very low temperatures.¹

The electrocaloric effect has not been widely used; it usually is too small to measure directly except in ferroelectric and pyroelectric substances. In 1930, before the current theories of ferroelectricity were developed, Kobeko and Kurtschatov² studied the electrocaloric effect in ferroelectric Rochelle salt. They did not report numerical values, but they found a maximum effect near the upper Curie temperature. In 1943 Hautzenlaub³ made qualitative measurements of the effect in Rochelle salt. He also studied potassium dihydrogen phosphate and found an electrocaloric temperature change that was a quadratic function of the applied field above the Curie temperature and a linear function of the applied field (but only 30% of the computed value) below the Curie temperature. Later, Baumgartner⁴ determined indirectly the electrocaloric effect in a crystal of KH_2PO_4 from changes in its resonant frequency. Roberts⁵ employed the electrocaloric effect to distinguish between a first- and second-order transition in ceramic BaTiO_3 . Schmidt⁶ made measurements of the same material near 4°K to show that its macroscopic polarization at low temperatures is thermodynamically irreversible, and Karchevskii⁷ has shown that the maximum electrocaloric effect in this substance occurs at the Curie temperature. Wiseman and Kuebler⁸ have measured the electrocaloric effect in crystalline Rochelle salt throughout its ferroelectric range (i.e., between its two Curie temperatures) and thereby determined the Devonshire "dielectric stiffness" coefficient, the ferroelectric Curie temperatures, and the spontaneous polarization close to both Curie temperatures. These results were quantitatively consistent with the thermodynamic properties of Rochelle salt determined by standard methods.

Because of the reciprocal relationship between the electrocaloric effect and pyroelectricity,* the present study included some experiments with a pyro-

*The pyroelectric effect is the change in the electrical polarization of a dielectric that is produced by a change in temperature. All ferroelectric materials are pyroelectric but not vice versa.

electric substance. Pyroelectric measurements of ferroelectric substances have been made by Chynoweth,^{9,10,11} and NASA has sponsored research on pyroelectric radiation detectors.^{12,13,14}

We made this study to exploit further the electrocaloric effect as a means of obtaining a better understanding of the spontaneous electrical polarization in ferroelectric and pyroelectric substances; these substances have present and potential uses in radiation detectors, minified electronic circuits, and optical modulators.

THERMODYNAMICS OF THE ELECTROCALORIC EFFECT

The Basic Electrocaloric Equations

The combined first and second laws of thermodynamics for a dielectric solid which is subjected to a tensile stress X and an electric field E is

$$dU = TdS + Xdx + EdP \quad (1)$$

where U is the internal energy, S the entropy, x the strain, and P the electrical polarization of a unit amount of material.*

Since dU is exact and the applied stresses are to be kept small in these experiments, Eq. (1) can be reduced to

$$(\partial T / \partial P)_S = (T / \rho c_p)(\partial E / \partial T)_P \quad (2)$$

which for very small temperature changes becomes

$$(\Delta T / \Delta P)_S = (T / \rho c_p)(\Delta E / \Delta T)_P \quad (2a)$$

where ρ is the density and c_p is the specific heat of the crystal at constant polarization. This equation will be called the " ΔP form" of the electrocaloric equation.

Another expression for the reversible electrocaloric effect can be obtained by employing the electric Gibbs function G_2 of Mason,¹⁵

$$G_2 = U - TS - Xx - EP. \quad (3)$$

Adding the derivative of this equation to Eq. (1) and choosing $S = S(T, X, \text{ and } E)$ yields for an adiabatic change in the field applied to an unclamped ($X = 0$) crystal, another pair of expressions analagous to Eq. (2) and (2a) for the reversible electrocaloric effect,

$$(\partial T / \partial E)_S = -(T \rho c_E)(\partial P / \partial T)_E \quad (4)$$

*The last term in Eq. (1) could have been written EdD , but the electrostatic energy $\epsilon_0 EdE$ of empty space has been excluded from the system for convenience, leaving EdP allocated to the crystalline substance.

or

$$(\Delta T / \Delta E)_S = -(T \rho c_E)(\partial P / \partial T)_E, \quad (4a)$$

where c_E is the specific heat of the substance at constant field. Eq. (4a) will be called the " ΔE form" of the electrocaloric equation.

To apply these two equations to a specific material, we need an equation of state which relates the thermodynamic variables.

The Paraelectric State

The Curie-Weiss Law is such an equation of state for ferroelectric substances but only above the Curie temperature; that is, above the Curie temperature ferroelectric substances exhibit paraelectric behavior. When the polarization is large compared to $\epsilon_0 D$, the Curie law can be written as $P = \epsilon_0 C(T - T_p)$ instead of $D = \epsilon_0 C(T - T_p)$. The paraelectric Curie temperature T_p and the Curie constant C of a substance are ordinarily determined by measurements taken in its paraelectric phase. Differentiation of the Curie-Weiss equations yields a value for the factor $(\partial P / \partial T)_E$ appearing in Eq. (4), which can then be written

$$(\partial T / \partial E)_S = \epsilon_0 C T E / \rho c_E (T - T_p)^2. \quad (5)$$

Integration of this expression over a very small range of temperature gives a useful expression for the electrocaloric effect in the paraelectric phase,

$$T = \epsilon_0 C T E^2 / 2 \rho c_E (T - T_p)^2 \quad (6)$$

which is notable for its quadratic dependence on the applied field.

The Curie-Weiss law also yields a value for the factor $(\partial E / \partial T)_P$ in Eq. (2), and Eq. (2) becomes

$$(\partial T / \partial P)_S = T P / \epsilon_0 C \rho c_P.$$

Integration of this expression over a small range of temperature gives another useful expression for the electrocaloric effect of a substance in its paraelectric phase,

$$T = T P^2 / 2 \epsilon_0 C \rho c_P. \quad (7)$$

This expression shows a quadratic dependence of ΔT on the polarization. Note that ΔP^2 does not mean $(P_2 - P_1)^2$ but rather $\Delta P^2 = P_2^2 - P_1^2$. Fortunately, the heat capacities at constant field and at constant polarization, c_E and c_P , which appear in Eq. (6) and (7) are approximately equal to each other above the Curie temperature if the polarization is not too large.

The Inner Field Equations for the Ferroelectric State

An equation of state for ferroelectric substances in their ferroelectric phase is not available. Various "models" have been proposed from which an equation of state might be inferred. A Langevin-like inner field model of a ferroelectric substance will lead to an equation of state. Although such a model based on cooperative interactions between rotatable dipoles of fixed moment is unrealistic for a number of reasons,¹⁶ most theories of ferroelectric mechanisms invoke an inner field of some sort to explain the non-linear effects that must exist to produce ferroelectric polarization. In some cases, the simple model is rather successful. If the field F which is effective in aligning a dipole of moment p parallel to the applied field E is written as $F = E + \gamma P$ where γ is the inner field constant and P is the polarization per unit volume, then a Langevin-type expression, $f(a)$, can be derived for the polarization as a function of temperature and field; i.e.,

$$P = f(a) = f[p(E + \gamma P)/kT]. \quad (8)$$

Setting $dP/dT = 0$ will yield the expression $(\partial E/\partial T)_P = (E + \gamma P)/T$. Combining this expression with Eq. (2) yields

$$dT = (T/\rho c_P)(E/T + \gamma P/T)dP.$$

In or near the ferroelectric region where P is so large that E/T is negligible,

$$dT = (\gamma/\rho c_P)P dP. \quad (9)$$

Thus, measurements of the electrocaloric effect will yield values for the inner field constant γ .

The early direct measurements of the electrocaloric effect in Rochelle salt by Kobeko and Kurtschatov² together with later measurements in this laboratory¹⁷ provide one of the severe indictments of the simple inner field model. These

measurements yield values of γ throughout the ferroelectric range and reveal that γ as determined from Eq. (9) is strongly temperature dependent and has negative values below 2.5°C, the temperature of maximum spontaneous polarization. The results in addition to other reasons² show that a description of ferroelectricity in Rochelle salt in terms of the inner field constant γ is of doubtful value.

On the other hand, Baumgartner's⁴ indirect measurements of the electrocaloric effect in KH_2PO_4 (by means of changes in the resonance frequency of his specimen) are consistent with a nearly constant value of γ over a small range of temperature. Baumgartner was able to account for the observed changes in γ with temperature by putting a weak functional dependence on temperature, $\psi(T)$, into the denominator of Eq. (8)

Whether or not the inner field model is valid, electrocaloric measurements can throw some light on the behavior of the thermodynamic parameters near the Curie temperature. But since a generally valid mechanism of ferroelectric transitions is not available, and since the roles played by thermal agitation, strengths and directions of covalent or hydrogen bonds etc. are not well understood, a more phenomenological approach is chosen which leaves the detailed mechanisms unspecified.

Phenomenological Description of Ferroelectricity

A phenomenological description has been formulated by Devonshire.¹⁸ He introduces an elastic Gibbs function, (free energy) $G_1 = U - TS - Xx$. Subtraction of the derivative of this equation from Eq. (1) gives

$$dG_1 = -SdT - xdx + EdP. \quad (10)$$

For a substance to exhibit ferroelectric behavior, its polarization must be a non-linear function of the field, and the value for the Gibbs function must be independent of the direction of the polarization. For the one-dimensional case (i.e., continuing to omit the subscripts on P), Devonshire postulates

$$G_1 = G_{10} + P^2/2 + \xi P^4/4 + \zeta P^6/6 + \dots \quad (11)$$

where G_{10} is the value G_1 at some arbitrary reference temperature and the coefficients are functions of the temperature at constant stress. The numerical factors are introduced for later convenience. Terms beyond fourth order are usually neglected.

A second-order ferroelectric transition can be explained in terms of G_1 by assuming that only the coefficient ω is a function of T and that the other coefficients are positive and relatively constant; then we have

$$(\partial G_1 / \partial P)_{X,T} = E = \omega(T)P + \xi P^3 + \zeta P^5 \quad (12)$$

and
$$(\partial E / \partial T)_P = (\partial \omega / \partial T)_P P.$$

Substituting this expression into Eq. (2a) gives

$$(\Delta T / \Delta P)_S = (TP / \rho c_p) (\partial \omega / \partial T)_P \quad (13)$$

or

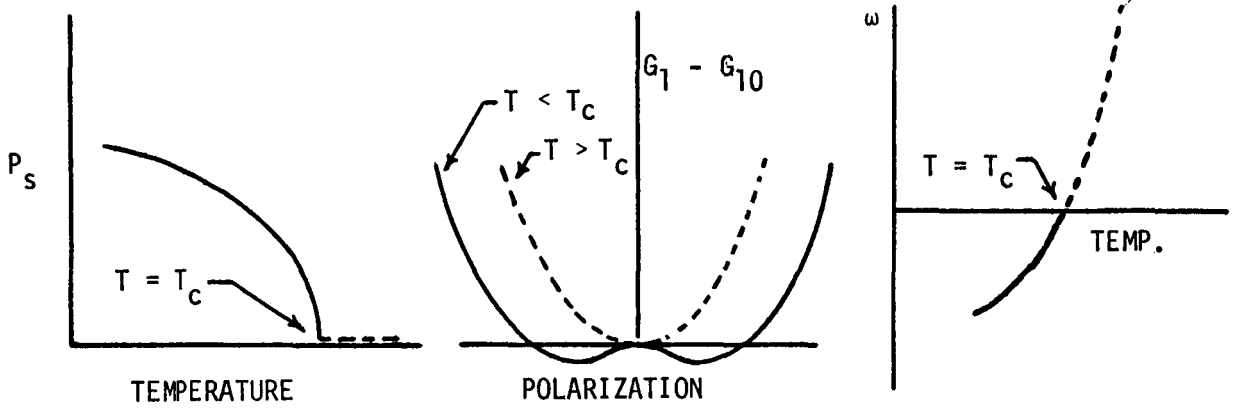
$$(\Delta T / \Delta P^2)_S = (T / 2\rho c_p) (\partial \omega / \partial T)_P. \quad (13')$$

The condition for a stable state is a minimum in G_1 or $(\partial G_1 / \partial P)_{X,T} = 0$; this condition together with the fact that P is small at the Curie temperature gives a boundary condition that $\omega(T_C) = 0$. Thus, measurements of the electrocaloric effect give values for the important Devonshire coefficient $\omega(T)$. Above the Curie temperature (in the paraelectric phase) where the polarization is small, ω can be determined experimentally from the paraelectric susceptibility χ_p by using an expression that is obtained by taking the derivative of Eq. (12),

$$\omega(T > T_C) = (\partial E / \partial P)_T = 1/\epsilon_0 \chi_p. \quad (14)$$

Thus, the Devonshire coefficient ω is seen to be, aside from a numerical constant, the reciprocal susceptibility or the "dielectric stiffness" in the paraelectric region. Fortunately, electrocaloric effects are so small in this region that no distinction needs to be made between the isothermal and the adiabatic susceptibility. The value of ω in the paraelectric region is strongly dependent upon temperature, the susceptibility obeying the Curie-Weiss law, $\omega = 1/\epsilon_0 \chi = (T - T_C)/\epsilon_0 C$, down to the Curie temperature. The question is whether ω continues to be a well-behaved function of temperature right on through the Curie temperature and below as would be the case if the elastic Gibbs function G_1 describes the dielectric behavior below the Curie temperature where ω is not a directly observable quantity but can be determined from the electrocaloric effect. Hopefully, $\omega(T)$ would suffer no discontinuity in value or slope near the Curie temperature (though the reciprocal susceptibility may) as shown in the accompanying diagram. The dotted

and solid lines serve to distinguish between behaviors above and below the Curie temperature. A smooth fit of the experimental values of ω obtained above and below T_c from electrocaloric data would corroborate the general picture.



An expression for the spontaneous polarization P_s in terms of the Devonshire coefficients can be gotten from Eq. (12) by setting $E = 0$; this gives

$$P_s^2 = -\omega/\xi \quad (15)$$

and

$$(T > T_c) = -1/2\epsilon_0\chi_f \quad (16)$$

where χ_f is the low-field reversible susceptibility in the ferroelectric region. Eq. (15) allows ξ to be determined from electrocaloric measurements, and Eq. (16) provides a means of verifying the electrocaloric determination of $\omega(t)$ below the Curie temperature.

The term $(\partial\omega/\partial T)_P$ of Eq. (13) is also related to the specific heat anomaly near the transition. Defining dS' as that part of the differential increase in entropy associated with dP in the temperature range dT , we can write the specific heat anomaly as

$$(c_E - c_P) = TdS'/\rho dT. \quad (17)$$

From Eq. (10) and (11), $S = -(\partial G_1/\partial T)_P = -(\partial G_{10}/\partial T)_P - (\partial\omega/\partial T)_P P_s^2/2$. The term $(\partial G_{10}/\partial T)_P$ represents the ordinary "thermal" entropy, and the term $(\partial\omega/\partial T)_P P_s^2/2$ represents S' the entropy of polarization. Consequently,

$$(c_E - c_P) = -(T/2\rho)(\partial\omega/\partial T)_P dP_s^2/dT. \quad (18)$$

Rewriting Eq. (11) in terms of the Curie-Weiss law which the substance obeys at $T > T_C$, gives $\omega = (T - T_C)/\epsilon_0 C$ where C is the Curie constant. Eq. (15) then becomes

$$(c_E - c_P) = -(T/2\epsilon_0 C) dP_S^2/dT, \quad (19)$$

which is a less general relationship than Eq. (18) because constancy of $(\partial\omega/\partial T)_P$ below T_C is assumed. If the inner field description were valid, the specific heat anomaly would reduce to the well-known expression,

$$(c_E - c_P) = -(\gamma/2\rho)dP^2/dT. \quad (20)$$

Eq. (12) through (19) are applicable to a substance which undergoes a second order ferroelectric transition. A first order transition can be described in terms of G_1 by assuming that ω is a function of temperature (as before) and that either ξ or ζ is negative. An analysis similar to that for the second order transition gives the following relationships near the Curie temperature:

$$\omega(T_C) = 3\xi^2/16\zeta \quad (21)$$

and

$$P_S^2(T_C) = -3\xi^2/4\zeta. \quad (22)$$

The Pyroelectric Effect

A relationship between pyroelectricity and the electrocaloric effect is evident from their definitions. The nature of this relationship would be expected to depend upon the experimental conditions under which the effects were observed, in particular, which of the state variables (X , x , E , P , S , and T) are held constant. Most processes can take place by alternative roundabout paths; for example, the "primary" pyroelectric effect ($dT \rightarrow dP$) at constant strain is usually less than half as large as the "secondary" effect ($dT \rightarrow dx \rightarrow dP$) in which thermal expansion ($dT \rightarrow dx$) produces a piezoelectric effect ($dx \rightarrow dP$). The relative importance of the various possible paths is determined by the experimental conditions imposed (constant stress, constant field, constant entropy, etc.) and by the magnitude of the coefficients (thermal expansion, piezoelectric, etc.) involved. This situation can be clarified by specifying the imposed conditions, and by distinguishing between independent and dependent variables.

A convenient choice of independent variables sufficient to specify the state of pyroelectric (electrocaloric) material is X , E , and T ; the dependent variables are then x , P (or D), and S . A differential change in the polarization $dP(X, E, T)$ is then written,

$$dP = (\partial P / \partial X)_{E, T} dX + (\partial P / \partial E)_{X, T} dE + (\partial P / \partial T)_{X, E} dT. \quad (23)$$

If the crystal is short-circuited ($E = 0$) and mechanically free ($X = 0$), only the dT term remains which is commonly written

$$dP = p^{X, E} dT \quad (24)$$

Another view of the same process is obtained by choosing x , E , and T as the independent variables which gives

$$dP = (\partial P / \partial x)_{E, T} dx + (\partial P / \partial T)_{x, T} dT;$$

substituting $dx = (\partial x / \partial T)_{X, E} dT$

gives
$$dP = [(\partial P / \partial x)_{E, T} (\partial x / \partial T)_{X, E} + (\partial P / \partial T)_{x, E}] dT. \quad (25)$$

This equation signifies that the pyroelectric polarization can be regarded as the sum of a primary effect ($dT \rightarrow dP$) for a clamped ($x = 0$) crystal superimposed upon a secondary effect which occurs via a roundabout path ($dT \rightarrow dx \rightarrow dP$), a path which is interpreted as a thermal expansion $dx = \alpha^{X, E} dT$ which produces a piezoelectric charge $e^{E, T} dx$. Writing $p^{X, E}$ for $(\partial P / \partial T)_{x, E}$, the primary pyroelectric coefficient of the clamped crystal, gives

$$dP = (e^{E, T} \alpha^{X, E} + p^{X, E}) dT$$

and so
$$p^{X, E} - p^{X, E} = e^{E, T} \alpha^{X, E}. \quad (26)$$

Continuing the analysis reveals that $e^{E, T}$ can be regarded as strain-induced stress ($dX \rightarrow dx$) which induces a direct piezoelectric effect:

$$(\partial P / \partial x)_{ET} = (\partial P / \partial X)_{E, T} (\partial X / \partial x)_{E, T}$$

which can be written as $e^{E,T} = d^{E,T}_c E, T$ so that

$$p^{X,E} - p^{X,E} = d^{E,T}_\alpha X, E E, T. \quad (27)$$

Thus the pyroelectric effect in a free, short-circuited crystal can be regarded as being comprised of a primary effect ($dT \rightarrow dP$) at constant strain plus a round-about virtual path ($dT \rightarrow dx \rightarrow dX \rightarrow dP$).

Studies of pyroelectric radiation detectors¹² has shown that the external impedance into which the pyroelectric device is delivering its signal is important. The case just discussed ($dE \approx 0$) is relevant to the use of a low-impedance detector. If a high-impedance detector is used, $dD \approx 0$ rather than $dE \approx 0$, and Eq. (23) will give

$$dE = -(1/\epsilon_0 \chi^{S,T})(\partial P/\partial T)_{X,E} dT = -(1/\epsilon_0 \chi^{X,T}) p^{X,E} dT \quad (28)$$

where $\epsilon_0 \chi^{X,T}$ is written in place of $(\partial P/\partial E)_{X,T}$.

The important feature is the appearance of the factor $p^{X,E} \equiv (\partial P/\partial T)_{E,X}$ which appears in the dE form of the electrocaloric equation, Eq. (4) as well as in the pyroelectric equations, Eq. (24) and (28). Thus the same crystalline property gives rise to both effects.

In addition to distinguishing between the primary and secondary effects which can occur in both pyroelectric and electrocaloric measurements, one must recognize the tertiary effects which arise from inhomogeneous temperatures or fields. These effects are much more easily eliminated in the electrocaloric experiments than in the pyroelectric experiments.

APPARATUS AND TECHNIQUES

Crystalline Samples

Large crystals, about 1 cm x 1 cm x 2 mm, are needed for accurate electrocaloric measurements, and they must also be oriented with their major faces perpendicular to the polar axis. Moreover, several equivalent specimens are needed because they frequently crack when subjected to high fields near the critical temperature. Many of the crystals tested were grown in these laboratories, but most of the data used were taken from commercially-grown specimens.

Each crystal was given a coat of air-drying silver paste over its entire major surfaces. The lower surface was then sprayed with a very thin insulating layer of Formvar to which a copper-constantan thermocouple was attached. This thermocouple was used to measure the electrocaloric effect. The crystal was suspended by cotton threads in a massive copper chamber which is depicted in Fig. 1. The sandwich-like mount previously used for Rochelle salt⁸ proved to be impractical for most of these studies because the large piezoelectric stresses between the two plates and the cement between them caused the crystals to shatter. Without the cement, cumulative slippage between the two crystals occurred until the high voltage lead connecting the outside layers of the sandwich would be short-circuited to one of the central electrodes.

A critical feature of the mounting of the crystal is the compromise that must be made in attempting to achieve both high electrical resistance and intimate thermal contact between the thermocouple and the specimen's electrodes; a leakage signal of a few hundredths of a microvolt per second could invalidate the measurements, and several trials are sometimes needed to achieve the desired conditions.

Prevention of electrical arcs by evacuating the inner chamber at the lower temperatures and higher applied fields was sometimes unsuccessful. In these instances arcing was prevented by adding nitrogen or helium gas at atmospheric pressure. Of course such gas greatly decreased the thermal insulation of the specimen, but the temperature recorder responded to the largest temperature change observed in about one second which was fast enough to permit identification and elimination of spurious effects due to non-adiabatic conditions as well as switching pulses, etc.

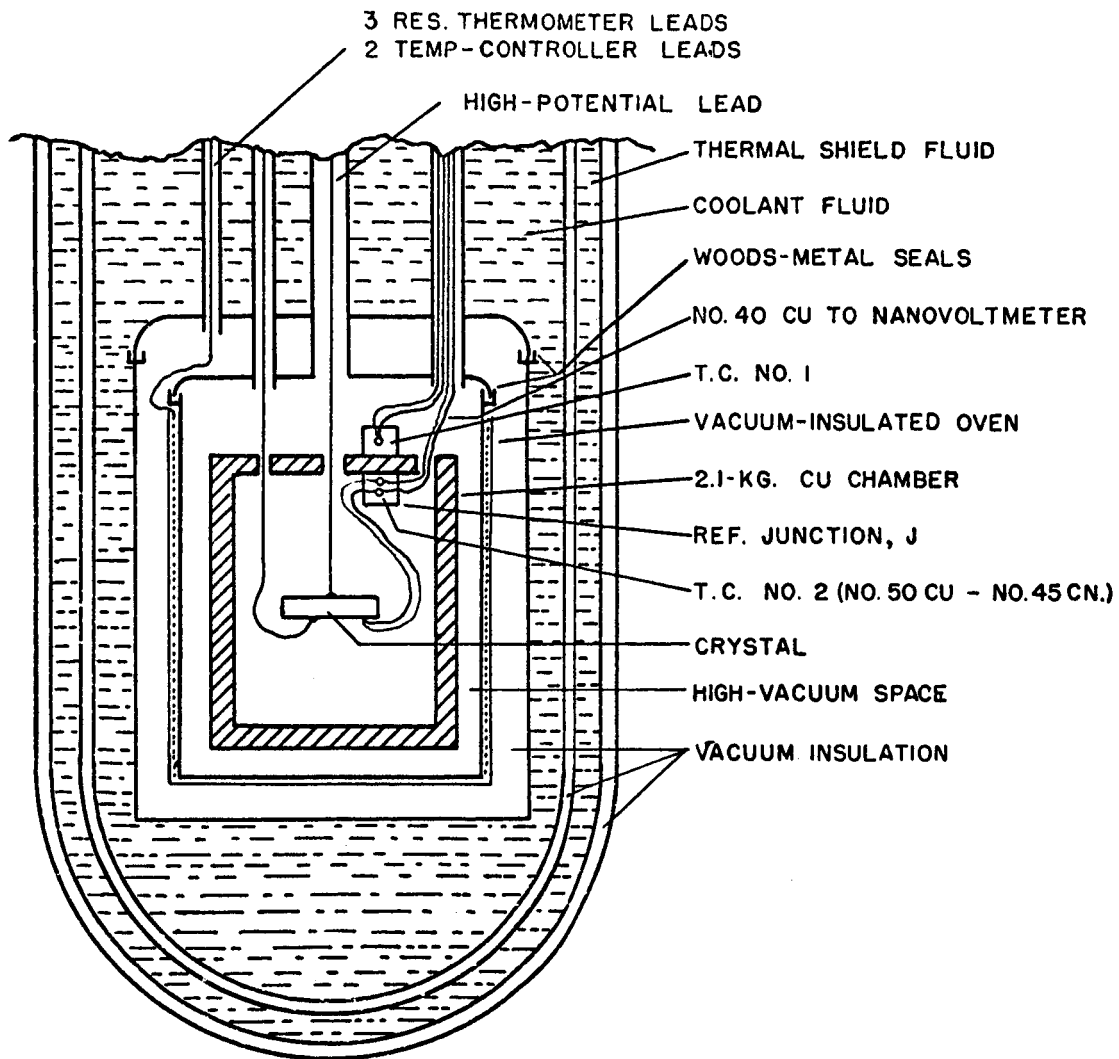


FIG.1 CONSTANT TEMPERATURE CHAMBER

Temperature Regulation of the Sample Chamber

Electrocaloric temperature changes are small, often in the fractional milli-degree range, so that very stable regulation of the sample chamber was required. An a-c Wheatstone bridge and phase-sensitive thyatron controller similar to the kind described by Brooks¹⁹ was used which controlled the reference junction to about 0.01 microvolt (approximately $4 \times 10^{-4}^{\circ}\text{K}$).

Measurements of Electrocaloric Temperature Changes

Electrocaloric temperature changes were measured with the thermocouple which was made of No. 50 copper vs. No. 45 constantan and was glued to be electrically insulated from the lower electrode. See Fig. 2. The massive copper chamber served as the reference junction. The emf of the thermocouple was amplified by either a Liston-Becker breaker amplifier or a Keithley Nanovolt Null Detector and then displayed on an 11-inch strip-chart recorder. At the highest sensitivity employed, the peak-to-peak noise signal was about 3 nanovolts which corresponds to a temperature difference of about $8 \times 10^{-5}^{\circ}\text{K}$. Any desired amplification was obtainable, and the appearance of the noise on the strip chart was such that electrocaloric signals as small as the noise level could be observed.

The heat capacity of the leads, electrodes, etc. is small compared to heat capacity of the specimens, and the heat losses were so low that no correction for them (which could have been made by extrapolating the temperature record backwards) was necessary.

Measurement of Electrical Polarization

The electrical polarization of the specimen was measured by means of a breaker preamplifier or Keithley electrometer connected across the polystyrene-film capacitor C_D as shown in Fig. 2. The charge was read on a strip-chart recorder.

Provision was also made for observing and photographing 60-hz hysteresis loops as presented on an oscilloscope. The observations were used for preliminary measurements and general survey purposes only.

Procedure of Measurement

Simultaneous records were made of the temperature of the chamber (the ambient temperature), changes in the electrical polarization of the specimen and changes in the temperature that occurred in the specimen. At each ambient temperature, several cycles of polarization were traversed in order to establish steady-state conditions before data were taken. After that, the hysteresis cycle

was ordinarily traversed "point-by-point" in a series of pre-determined step-wise changes in the applied field. Each step required about one second, fast enough to insure adiabatic processes and slow enough to avoid sudden crystalline strains and spurious electrical pulses. The steps were spaced either one or two minutes apart. Some "single-step" measurements were taken in which the field was switched completely on or off.

Out in the tail of the hysteresis loop where measurements are especially valid because the polarization is thermodynamically reversible but where measurements are difficult because the polarization is nearly saturated, the sensitivity of the measurements was greatly increased by applying a known biasing charge to the capacitor C_p to suppress the zero of the charge-measuring equipment and then increasing the amplification of the electrometer.

A program for processing the data obtained from the recorder traces and automatically plotting the more important computed quantities was written in Fortran IV for IBM 7040 computer and was modified later for use with a GE 625. For each temperature, both a graph of the hysteresis loop (P vs. E) and the electrocaloric effect (cumulative changes in T vs. E) were obtained together with tables of other significant quantities. The plotted results presented in this report were redrawn by hand.

Special procedures required for the experiments with tartaric acid are described later in this report.

DISCUSSION OF RESULTS

Potassium Dihydrogen Phosphate KH_2PO_4

Potassium dihydrogen phosphate is one of a dozen or so phosphates or arsenates that are known to become ferroelectric. The dielectric properties of crystalline KH_2PO_4 have been extensively studied by Busch and Scherrer,²⁰ by Baumgartner,²¹ and by Barkla and Finlayson.²² The specific heat anomaly was observed by Stephenson and Hooley.²³

Chemical formula	KH_2PO_4
Dimensions of crystal	23.85 mm x 13.93 mm x 2.974 mm
Density	2.32 g/cm ³
Crystal symmetry (above T_c)	Tetragonal
Ferroelectric axis	Tetragonal c
Specific heat	From Stephenson and Hooley ²³
Curie temperature	123°K
Range of temperature studied	78°K to 136°K

KH_2PO_4 in the Paraelectric Phase

Eq. (6) and (7) for the electrocaloric effect in a paraelectric substance are particularly useful; if the Curie constant, density, and specific heat of a sample are known, then the degree of agreement between the measured electrocaloric effect and these two equations serves as a criterion for the validity of the electrocaloric measurements. Conversely, once the validity of the method is established, the electrocaloric measurements can be used to determine properties such as the Curie constant.

Eq. (6) predicts that the electrocaloric temperature change is quadratic in the applied field,

$$\Delta T = \epsilon_0 C T \Delta E^2 / 2 \rho C_E (T - T_p)^2 \quad (6)$$

Fig. 3 displays typical results of step-by-step dielectric and electrocaloric measurements above the Curie temperature. The plotted values of ΔP and ΔT are cumulative changes so that any error of closure for a complete cycle of electrocaloric (ΔT) measurements represents the cumulative errors in the measurements of ΔT for the individual steps, irreversible effects in the specimen being ruled out in this instance because of the obvious reversibility exhibited by

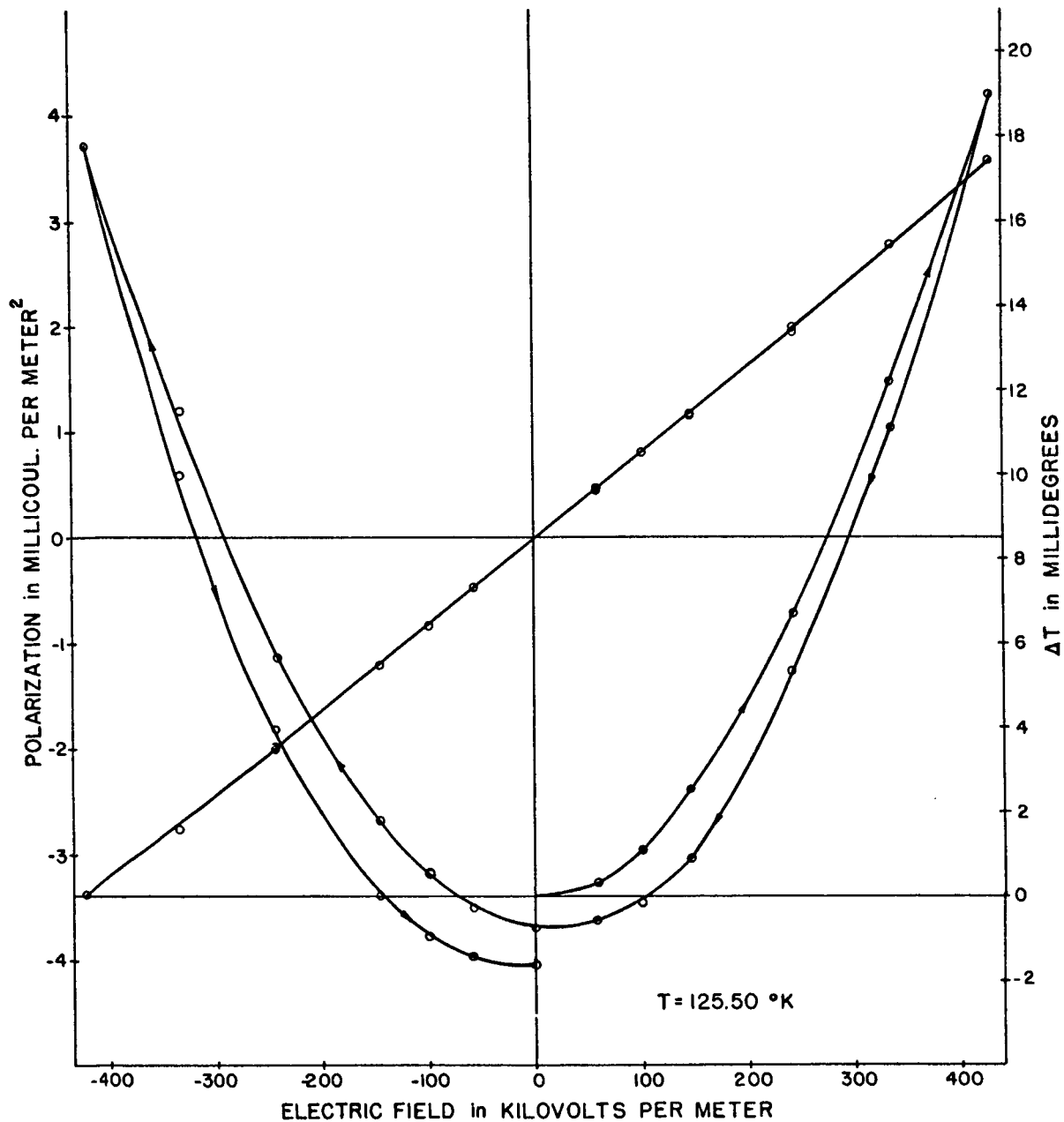


FIG. 3 DIELECTRIC & ELECTROCALORIC MEASUREMENTS ABOVE THE CURIE TEMPERATURE

the polarization. The excellent agreement between the experimental results and those predicted by the theory is evident: P is a linear function of E , and ΔT is a quadratic function of E . A parabola (not drawn in Fig. 3) that was fitted to the maximum value of polarization fell neatly between the two traces for positive values of E . The other measurements in the paraelectric region gave similar results at temperature ranging from 136°K (where the effect becomes very small) down to within a few tenths of a degree above the Curie temperature.

Eq. (7) predicts that the electrocaloric effect has a quadratic dependence on the polarization,

$$\Delta T = T \Delta P^2 / 2 \epsilon_0 C_p c_p. \quad (7)$$

This seems obvious from the dependence of ΔT on E^2 and the linear dependence of P upon E . However, a different specific heat appears in Eq. 7, c_p instead of c_E , and the measurements on KH_2PO_4 above T_c were taken primarily to determine the validity of the measurements. So, with the use of Eq. (7) in mind, experimental values of ΔT were plotted against ΔP^2 with the results shown in Fig. 4. The straight lines which intersect the origin are in agreement with Eq. (7). These data can be used to determine the Curie constant: Eq. (7) together with the known values of density and specific heat at constant polarization, yields values for $1/\epsilon_0 C$ that are in fair agreement with Baumgartner's measurements²¹ and with the values we obtain from dielectric measurements. Fig. 5 represents these comparisons.

The use of Eq. (13) in obtaining the first Devonshire coefficient ω from electrocaloric measurements can be illustrated for KH_2PO_4 in the paraelectric state. (Of course, a more accurate value can be obtained directly from the dielectric measurements in this instance.) Integration of Eq. (13) over a small range of temperature ΔT gives

$$(\partial \omega / \partial T)_p = (2 \rho c_p / T) \Delta T \Delta P^2. \quad (29)$$

The value of ω at the paraelectric Curie temperature is practically zero because the Curie-Weiss law gives infinite susceptibility at this temperature. With $\omega \rightarrow 0$ as $T \rightarrow T_p$ as a boundary condition, $\Delta(T)$ can be determined from the electrocaloric measurements. Fig. 5 gives the values of $\partial \omega / \partial T$, so the values of $\omega(T)$ in the paraelectric range are established.

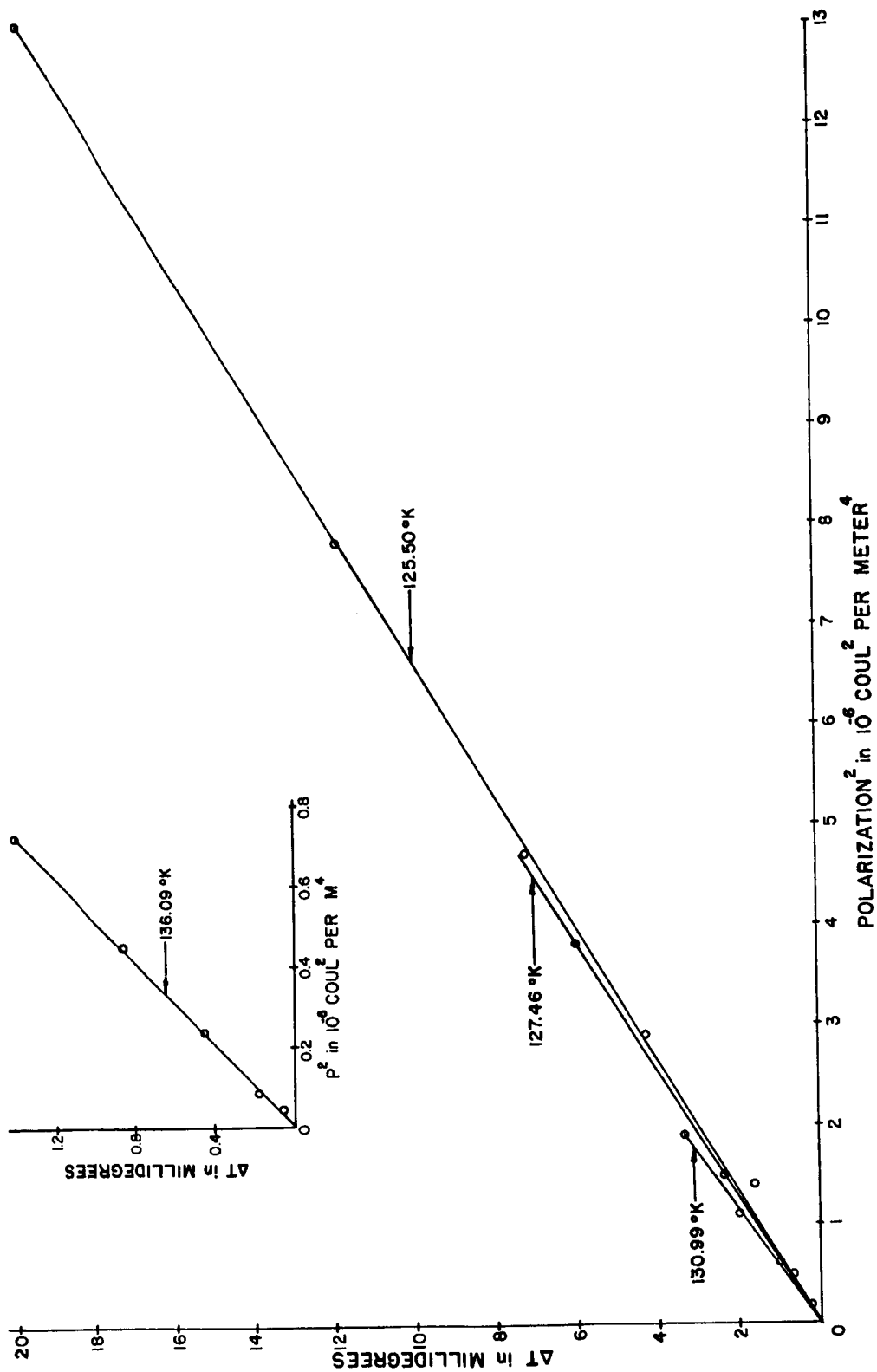


FIG. 4 ΔT vs. ΔP^2 ABOVE THE CURIE TEMPERATURE

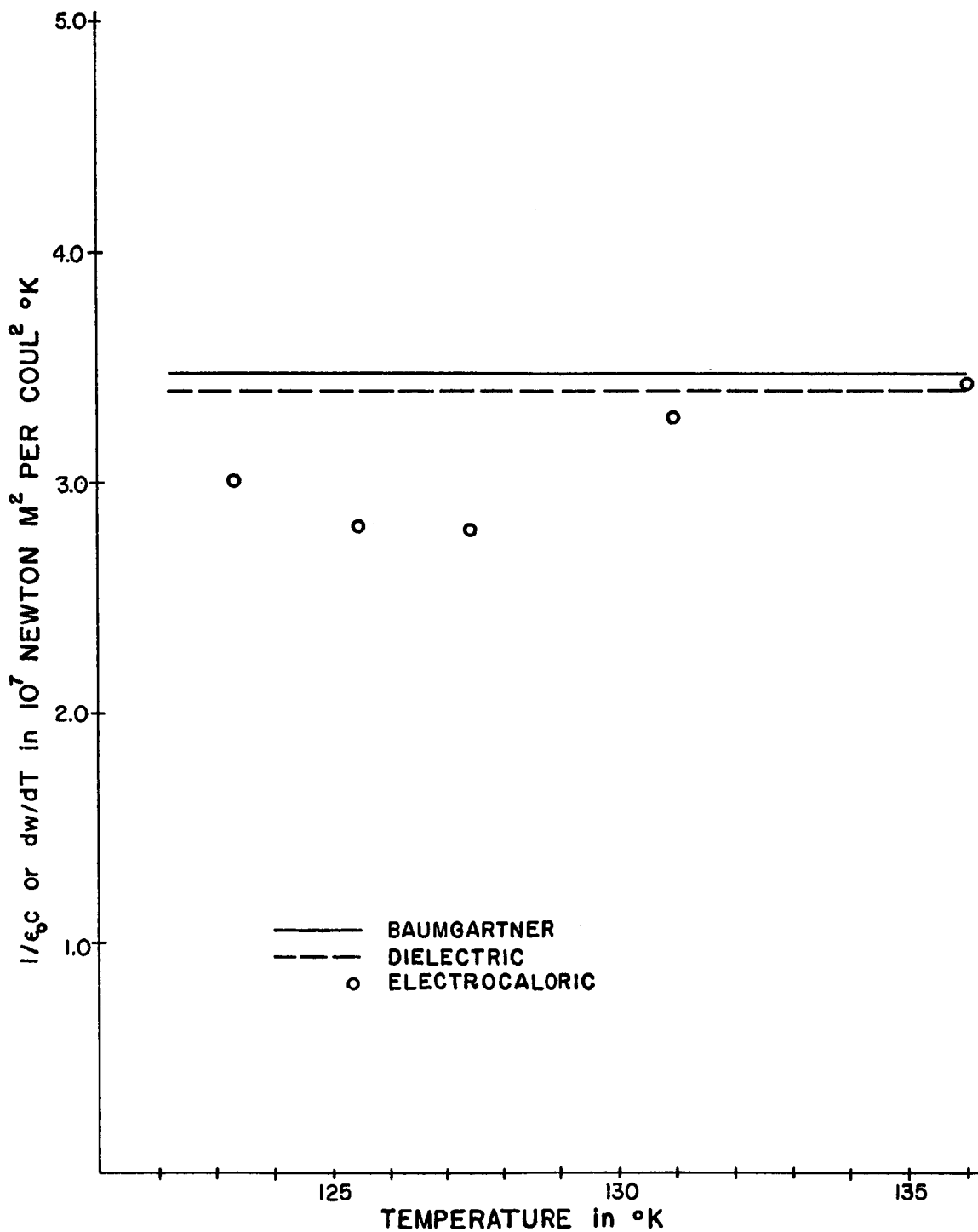


FIG. 5 ELECTROCALORIC MEASUREMENTS RELATED TO DIELECTRIC MEASUREMENTS ABOVE THE CURIE TEMPERATURE

KH₂PO₄ in the Ferroelectric Phase

Below the Curie temperature, the Curie-Weiss law will obviously not serve as an equation of state; the electrocaloric effect obtained below the Curie temperature, shown in Fig. 6, is qualitatively different from the effect obtained above the Curie temperature, shown in Fig. 3. The measurements shown in Fig. 6, though taken just below the Curie temperature for contrast with Fig. 3, illustrate the type of results obtained down to the lowest temperature, 78°K.

Of course, the more general thermodynamic relations of Eq. (2) and (4) are still valid. Consider first the ΔP form of the electrocaloric equation,

$$\Delta T / \Delta P = (T / \rho c_p) (\Delta E / \Delta T)_P. \quad (2a)$$

One would expect to be able to evaluate $(\Delta E / \Delta T)_P$ directly from Eq. 2a by measuring the electrocaloric effect and obtain an equation of state, $E = f(T, P)$, by integrating Eq. (2a). The difficulty is that the electrocaloric effect (or other effects for that matter) cannot be measured at arbitrarily-selected values of P ; in particular, values of P smaller than P_s are not experimentally accessible, values of P corresponding to low values of E are not thermodynamically reversible because of hysteresis, and P does not change much beyond its saturation value at high values of E .

The recourse employed was to look at the general features of the ferroelectric transition (i.e., whether it is of first or second order), assume a physically reasonable expression for the equation of state (or an equivalent expression for the Elastic Gibbs function G_1), and then compare the computed values of the electrocaloric effect to the measured values.

If KH₂PO₄ undergoes a second order ferroelectric transition and if the only temperature-dependent coefficient in the expansion of G_1 is ω (see Eq. (11)), then Eq. (2a) becomes identical to Eq. (13) which can be written for a path $a \rightarrow b$ as

$$\Delta T = (T_a - T_b) = (T / \rho c_p) (\partial \omega / \partial T)_P (P_a^2 - P_b^2). \quad \text{Eq. (13)}$$

Therefore, a plot of ΔT vs. P_a^2 obtained when the applied field is removed should yield a straight line which intersects the P_b^2 axis at P_b^2 . Fig. 7 shows such plots. The departures from linearity at low values of P are due to irreversibility (hysteresis); they should disappear as the Curie temperature is approached as indeed they do. Extrapolation of the linear portions of Fig. 7 give values for

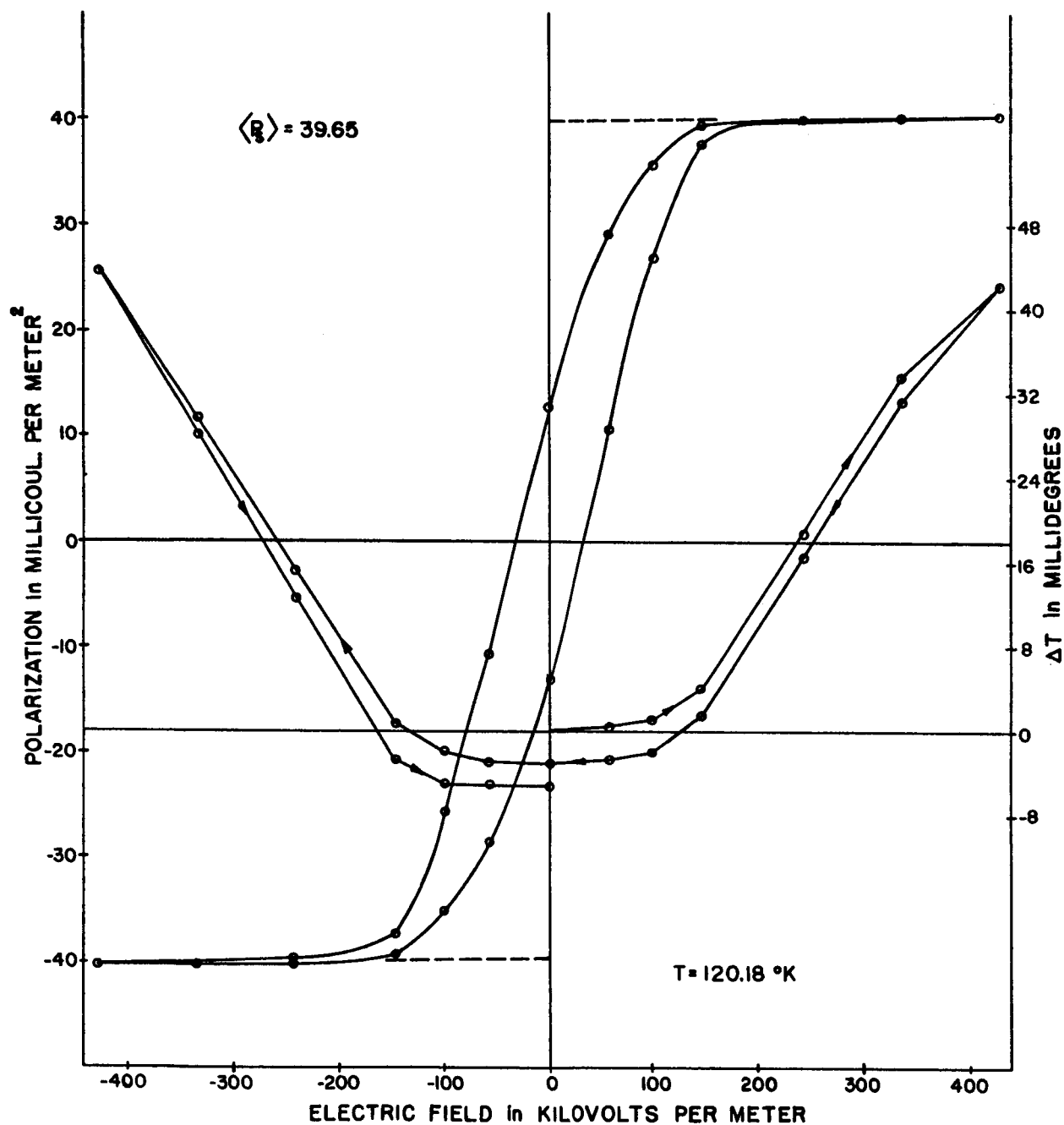


FIG. 6 DIELECTRIC & ELECTROCALORIC MEASUREMENTS BELOW THE CURIE TEMPERATURE

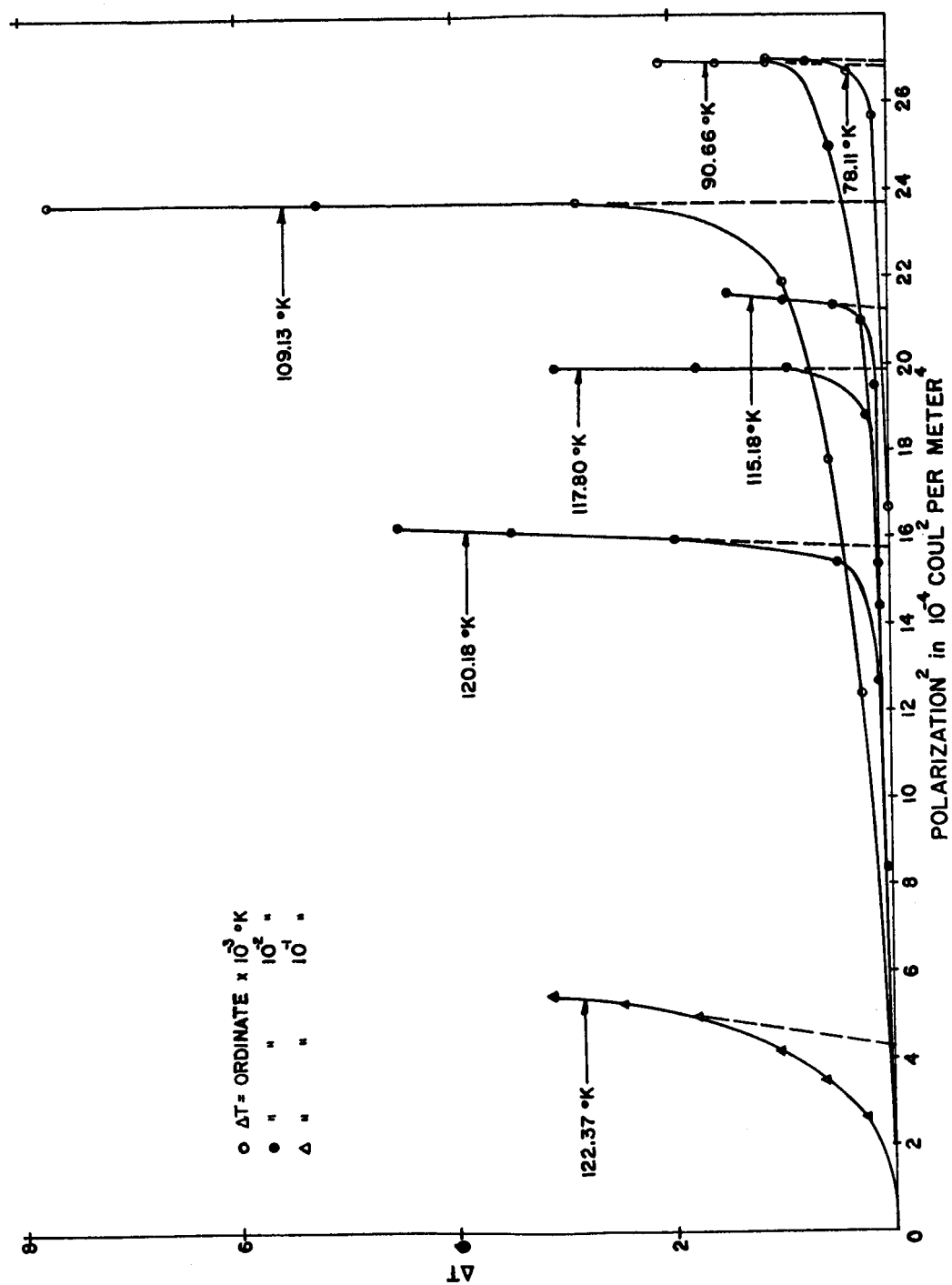


FIG. 7 ΔT vs ΔP^2 BELOW THE CURIE TEMPERATURE

P_s . These "electrocaloric" values are shown in Fig. 8 together with the values obtained from static dielectric measurements of the hysteresis cycle on the same specimen. The agreement is good; moreover, the electrocaloric data require less extrapolation and give their most reliable values for $P_s(T)$ near the Curie temperature, the very region where the extrapolation of the hysteresis curve to $E = 0$ is less certain. The ferroelectric Curie temperature given by these electrocaloric data is 123°K. The short lines on Fig. 8 are values of $\partial P/\partial T$ computed from the electrocaloric measurements by means of Eq. (4a). The values of P and T (represented by open triangles) through which the lines representing $\partial P/\partial T$ are drawn are located above the curve representing P_s vs. T because the electrocaloric measurements were made in the reversible region near the tips of the hysteresis loops. These results indicate that, unlike Rochelle salt,⁸ the value of $\partial P/\partial T$ is approximately independent of electric field even within a few degrees of the Curie temperature.

Unfortunately these data are not sufficiently accurate to permit a determination of $\partial \omega/\partial T$ throughout the ferroelectric region. The inaccuracy lies not in the measurements of ΔT but in the measurement of the relatively small changes in polarization that occur near the tips of the hysteresis loops, i.e. in the nearly reversible region. The accuracy of the measurements in this region were improved by applying a known biasing charge to suppress the zero of the charge-measuring equipment, increasing the sensitivity of the charge measurements and then measuring ΔP and ΔT for stepwise changes in E in the tips of the hysteresis loops. Typical results at the highest fields are shown in Fig. 9 on a magnified scale. An incidental conclusion is evident from Fig. 9: the polarization of KH_2PO_4 does not become linear in E at the highest fields used. This is consistent with the Devonshire formalism.

With Eq. (2) in mind, measured values of the quantity $(\rho c_p/T)(\Delta T/\Delta P)_s$ which is equivalent to $(\partial E/\partial T)_p$ are plotted as a function of temperature (Fig. 10) and of polarization (Fig. 11) over the entire temperature range of interest. These figures show that $(\partial E/\partial T)_p$ is not a function of temperature alone or of polarization alone. Attempts were made to fit the measured values of $(\rho c_p/T)(\Delta T/\Delta P)_s$ to an analytical expression for $(\partial E/\partial T)_p$ that was derivable from an expansion of G_1 according to Eq. (11),

$$G_1 = G_{10} + \omega P^2/2 + \xi P^4/4 + \zeta P^6/6 + \dots \quad (11)$$

from which

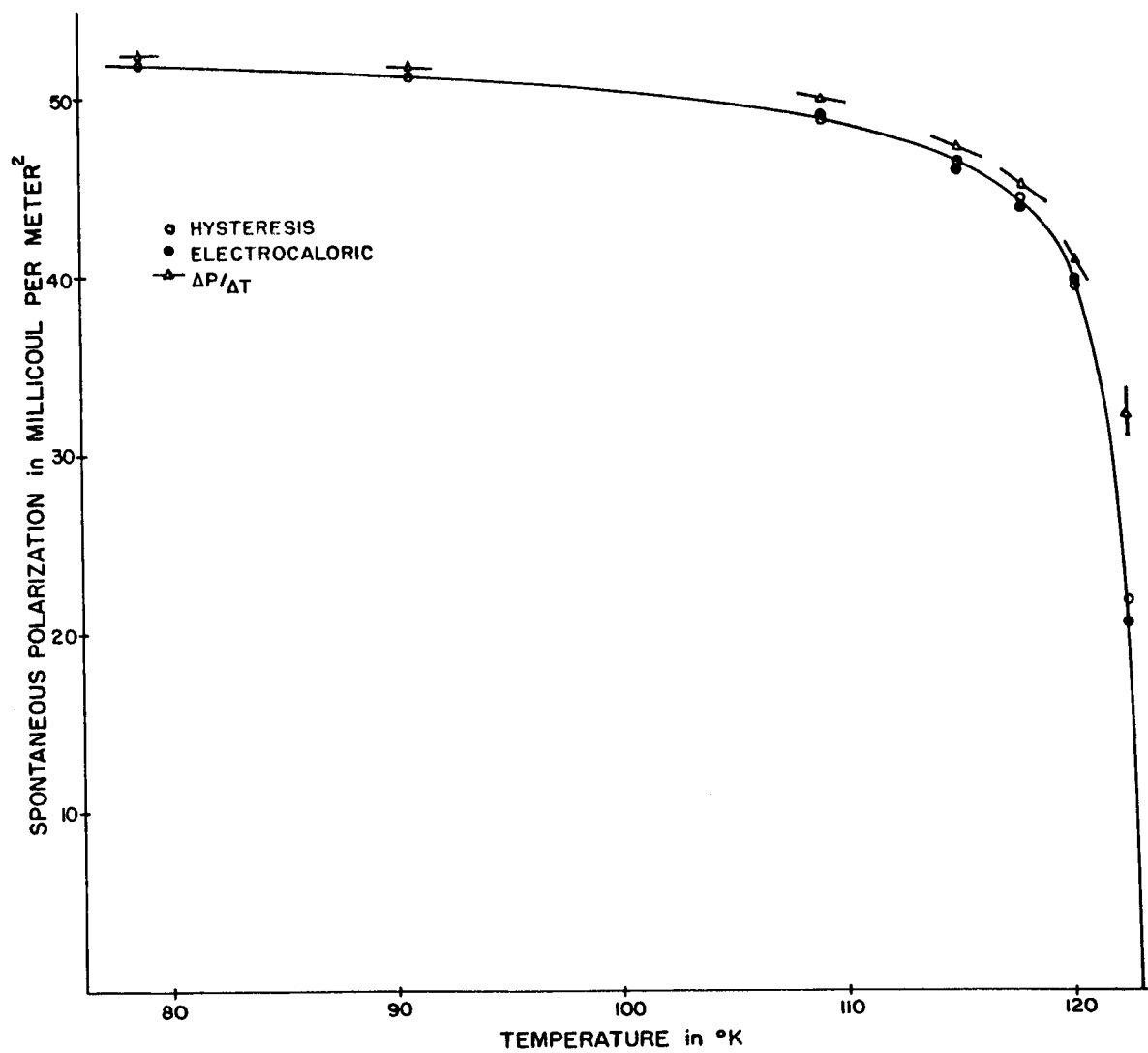


FIG. 8 SPONTANEOUS POLARIZATION & $\Delta P/\Delta T$ vs. TEMPERATURE

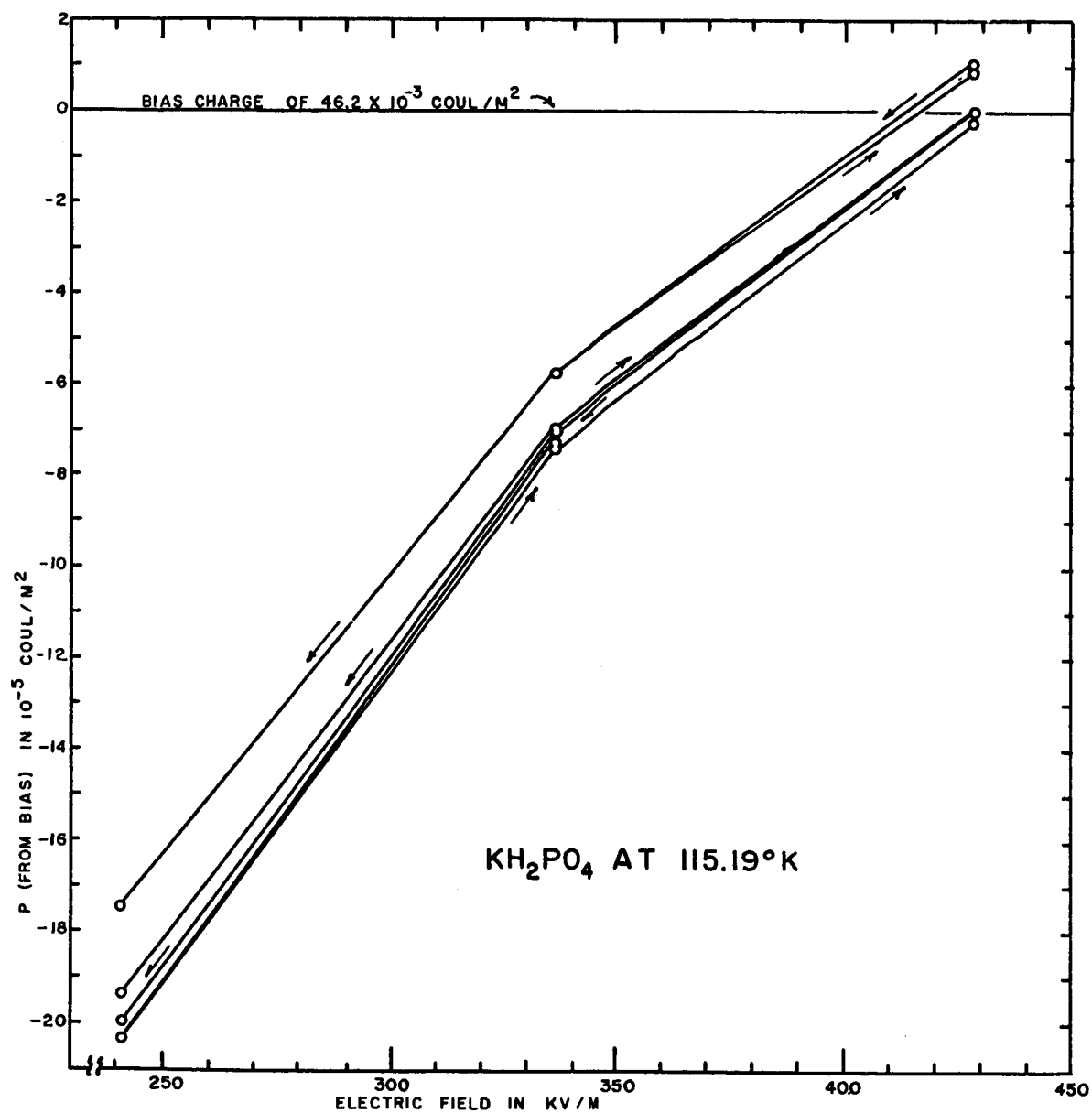


FIG.9 REPETITION OF ΔP NEAR TAIL OF HYSTERESIS CYCLE

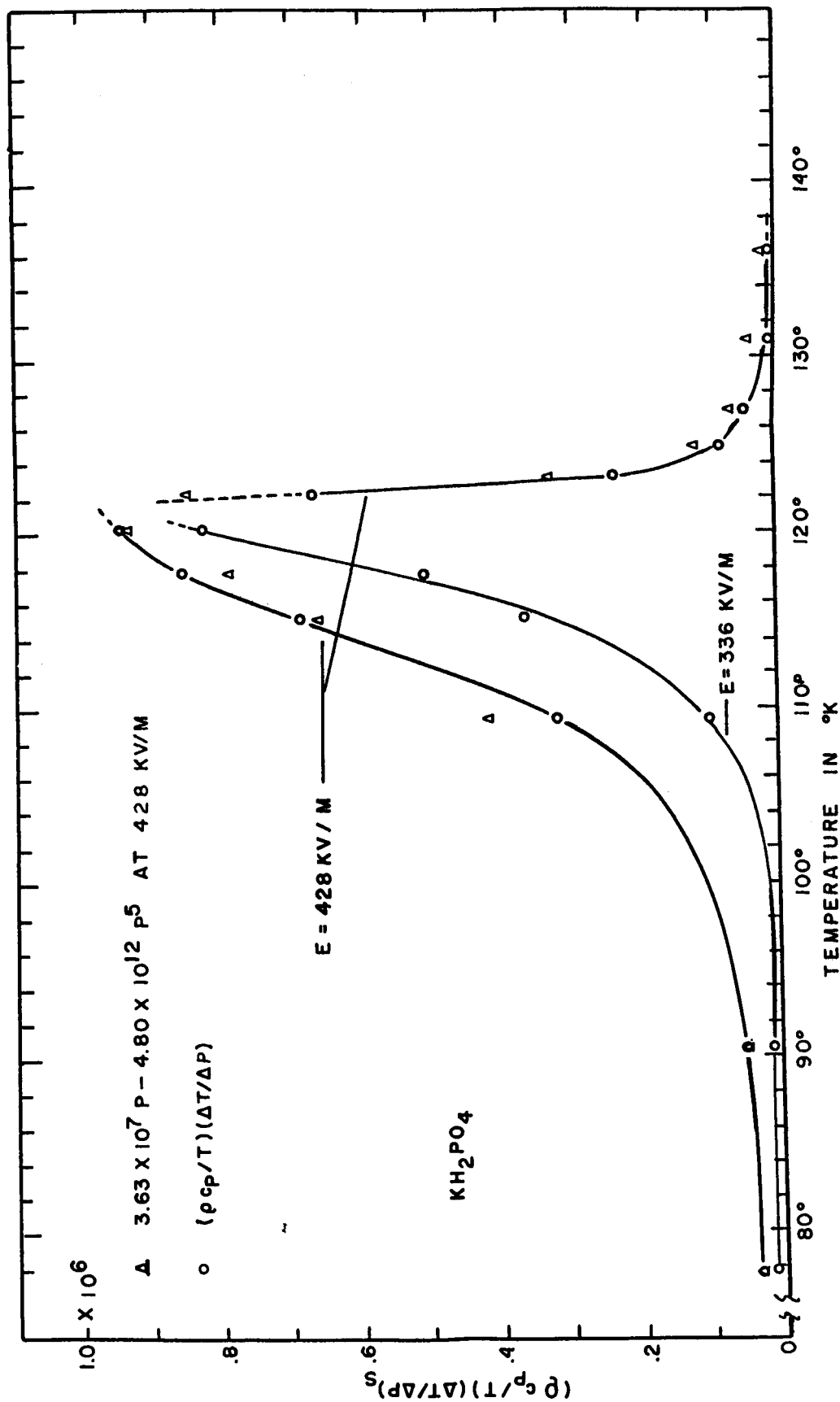


FIG. 10 ELECTROCALORIC EFFECT ABOVE AND BELOW T_C

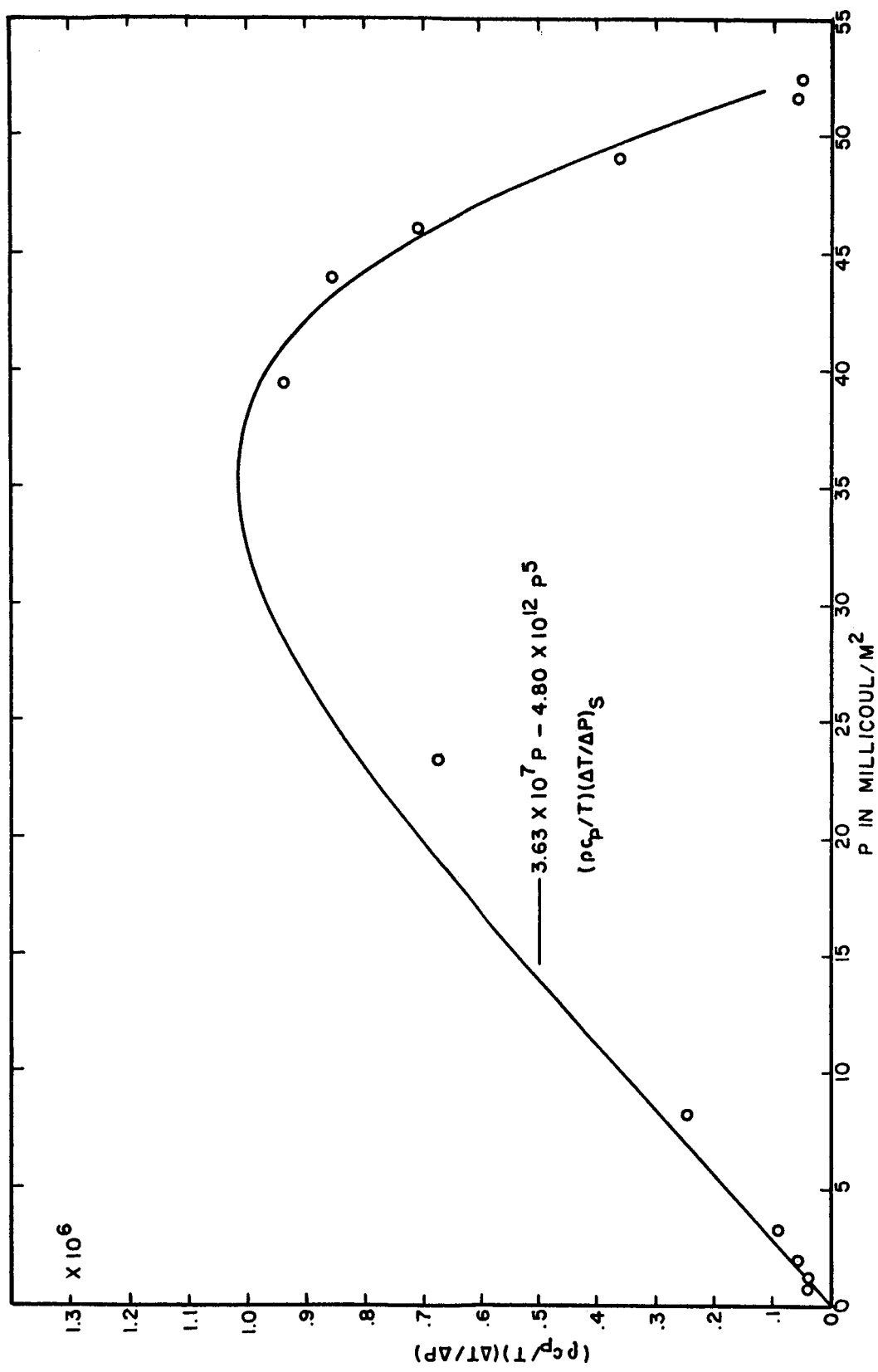


FIG.II ELECTROCALORIC EFFECT IN KH₂PO₄ AS f(P)

$$E = (\partial G / \partial P)_T = \omega P + \xi P^3 + \zeta P^5 + \dots$$

The best fit was obtained for $\omega = 3.63 \times 10^7$, $\xi = 0$, and $\zeta = -4.80 \times 10^{12}$, the degree of fit being evident from Figs. 10 and 11. With these constants, Eq. (11) fits the high-field electrocaloric measurements fairly well right on through the Curie temperature, but it predicts erroneously that the value of $(\partial E / \partial T)_P$ should increase at lower values of E and P . A non-zero value for ξ (a P^3 term in the equation for E) did not correct this discrepancy.

The cause of the discrepancy is not known. It is not due to irreversible effects: integration of the entire hysteresis cycle at 115.19°K, for example, yields only 469 joules of heat which would increase the temperature of a specimen only 6×10^{-4} °K, and Fig. 9 shows that the polarization is nearly reversible in the tips of the hysteresis loops. Moreover, the small effects of irreversibility tend to be cancelled by our averaging of the measured values of $\Delta T / \Delta P$ for polarization and depolarization at each field step.

In spite of the inadequacy of the inner-field model of ferroelectricity, we felt that it was interesting to determine the inner field constant γ from the electrocaloric measurements, i.e. from Eq. (9) which can be written

$$\gamma = \rho C_P (\Delta T / \Delta P) / P. \quad (9)$$

Measured values of γ (below the Curie temperature only) are shown in Figs. 12 and 13. The solid line of Fig. 13 represents the equation

$$\gamma = 5.15 \times 10^3 \exp (0.1085T).$$

Comparison of these two figures shows that γ , far from being a simple constant, is not even dependent upon temperature alone. Thus the electrocaloric measurements confirm the idea that an internal field parameter γ which is based on long-range electrostatic forces between dipoles is not a proper foundation on which to build a model of ferroelectric polarization.

The Pyroelectric Coefficient for KH_2PO_4

For a stress-free crystal, the pyroelectric coefficient $p^{X,E}$ discussed earlier in this report reduces to

$$p^E \equiv (\partial P / \partial T)_E.$$

The subscript and superscript E denote a constant-field process; e.g., this

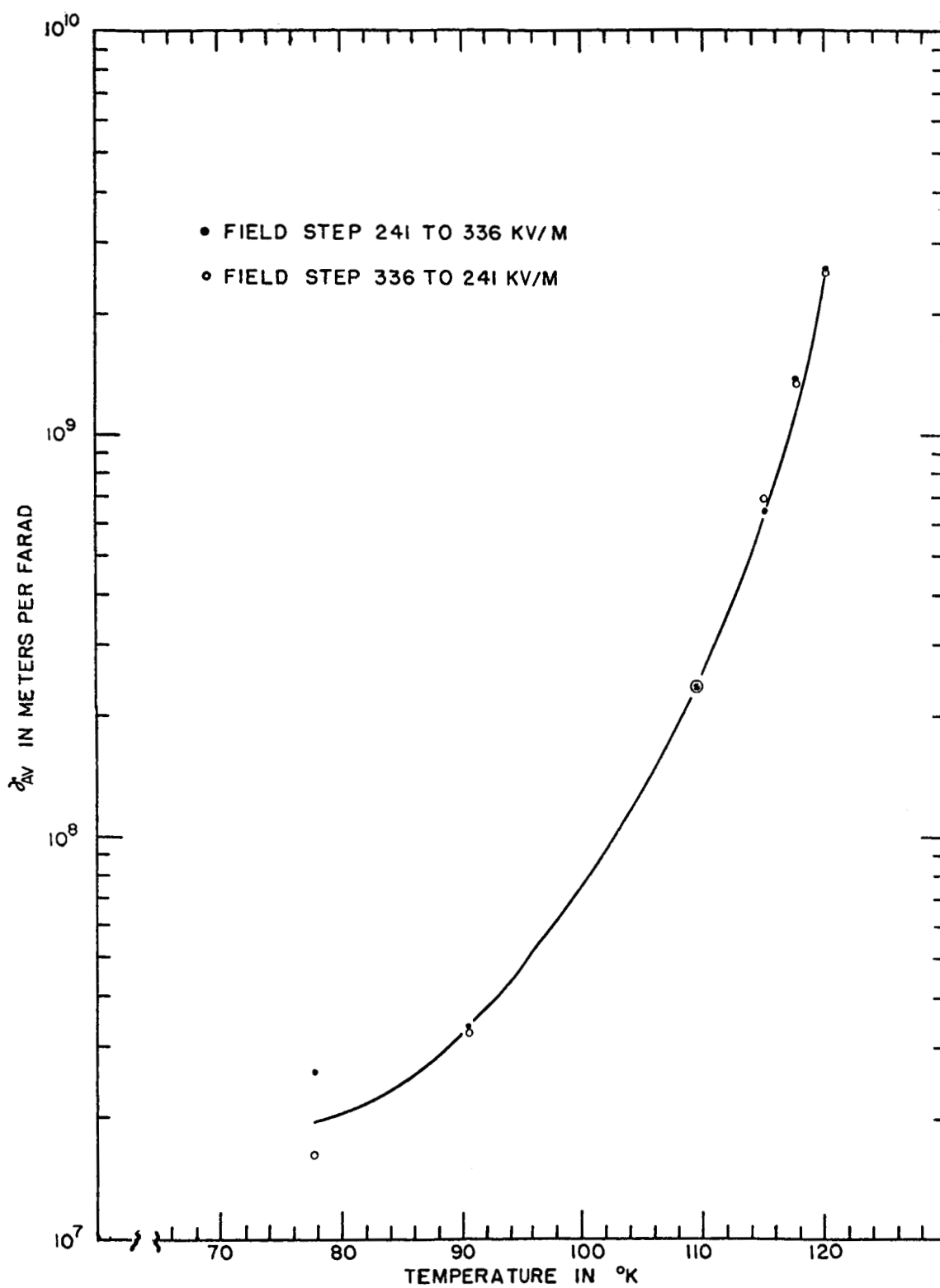


FIG.12 ELECTROCALORIC MEASUREMENT OF γ ,
 KH_2PO_4 AT 241-336 KV/M

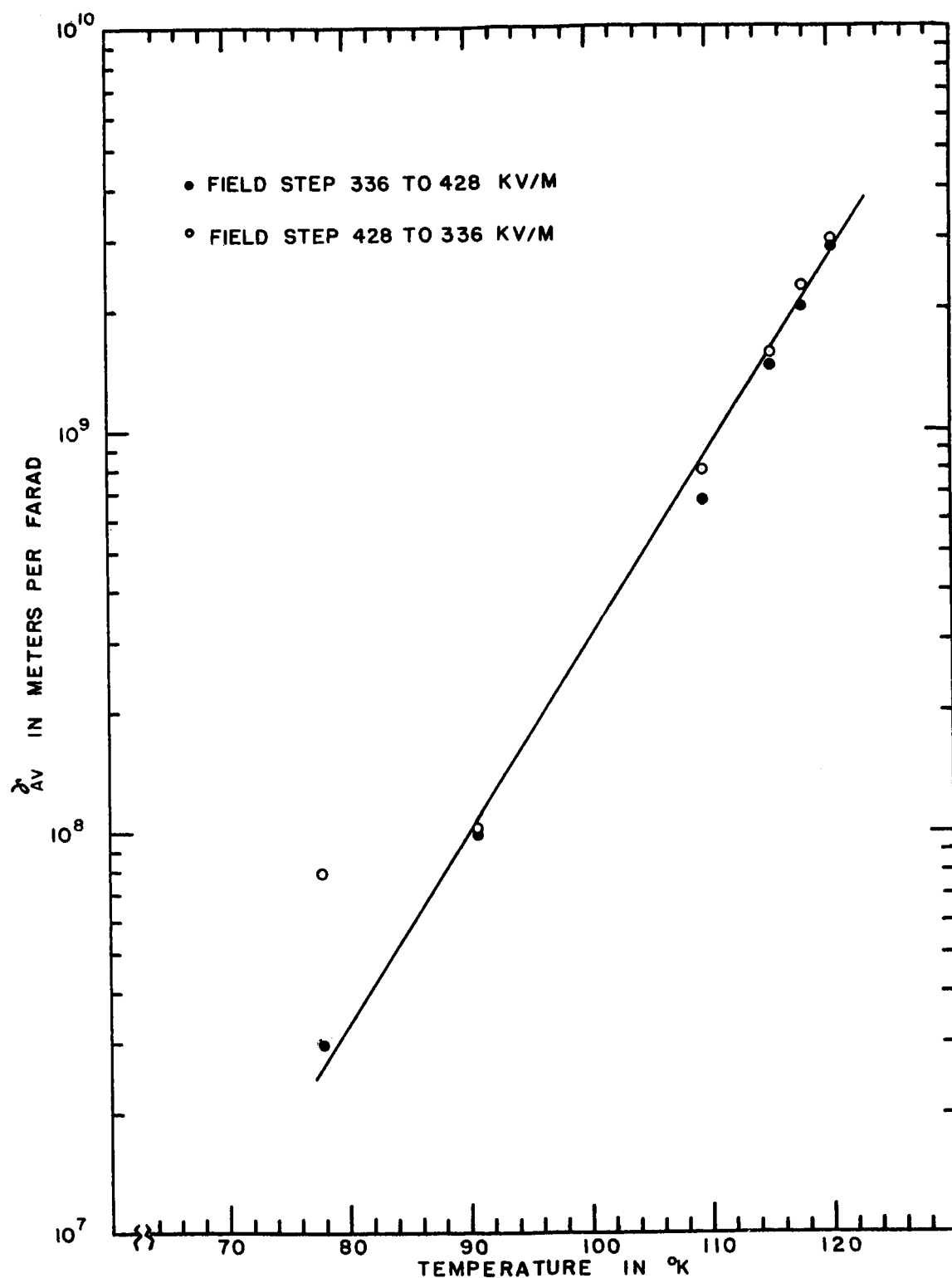


FIG. 13 ELECTROCALORIC MEASUREMENT OF γ , KH_2PO_4 AT 336-428 KV/M

expression is applicable when a pyroelectric signal is delivered to a low-impedance detector. Combining the definition of p^E with the E form of the electrocaloric equation Eq. (4a), gives

$$p^E = - (\rho c_E / T) (\Delta T / \Delta E). \quad (29)$$

We computed p^E at various temperatures from measured values of the electrocaloric effect as suggested by Eq. (29). Values of the specific heat c_E were obtained from Stephenson and Hooley.²³

The results of this computation are shown in Fig. 14 and should be compared with qualitatively similar results for other substances that are discussed later. Values of p^E in the paraelectric region are not plotted; they can be computed from the Curie-Weiss law.

Triglycine Sulfate $(\text{NH}_2\text{CH}_2\text{COOH})_3 \cdot \text{H}_2\text{SO}_4$

Triglycine sulfate undergoes one second order ferroelectric transition at 322.60°K (49.54°C). Its dielectric properties have been investigated by Hoshino²⁴ and others.²⁵ Its use as a pyroelectric detector has been considered by the Sperry Group^{12,13,14} and by Chynoweth.¹¹

Chemical formula	$(\text{NH}_2\text{CH}_2\text{COOH})_3 \cdot \text{H}_2\text{SO}_4$
Dimensions of crystal	2.82 cm ² x 3.19 mm
Density	1.68 g/cm ³
Crystal symmetry (above T_C)	Monoclinic
Ferroelectric axis	Monoclinic b
Specific heat ²⁴	$c_p = 419 + 1.747T$ joules/Kg
Curie temperature	322.60°K (49.45°C)
Range of temperature studied	273°K to 334°K

TGS in the Paraelectric Phase

The typical dielectric and electrocaloric behavior observed for triglycine sulfate (hereafter called TGS) in its paraelectric phase are shown in Fig. 15. The measurements for TGS are consistent with the Curie-Weiss law as shown in Fig. 16. The solid line represents the Curie-Weiss law with $T_C = 322.6^\circ\text{K}$ (49.45°C) and $C = 3260$. Both of these values are in reasonable agreement with published determinations by a-c methods; the most recent measurements are those of Gonzalo²⁶ who gives $T_C = 49.40^\circ\text{C}$ and $C = 3560$. Hoshino²⁴ reports $T_C = 48^\circ\text{C}$ and $C = 3280$. Measured values for the electrocaloric effect in the paraelectric phase are displayed below, along with those for the ferroelectric phase.

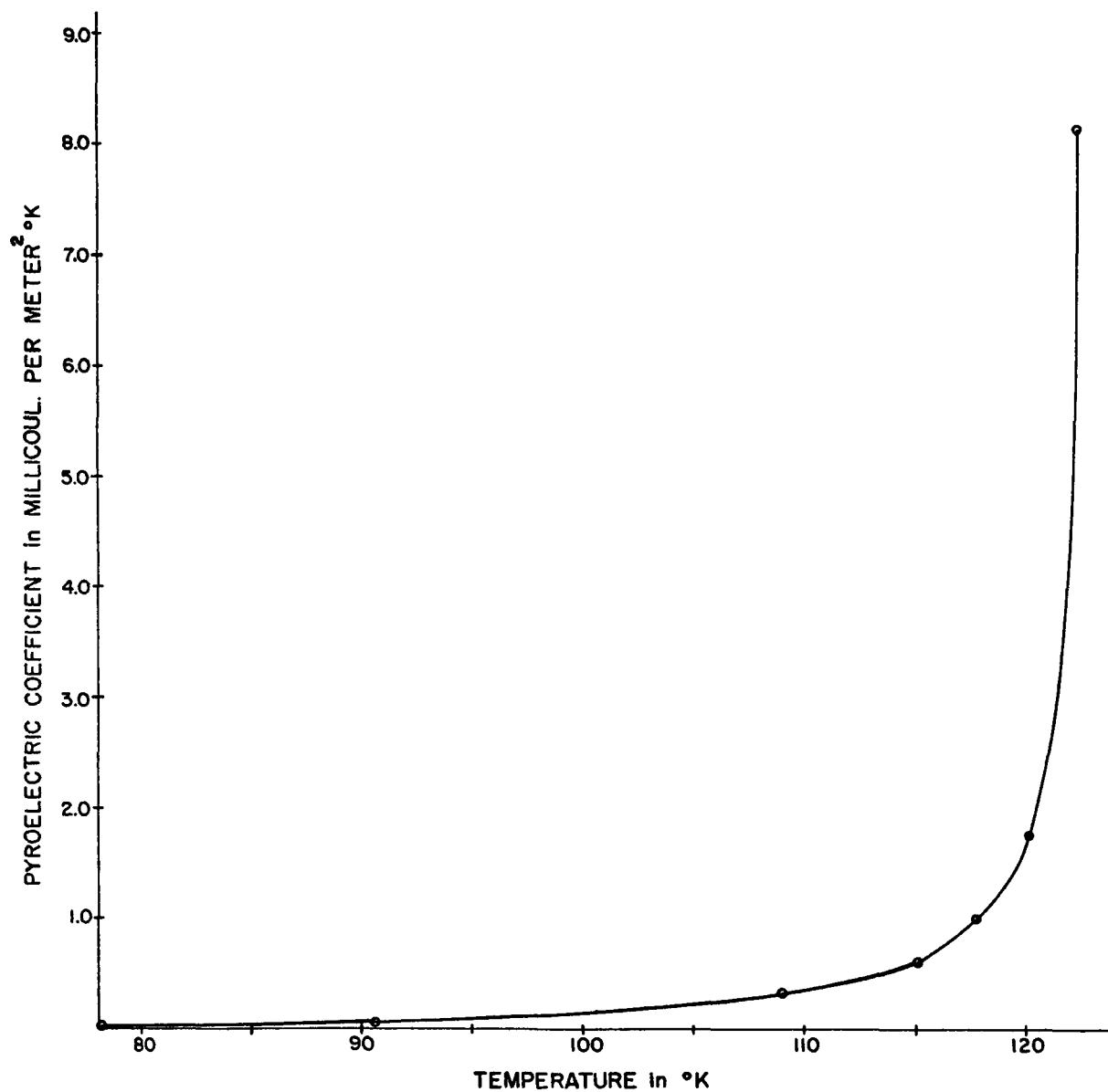


FIG.14 ELECTROCALORIC MEASUREMENT OF THE
PYROELECTRIC COEFFICIENT vs. TEMP.

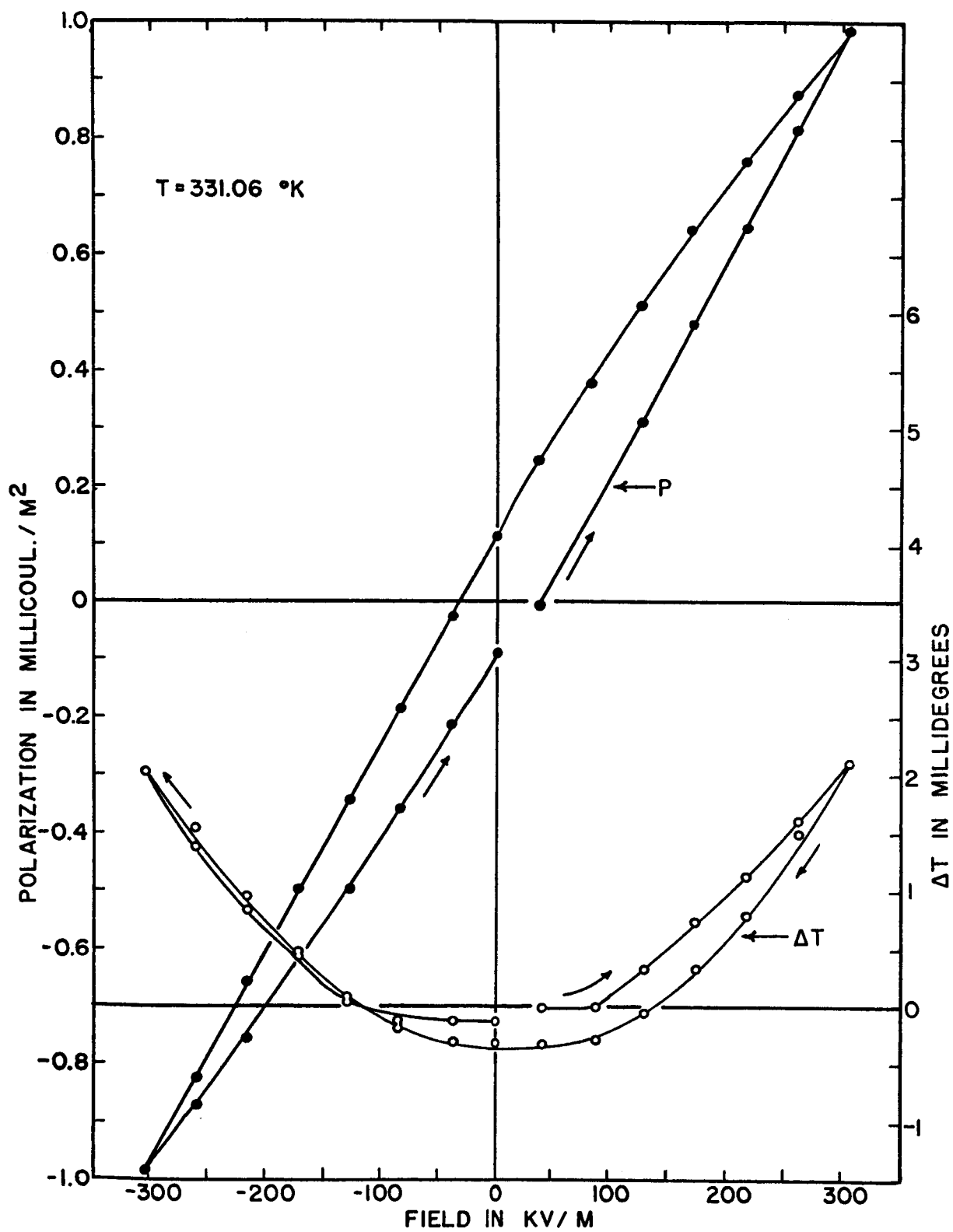


FIG. 15 TGS ABOVE THE CURIE TEMPERATURE

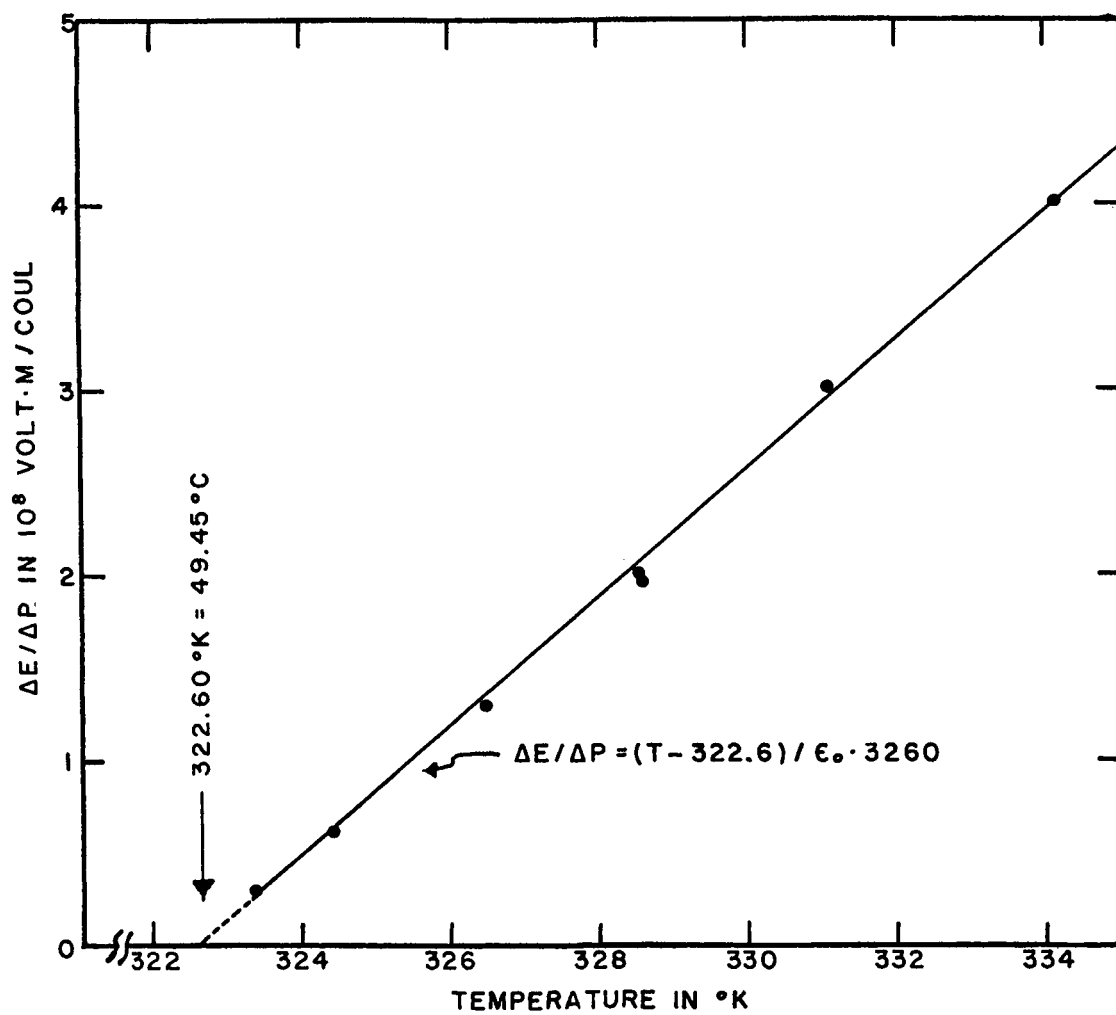


FIG.16 RECIPROCAL D-C SUSCEPTIBILITY OF TGS

TGS in the Ferroelectric Phase

As TGS is cooled through the Curie temperature, the electrocaloric effect changes abruptly from being quadratic in E (see Fig. 15) to being linear in E as shown by the typical measurements displayed in Fig. 17. In this instance the hysteresis effect is negligible except for small values of E .

The electrocaloric effect and the polarization in both of the two specimens studied extensively was asymmetrical with respect to E as shown in Fig. 17. The asymmetry disappears as the crystal is heated above the Curie temperature but reappears again in the same direction, though not always in the same amount, when the crystal is re-cooled. There are two aspects to this asymmetry: one is the often-reported internal bias of the ferroelectric phase, and the other is a gradually-slowng drift of charge that follows the "instantaneous" polarization accompanying each change in E . The rates and magnitudes of these drifts are also asymmetrical in E . We attribute these drifts to a combination of ferroelectric relaxation polarization and ohmic conduction within the crystal. Asymmetry in the polarization of TGS has also been observed by Hoshino²⁴ and by Chynoweth¹¹, Chynoweth having observed asymmetry in the pyroelectric effect as well. Large differences exist between the hysteresis loops taken at 60 hz, at 1 field step/minute, and 1 field step/5 minutes (see Status Report No. 4)¹⁷. For example, the short vertical solid and broken lines in Fig. 17 show the coercive field for the hysteresis loops taken at 60 hz and 1 step/5 min. respectively.

These relaxation effects are particularly vexing to us because they preclude accurate determinations of the "instantaneous" values of P from the recorder trace. Moreover, the asymmetry and relaxation properties of the crystals are not constant, their behavior becoming somewhat more consistent with use.

Fig. 18 shows the electrocaloric effect observed at various temperatures. The upper curve represents the cumulative sum of the step-wise electrocaloric temperature changes for a maximum applied field of 305.6 kV/m, and the lower curve represents corresponding values for a field of 128.4 kV/m.

Fig. 19 shows the variation of static polarization with temperature at $E = 306$ kV/m and at $E = 0$.

Detailed measurements of ΔP and ΔT vs. E near the tips of the hysteresis loops were made at increased sensitivity by employing the charge-biasing techniques previously cited.

When the electrocaloric measurements taken at increased sensitivity were compared to values computed from Eq. (11), it was found that only the P^2 term which includes the first Devonshire coefficient ω is needed to give the best fit.

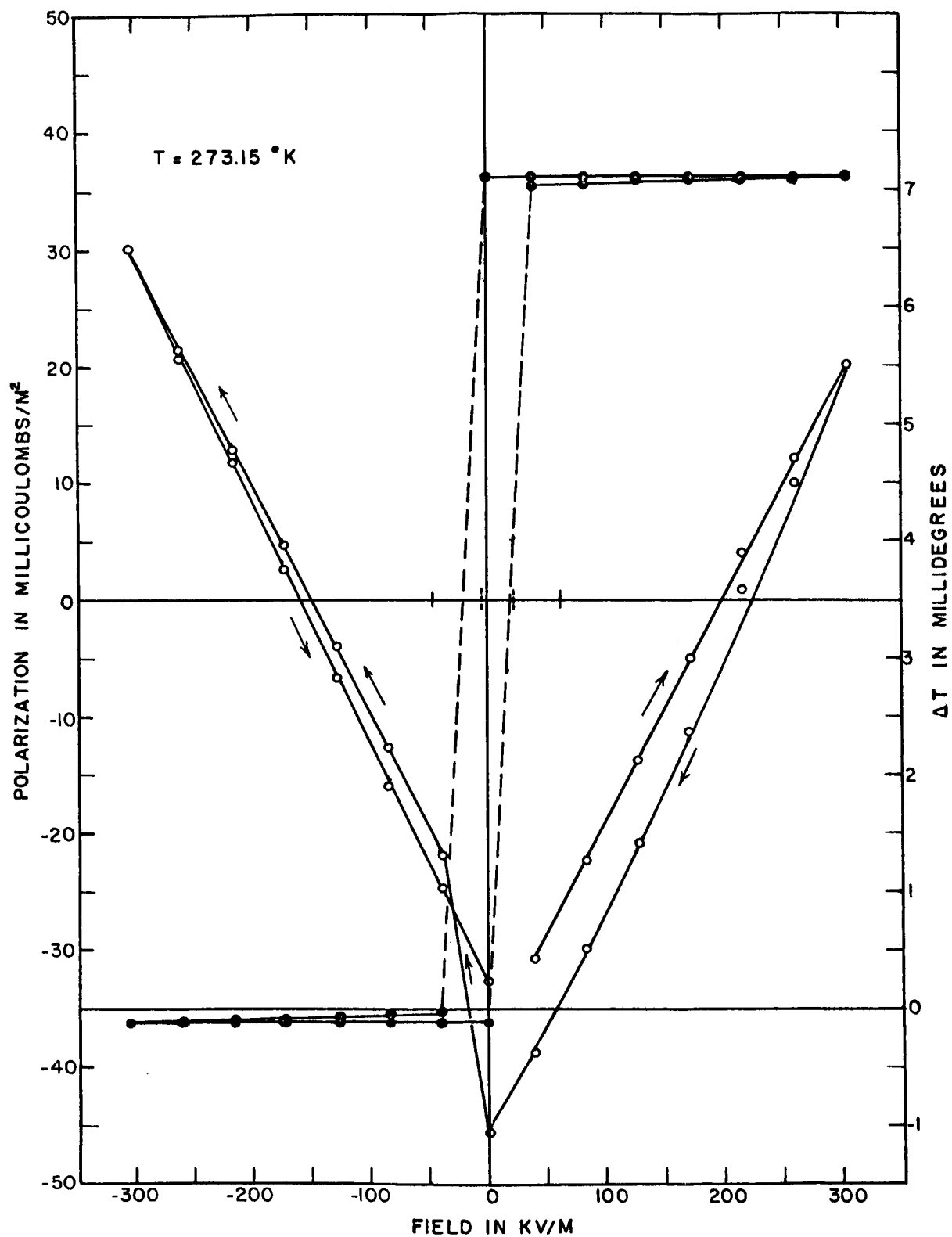


FIG.17 TGS BELOW THE CURIE TEMPERATURE

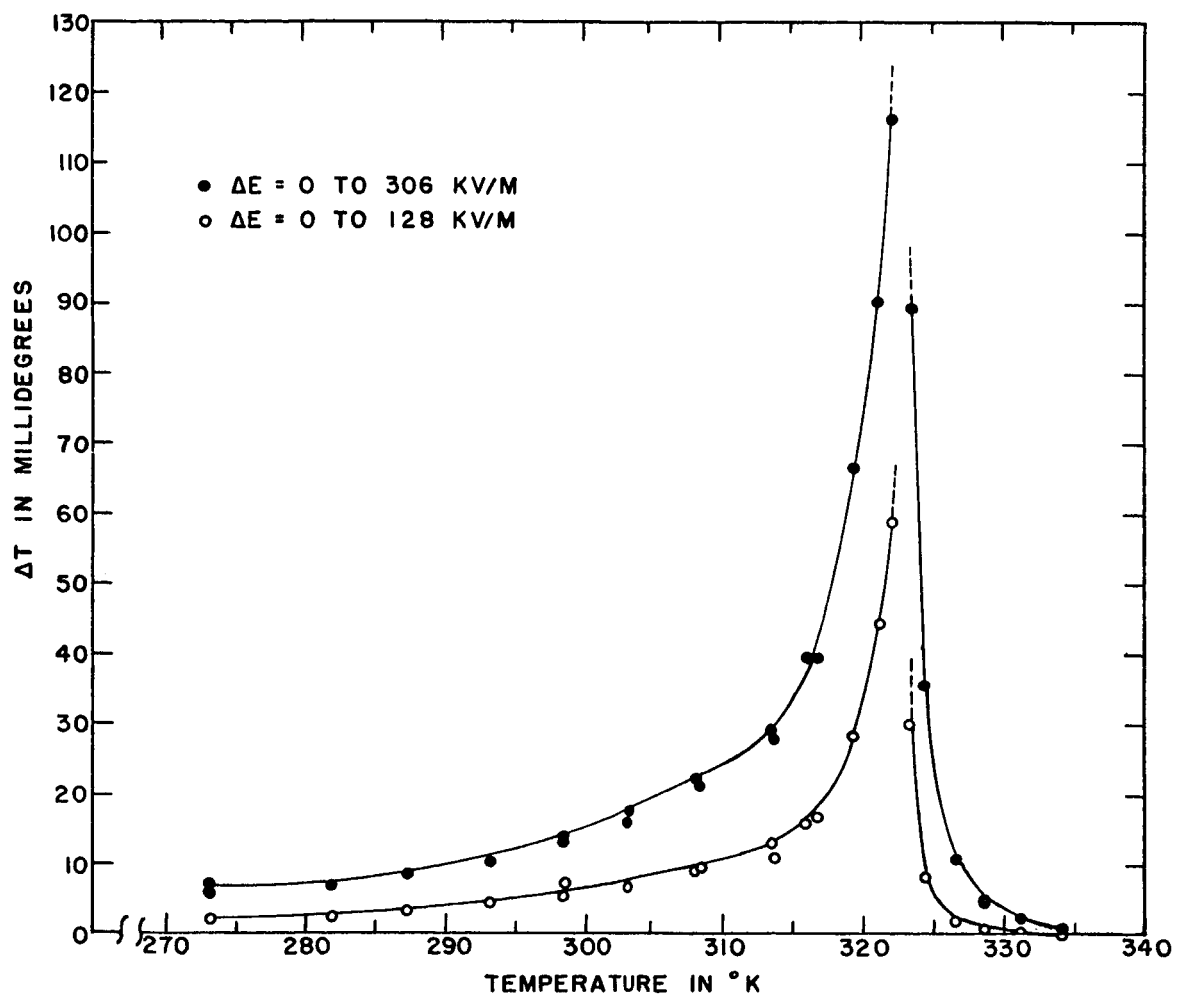


FIG.18 TOTAL ELECTROCALORIC EFFECT IN TGS

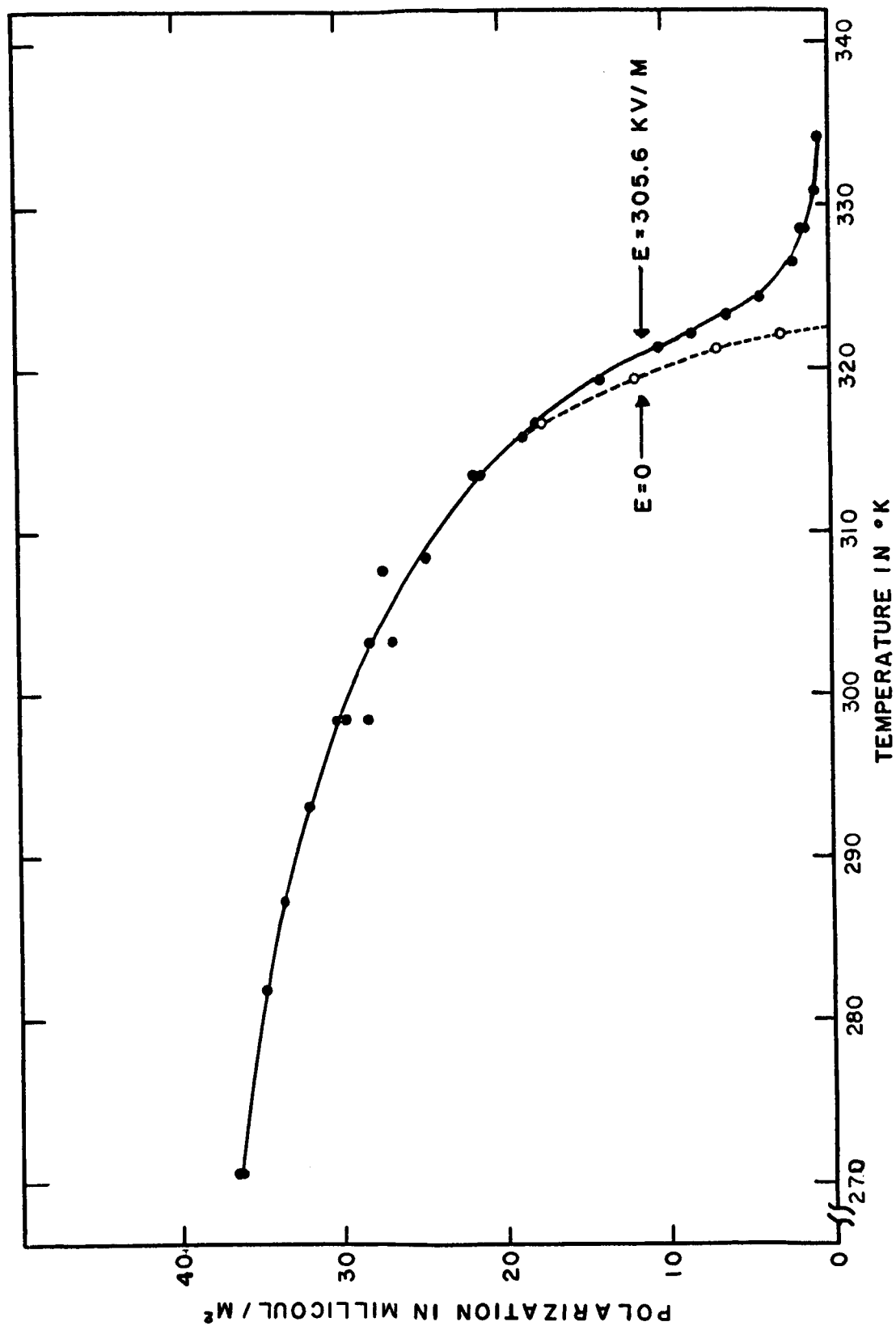


FIG. 19 POLARIZATION OF TGS

That is, unlike KH_2PO_4 , TGS is reasonably well described by Eq. (13) which can be rewritten

$$(\partial\omega/\partial T) = \rho c_p \Delta T / TP \Delta P$$

if $\Delta T \ll T$ and $\Delta P \ll P$ as is the case for measurements taken near the tips of the hysteresis loops. Fig. 20 shows the measured values $\rho c_p \Delta T / TP \Delta P$ throughout the temperature range over which the electrocaloric effect is appreciable.

The scatter of the points in Fig. 20 is due partly to the relaxation effects which make consistent measurements of ΔP difficult, but it is due mostly to actual changes in the crystal produced by the electrical and thermal treatment. The values indicated by the circles in Fig. 20 were obtained with a "fresh" specimen before it had ever been heated above the Curie temperature, and these values were given less weight in drawing the solid line.

Some uncertainties notwithstanding, two conclusions can be drawn: (1) there is continuity in the value of $\partial\omega/\partial T$ at the Curie temperature, and (2) the value of $\partial\omega/\partial T$ begins to drop appreciably at low temperatures. This continuity in the value of $\partial\omega/\partial T$ through the Curie temperature is greatly different from the behavior of potassium dihydrogen phosphate.

As shown by information contained in Figs. 15 and 17, TGS obeys the Curie-Weiss law so that Eq. (12) reduces to

$$E = \omega P = (T - T_p)P/\epsilon_0 C$$

above the Curie temperature. Consequently, ω must be zero at the Curie temperature. The value of $\omega(T)$ can then be obtained from Fig. 20 by integration. The resulting values of ω are displayed in Fig. 21 together with the values (shown by the broken line) predicted from the Curie constant.

The Pyroelectric Coefficient for TGS

The pyroelectric coefficient p^E was determined from measurements of the electrocaloric effect via Eq. (29),

$$p^E = -(\rho c_E/T)(\Delta T/\Delta E). \quad (29)$$

Values of c_E were obtained from Hoshino and Mitsui.²⁴ The variation of p^E with temperature is shown in Fig. 22. In the ferroelectric phase p^E is approximately independent of the field. In the paraelectric phase the electrocaloric temperature rise is quadratic in E as predicted by the Curie-Weiss law. Consequently

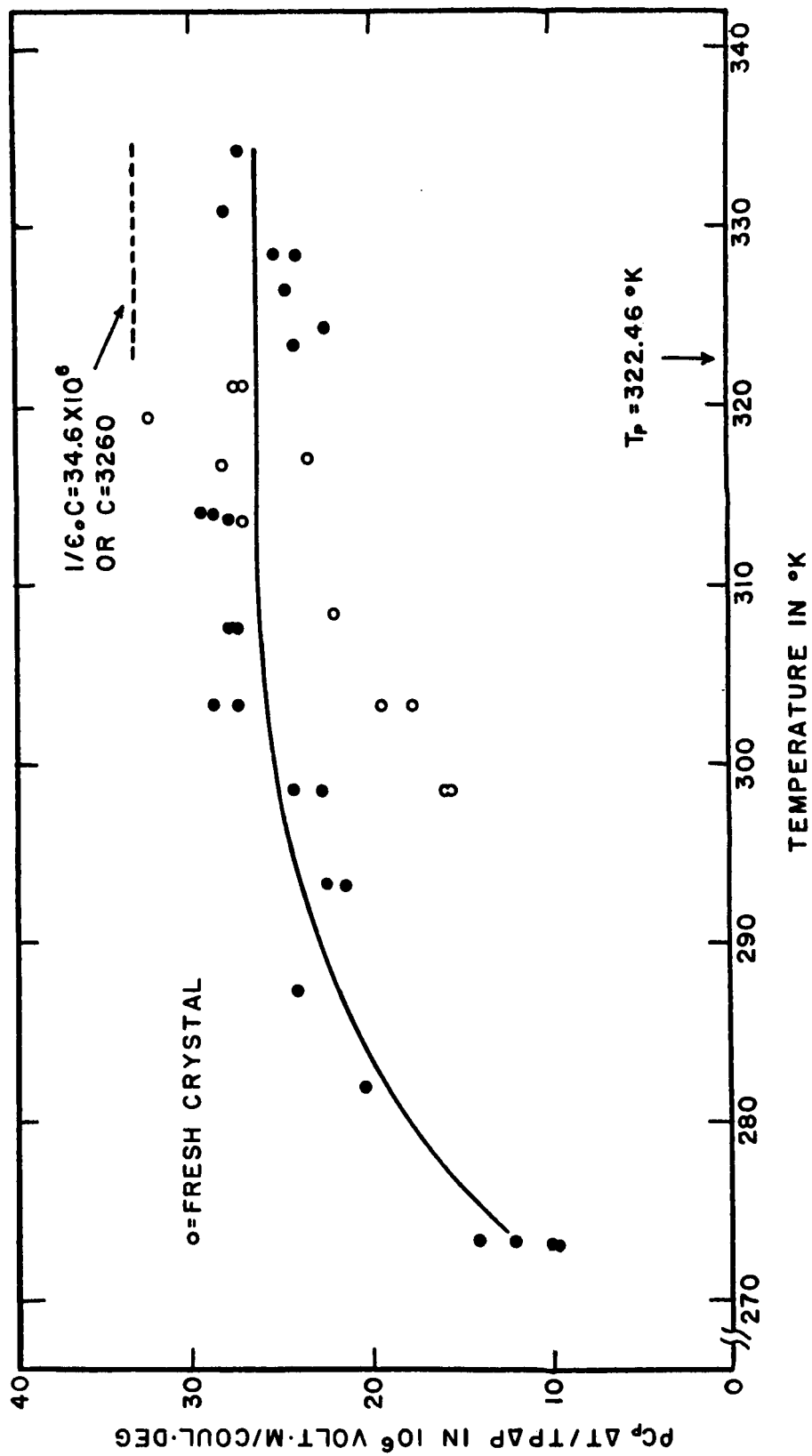


FIG.20 VALUES OF $(PC_p \Delta T / TP \Delta P)$ AT 261 KV/M

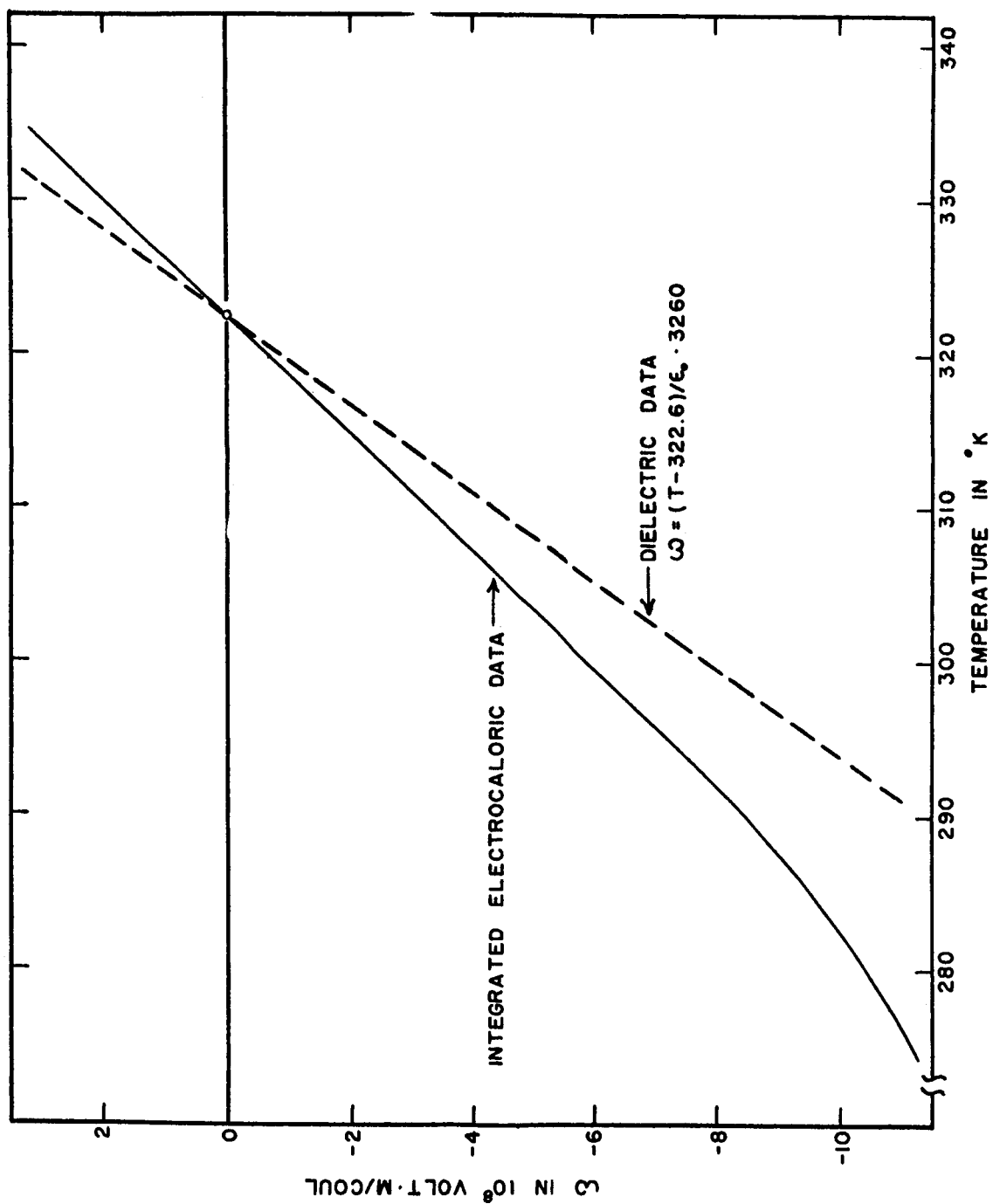


FIG. 21 $\omega(T)$ FROM ELECTROCALORIC AND DIELECTRIC MEASUREMENTS

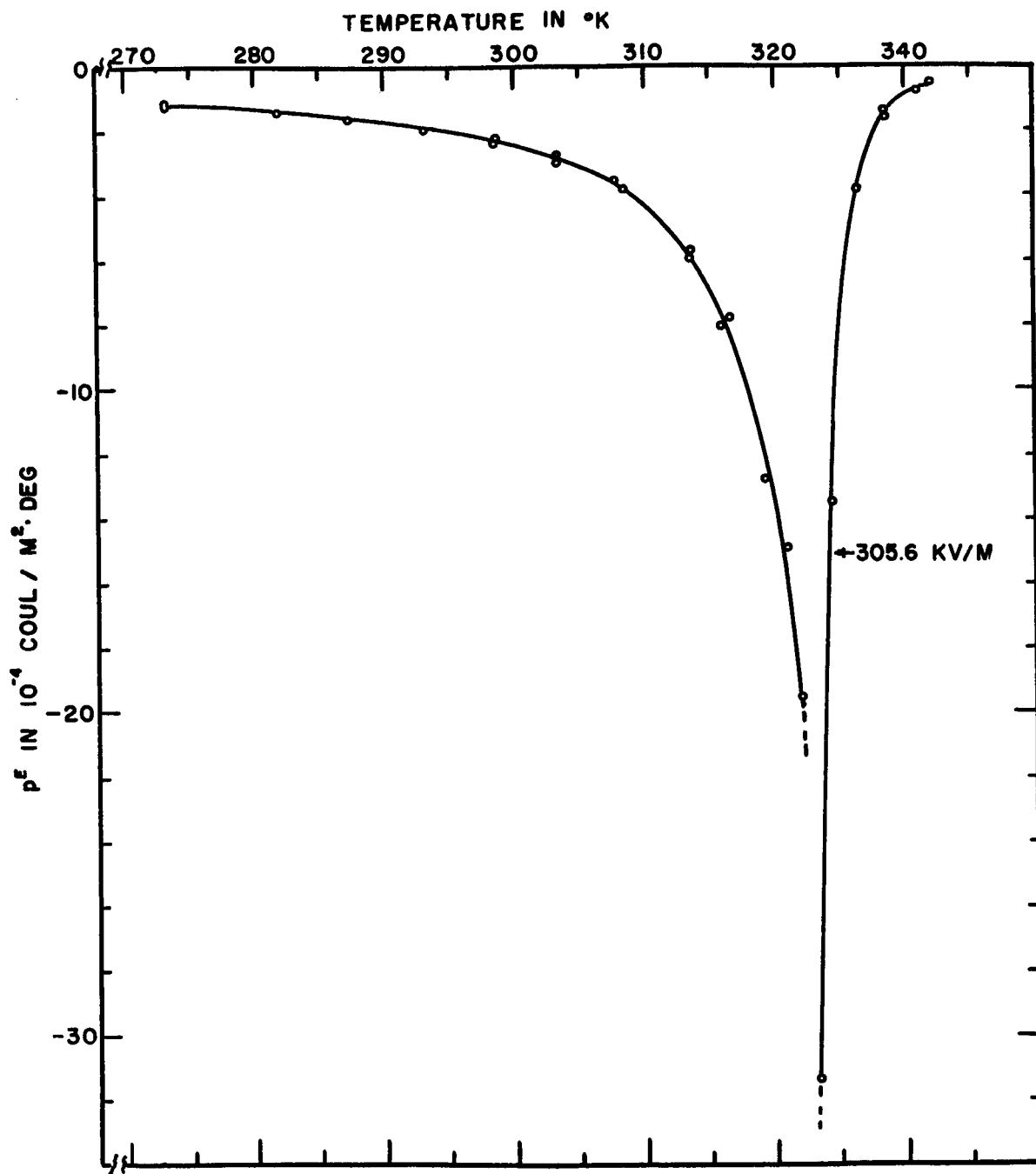


FIG.22 PYROELECTRIC COEFFICIENT OF TGS FROM ELECTROCALORIC DATA

the sensitivity of a radiation detector used in its paraelectric phase could be adjusted at will by changing the biasing field. The sensitivity at the maximum field used in these experiments (305.6 kV/m) is shown in Fig. 22.

Potassium Dihydrogen Arsenate KH_2AsO_4

This substance was selected for study because it is similar to KH_2PO_4 .^{27,28} As pointed out in the preceding sections of this report, the electrocaloric effect in KH_2PO_4 appeared to be unlike the effect in Rochelle salt⁸ and in tri-glycine sulfate.¹² In particular, we were unable to find a Gibbs function G_1 that would predict both the variation of the electrocaloric effect and the ferroelectric behavior with temperature; moreover, the first Devonshire coefficient ω for KH_2PO_4 was not well-behaved near the Curie temperature.

Chemical formula	KH_2AsO_4
Dimensions of crystal	0.868 cm ² x 2.65 mm
Density	2.87 g/cm ³
Crystal symmetry	Tetragonal
Ferroelectric axis	Tetragonal c
Specific heat	From Stephenson & Zettlemoyer ²⁹
Curie temperature	96°K
Range of temperature studied	90.45°K to 100.57°K

KH_2AsO_4 in the Paraelectric Phase

The behavior of KH_2AsO_4 proved to be similar to KH_2PO_4 in both the paraelectric and ferroelectric phases, thus corroborating the work on KH_2PO_4 . Typical static polarization and electrocaloric temperature changes for KH_2AsO_4 above the Curie temperature are shown in Fig. 23. Potassium dihydrogen arsenate obeys the Curie-Weiss law, the Curie temperature being 94.25°K and the Curie constant being 2349 as determined from the electrocaloric measurements.

KH_2AsO_4 in the Ferroelectric Phase

Fig. 24 illustrates the behavior of this substance below the Curie temperature. The lowest of the three curves in Fig. 25 represents the remanent polarization, the values of P at $E = 0$, as read from our step-wise hysteresis loops (e.g. Fig. 24).

The middle curve represents a near-coincidence of three values: (1) the polarization attained at the maximum applied field, (2) the spontaneous polarization P_s obtained by extrapolating the tips of the hysteresis loops to $E = 0$, and

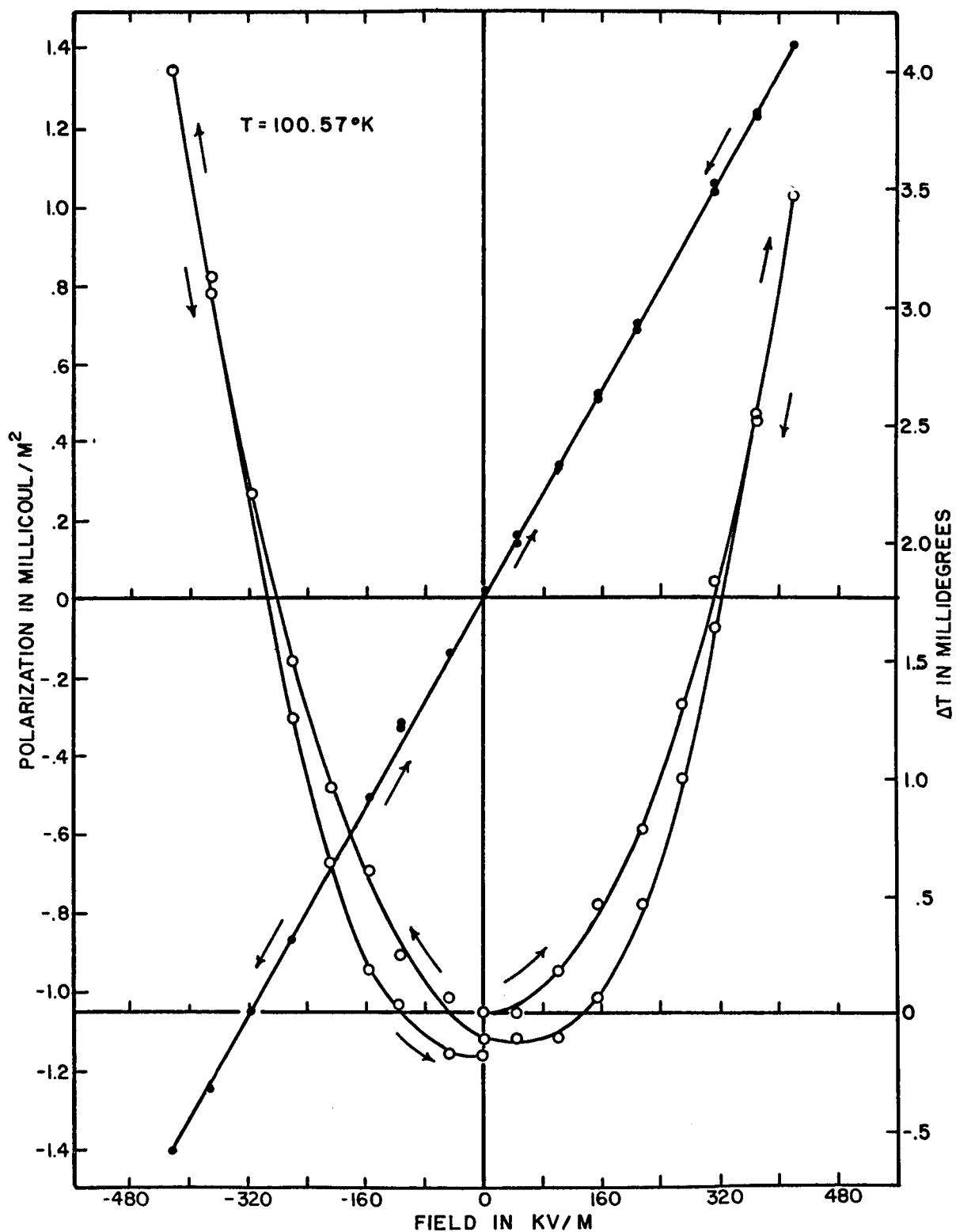


FIG.23 KDA ABOVE THE CURIE TEMPERATURE

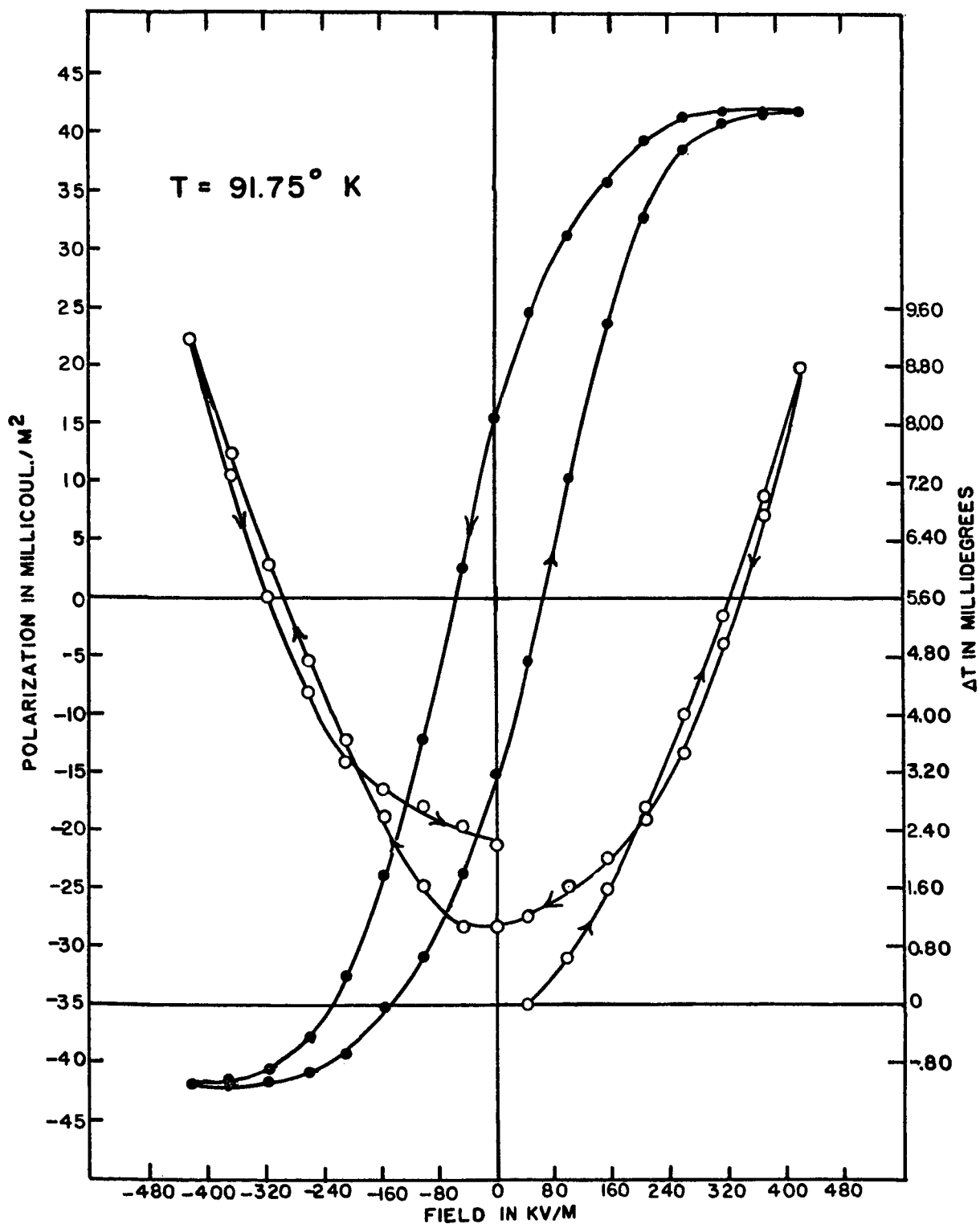


FIG. 24 KDA BELOW THE CURIE TEMPERATURE

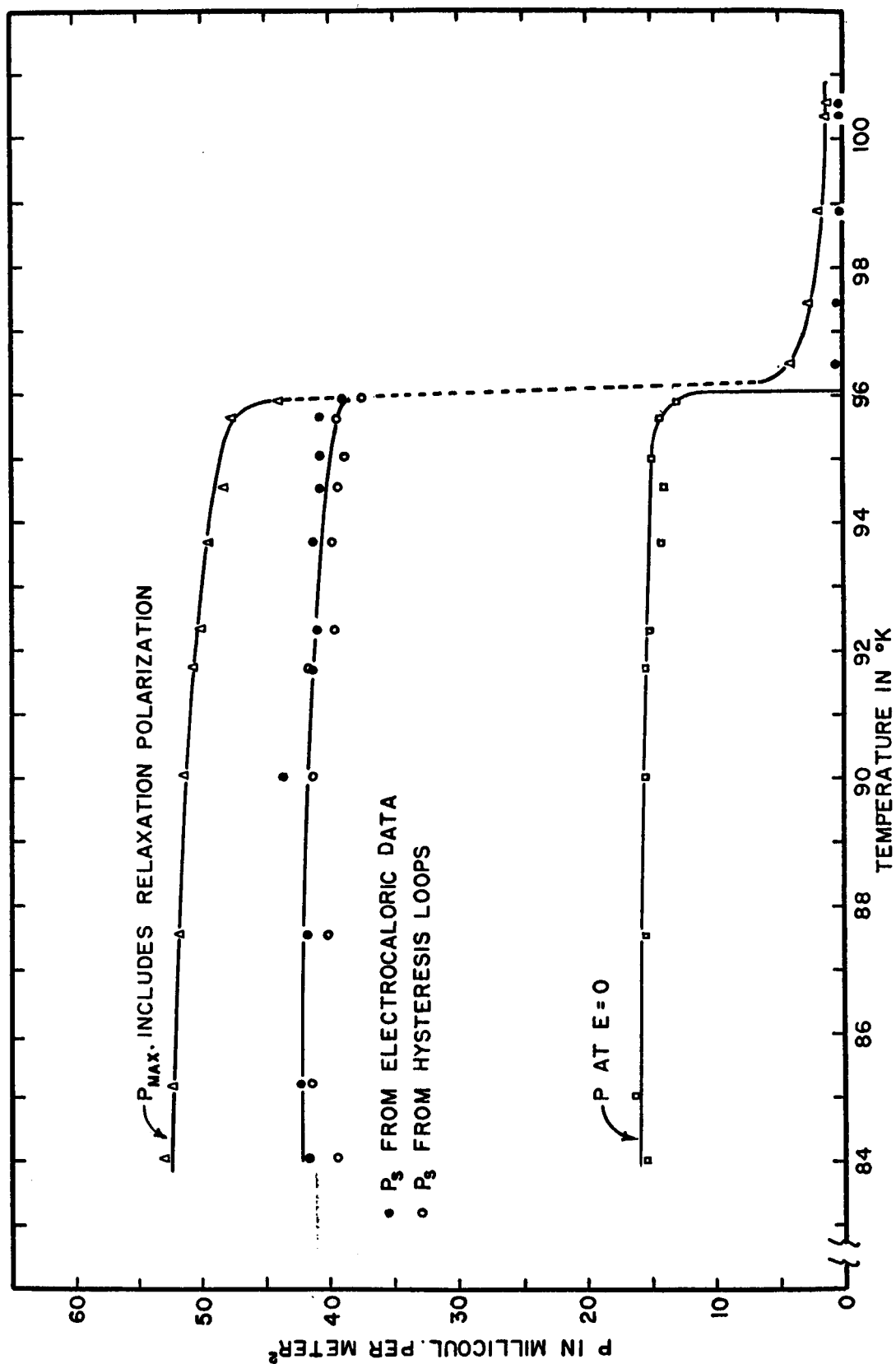


FIG. 25 POLARIZATION OF KDA

(3) values of P_s determined from the electrocaloric measurements by extrapolating plots of ΔT vs. P^2 to the $\Delta T = 0$ axis in the manner depicted in Fig. 7.

Each field step applied to KH_2AsO_4 produces a sudden change in polarization which is followed by a slow "relaxation" polarization similar to that observed with KH_2PO_4 but much smaller. Normally, only the part of the polarization that appeared to be "instantaneous" on the strip chart was measured. (There was a slight indication that a slow temperature change accompanied the slow part of the dielectric polarization, but only the "instantaneous" changes were included in the measurements.) The upper curve in Fig. 25 gives the polarization at maximum field with the slow "relaxation" part of the polarization included.

Evidently the ferroelectric Curie temperature T_f , the temperature at which P_s disappears when the substance is heated, is nearly 2°K higher than the paraelectric Curie temperature T_p . This behavior is characteristic of a first-order rather than a second-order transition.

With Eq. (2) in mind, measured values of the quantity $(\rho c_p/T)(\Delta T/\Delta P_s)_S$ which is equivalent to $(\partial E/\partial T)_P$ are plotted as a function of temperature in Fig. 26 which is analagous to Fig. 10 for KH_2PO_4 . As was the case for KH_2PO_4 , an expansion of the Gibbs function that agreed with the measured values both above and below the Curie temperature could not be found. Above T_c , the Curie-Weiss law agrees with the experimental values fairly well (see Fig. 26), but below T_c a better fit was obtained by putting the temperature dependence into the coefficient ξ rather than ω so that

$$\omega = 3.66 \times 10^8$$

and

$$\xi = -4.00 \times 10^{10} (T_c - T)^{1/4}$$

which gives

$$E = 3.66 \times 10^8 P - 4.00 \times 10^{10} (T_c - T)^{1/4} P^3,$$

$$(\partial E/\partial P)_T = 3.66 \times 10^8 = 12.0 \times 10^{10} (T_c - T)^{1/4} P^2,$$

and

$$(\partial E/\partial T)_P = 1.00 \times 10^{10} P^3 / (T_c - T)^{3/4}.$$

The latter expression is represented in Fig. 26 by the solid line below T_c . Setting the preceding expression for E equal to zero, correctly predicts a polarization catastrophe at $T = T_c$,

$$P_s = 9.15 \times 10^{-3} / (T_c - T)^{1/4}.$$

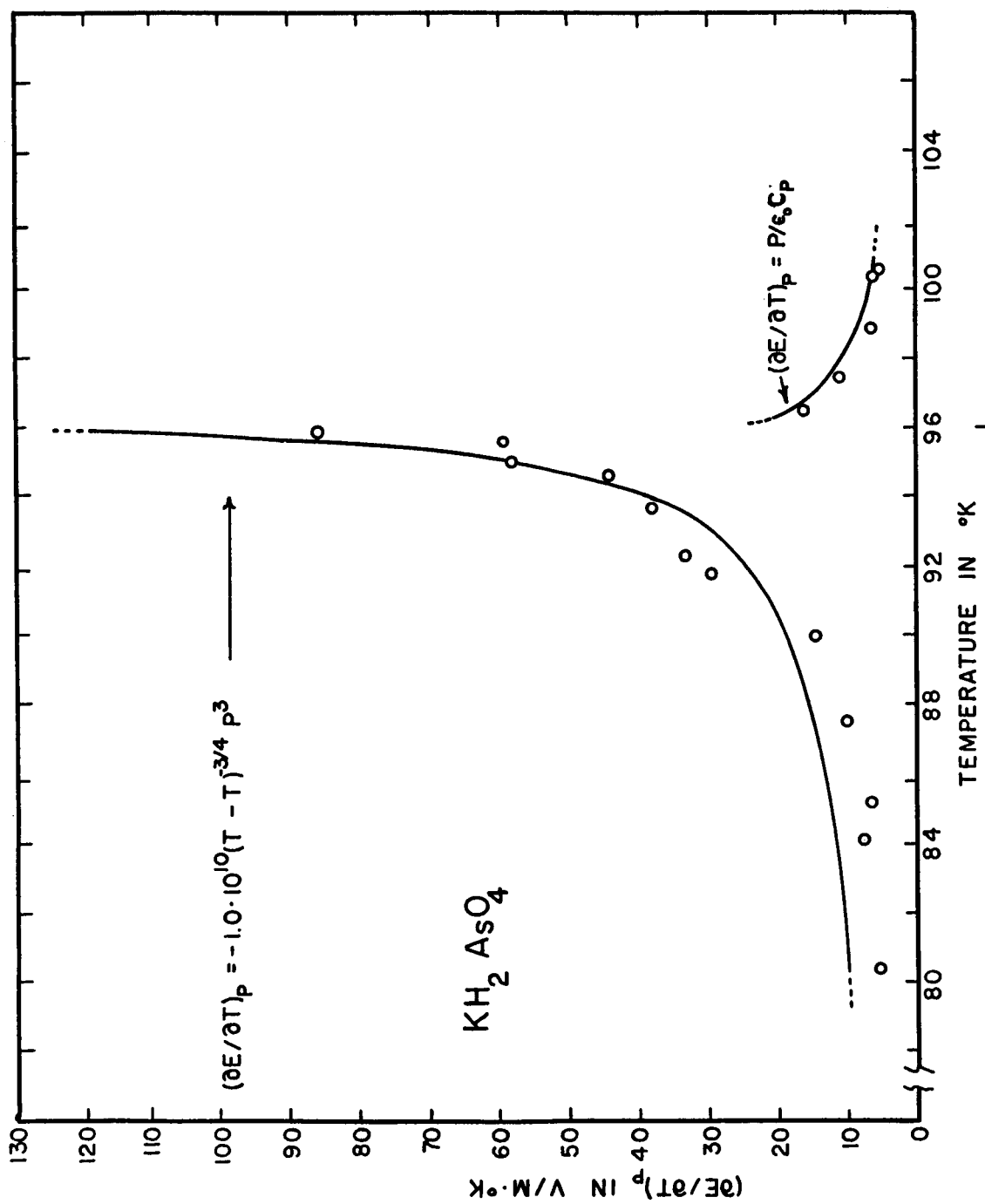


FIG. 26 ANALYTICAL & MEASURED VALUES OF $(\partial E/\partial T)_p$

The Order of the Transition in KH_2AsO_4

In practice, the distinction between a first and second order phase transition is often difficult; the latent heat may be small and confused by thermal hysteresis of the transition temperature and discontinuities in spontaneous polarization, the phase change may be a slow process, or susceptibility may be reduced to negligible values by the finite measuring field. Moreover, the transition may be spread over an appreciable temperature range because of crystalline strains, impurities, or other defects. Our measurements show a discontinuity in the spontaneous polarization (Fig. 25), a discrepancy between T_C and T_p , and an anomalous behavior of ω ; all of these suggest that the ferroelectric transition in KH_2AsO_4 is of first rather than second order. Consequently, we looked for a latent heat of transition by the method of cooling.

Only enough of such a cooling curve is reproduced in Fig. 27 to display the following features: the constant rate of cooling except in the transition region, the small "hook" in the cooling curve which suggests some supercooling, and the regressions in the behavior of polarization with respect to both time and temperature that appear in the region of the "hook." Our results differ from the careful measurements of Stephenson and Zetlemoyer²⁹ in two definite respects: our "transition temperature" is spread over about 1.3°K whereas theirs is spread over 9.2°K, and their cooling curves show no evidence of supercooling. We believe that these discrepancies arise because our measurements were made on a short-circuited single crystal whereas theirs were made on granular or powdered material in which the formation of domains and the lack of field-free conditions would smear out the transition. These discrepancies and the "hook" in our cooling curves tend to confirm the evidence from our dielectric and electrocaloric measurements that the ferroelectric transition in KH_2PO_4 is of first order and to verify our results obtained with KH_2PO_4 .

The Pyroelectric Coefficient for KH_2AsO_4

Above the Curie temperature, the measured values of the pyroelectric coefficient p^E agrees with the value computed from the Curie-Weiss law. Below T_C , the needed accurate values of c_E for a short-circuited single crystal are not available for the calculation.

Tartaric Acid $\text{C}_4\text{H}_6\text{O}_6$

The electrocaloric effect in crystalline tartaric acid was investigated because it is known to be pyroelectric. Tartaric acid presumably possesses a

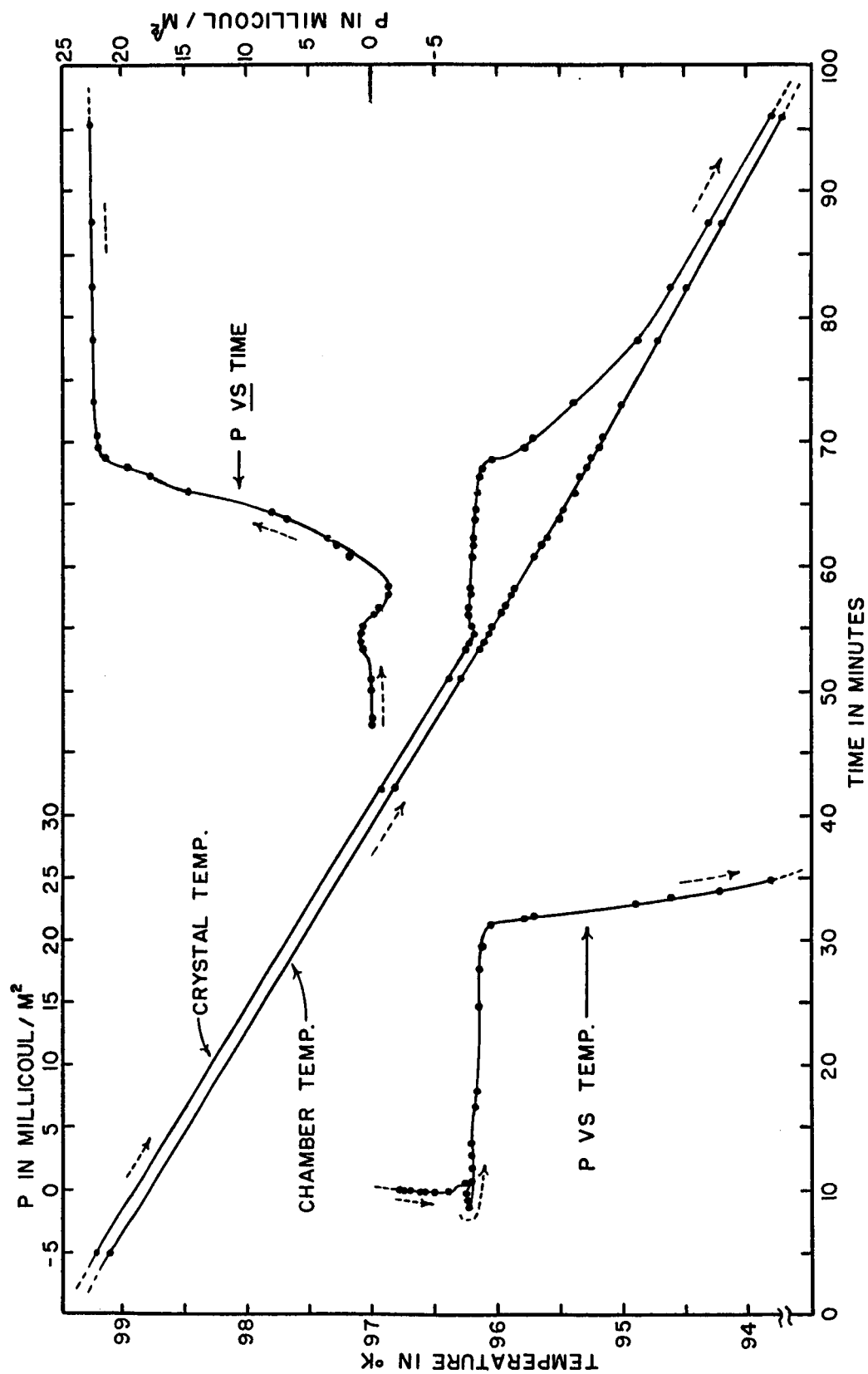


FIG. 27 COOLING RATE FOR KDA

spontaneous or intrinsic electrical polarization which, like the polarization in a ferroelectric substance, is temperature dependent but unlike the polarization in a ferroelectric substance is not reversible by the application of an electric field. The pyroelectric coefficient p^E of tartaric acid is known to be large,^{30,31}

$$p^E = (\partial P / \partial T)_E = (\partial D / \partial T)_E = 0 = 2.5 \times 10^{-5} \text{ coul/m}^2 \text{ deg},$$

and this quantity $(\partial P / \partial T)_E$ appears in the dE form of the electrocaloric equation

$$(\Delta T / \Delta E)_S = - (T \rho C_E) (\partial P / \partial T)_E. \quad (4a)$$

One would expect that tartaric acid with its non-reversible polarization, would exhibit electrocaloric behavior like that of a ferroelectric substance which had been electrically biased well into the reversible tail of its hysteresis loop. Thus the desirable condition in which there is negligible motion of domain walls (or perhaps no walls at all) would be automatically achieved.

Chemical formula	$C_4H_6O_6$
Dimensions of crystals (several used)	$1.5 \text{ cm}^2 \times 2 \text{ mm}$ (approx.)
Density	1.760 g/cm^3
Crystal symmetry	Monoclinic
Pyroelectric axis	Along [110]
Specific heat	Unknown
Range of temperature studied	$91.1^\circ\text{K} - 441^\circ\text{K}$

The Intrinsic Polarization of Tartaric Acid

The only published value that we have found for the intrinsic polarization P_s of a pyroelectric crystal is Voigt's estimated lower limit of 33 esu/cm^2 ($0.11 \text{ millicoul/m}^2$) cited by Cady³⁰ for tourmaline at 24°C . Voigt obtained this value by cleaving a crystal perpendicular to its pyroelectric axis and immersing the two parts in cups of mercury that were connected to an electrometer. This method is subject to much error. We have found that reproducible values of P_s can be obtained by measuring "thermally induced currents."

The thermally induced current in a polarized dielectric which is heated or cooled at the rate $\partial T / \partial t$ is given by the expression

$$i = A dP / dt = A (\partial P / \partial T) (\partial T / \partial t); \quad (30)$$

it is the current that flows when a short-circuited crystal is heated or cooled. In principle, if the crystal is heated until P_S is reduced to zero, the value of P_S as a function of temperature can be determined by integrating the thermally induced current; however, there is no way to know from measurements of the external current whether P_S really disappears or is masked by internal conductivity as the temperature is raised. Moreover, the true thermally induced currents may be mingled with currents arising from excessive temperature gradients (so-called tertiary pyroelectricity) or by internal migration of charge caused by previous electric fields, for example fields that were generated by the crystal's own pyroelectric effect.

A number of bothersome effects were found to occur near the temperature at which P_S disappears: large erratic currents flow, the crystal's surface appearance changes slightly, and the thermally induced currents become quantitatively irreversible with respect to temperature. The onset of irreversibility was chosen as the criterion for determining the temperature at which P_S disappeared.

To test its validity, the method of determining $P_S(T)$ from thermally induced currents was tried on triglycine sulfate for which $P_S(T)$ is known from both hysteresis and electrocaloric measurements.^{24,17} At temperatures below about 323°K the crystal chamber described in Fig. 1 and Fig. 2 was used but with the electrometer used as an ammeter rather than a coulombmeter. At higher temperatures where the Wood's-metal seals fail, the apparatus shown in Fig. 28 was used. A number of trial runs with triglycine sulfate demonstrated that $P_S(T)$ can be obtained with good accuracy by measuring thermally induced currents.

Values for the polarization of tartaric acid that were obtained by integrating the thermally induced depolarization current are shown in Fig. 29. It represents measurements on two virgin samples; one was heated from 298°K through its transition temperature, the other was cooled from 328.9°K to 104.8°, and the two sets of data were fitted at 305.4°K. Our values for P_S are much larger than the value 0.11 millicoul/m², previously cited.³⁰

Comparison of Fig. 29 with the well-known behavior of ferroelectric substances reveals a similarity between $P_S(T)$ for pyroelectric tartaric acid and ferroelectric substances which undergo a second-order transition. This phase change occurs at 396°K if deviation from thermally reversible polarization is taken as the criterion (but see Fig. 33 in the next section).

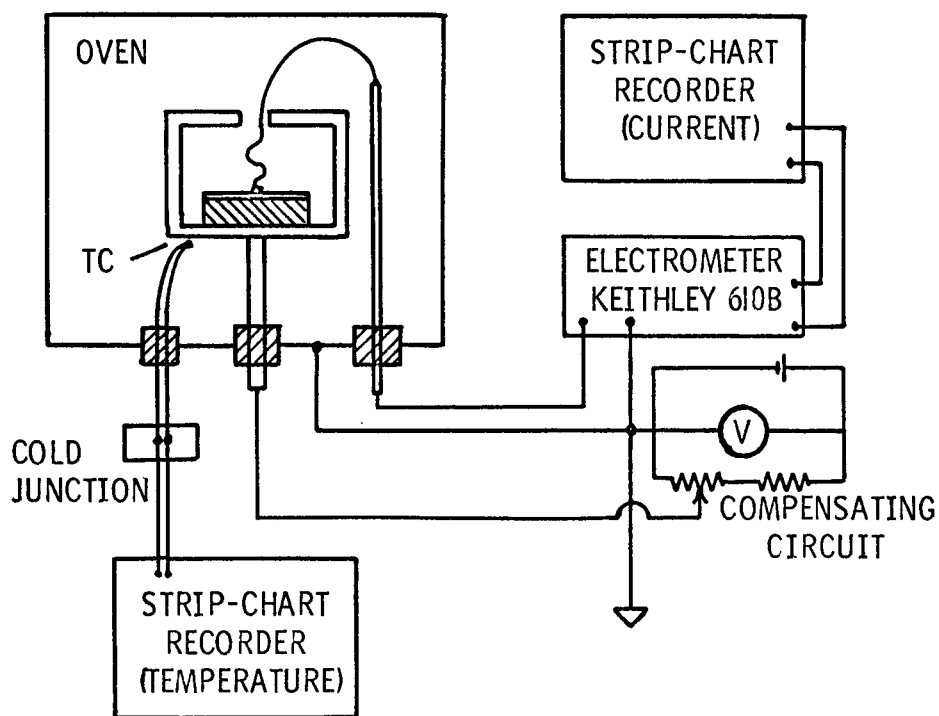


**FIG. 28 APPARATUS FOR MEASURING THERMAL
DEPOLARIZATION CURRENTS AT HIGHER TEMPERATURES**

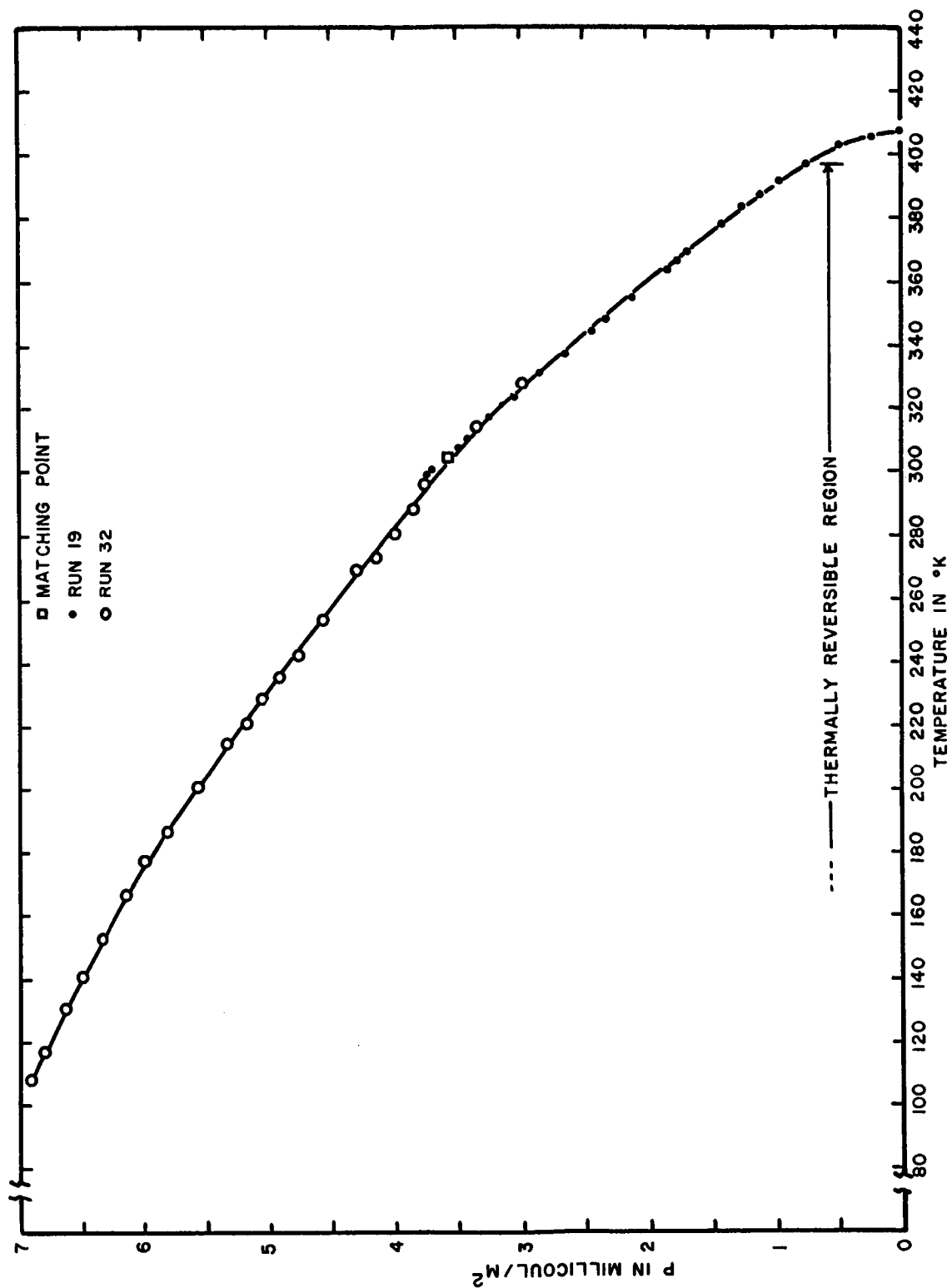


FIG. 29 INTRINSIC POLARIZATION OF TARTARIC ACID

The Pyroelectric Coefficient for $C_4H_6O_6$

The pyroelectric coefficient p^E for a short-circuited unstressed crystal is given by the slope $(\partial P/\partial T)_{\chi, E}$ of Fig. 29. Its value as a function of temperature is shown in Fig. 30.

The Electrocaloric Effect in Tartaric Acid

Electrocaloric and dielectric measurements were made on crystalline tartaric acid from 91.10°K to 320.16°K. Typical results for two different temperatures are shown in Figs. 31 and 32. The evident linearity of both the changes in polarization and the electrocaloric effect with applied field would be expected by analogy with a ferroelectric substance that is biased nearly to "saturation." Moreover, the reversal of the sign of ΔT at $E = 0$ shows that the polarization of tartaric acid does not reverse under the influence of the applied field; examination of the equation

$$\Delta T = -(T\rho C_E)(\partial P/\partial T)_E, \quad (4a)$$

reveals that unless $(\partial P/\partial T)_E$ fortuitously changes sign at $E = 0$, the sign of P does not change with E . A field applied adiabatically and antiparallel to P will tend to increase the entropy of the crystal, so its temperature will tend to fall. By contrast, a field in either direction tends to decrease the entropy of a ferroelectric crystal which is compensated for by a rise in temperature.

Some idea of the relative magnitude of the field-induced polarization compared with the spontaneous polarization can be obtained from the following numbers:

<u>Temperature</u>	<u>Induced P</u> <u>for $E = 3\text{ kV/cm}$</u>	<u>$P_S(E = 0)$</u>
90°K	13.5 $\mu\text{Coul/m}^2$	7,300 $\mu\text{Coul/m}^2$
300°K	13.5 $\mu\text{Coul/m}^2$	3,670 $\mu\text{Coul/m}^2$

Notice also that the static electric susceptibility seems to be independent of temperature, a result that was confirmed from the dielectric measurements from 90°K to 320°K and which is distinctly different from that obtained for ferroelectric substances. We obtained a mean value of $K = \Delta D/\epsilon_0 E = 5.22$ for the differential static dielectric constant which corresponds to $\chi = 4.22$. This value is somewhat larger than Mason's,¹⁵ but his value was evidently obtained at a frequency of 1000 hz, so our "static" value should be higher than his. Mason's

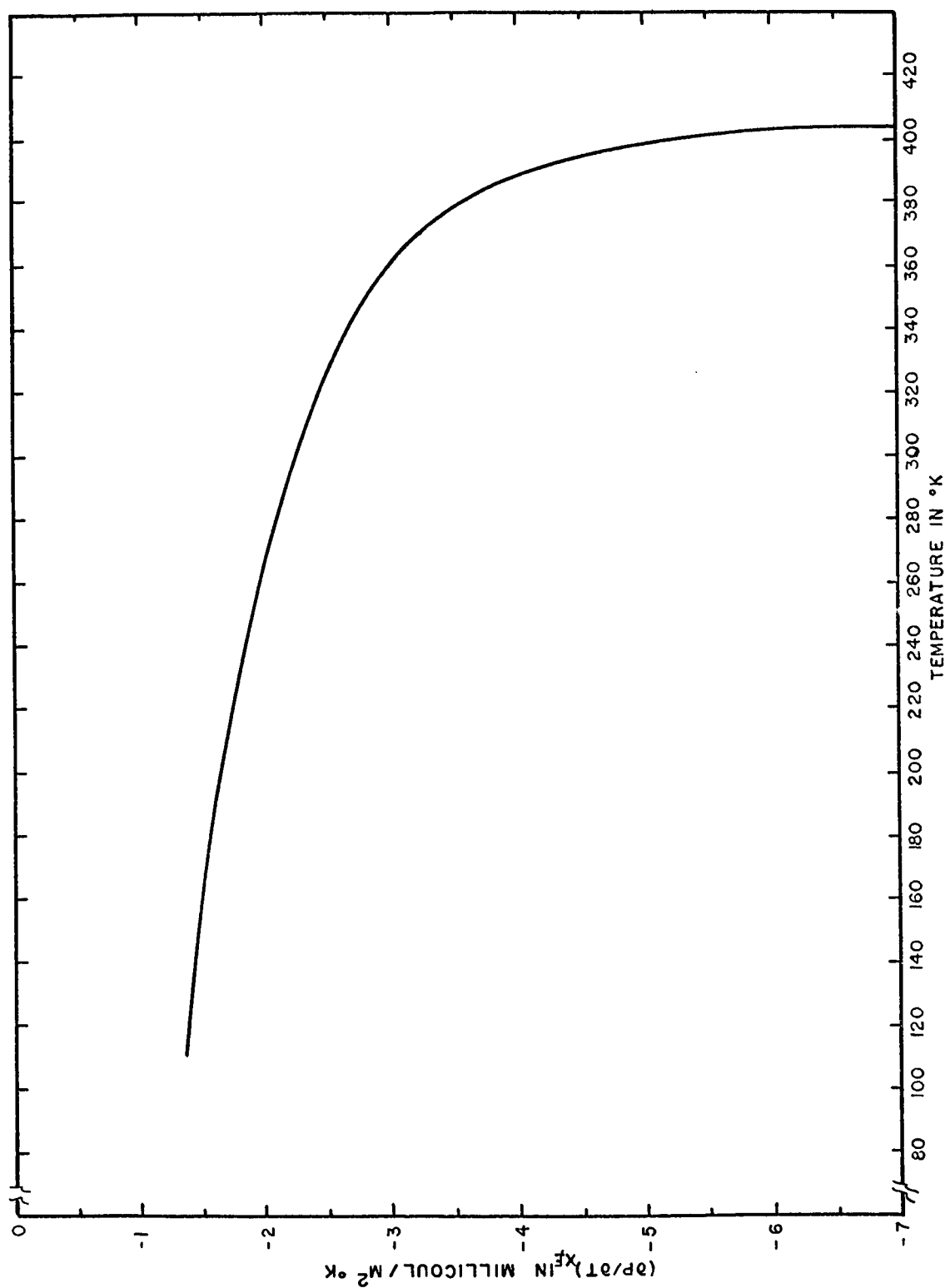


FIG. 30 THE PYROELECTRIC COEFFICIENT OF TARTARIC ACID

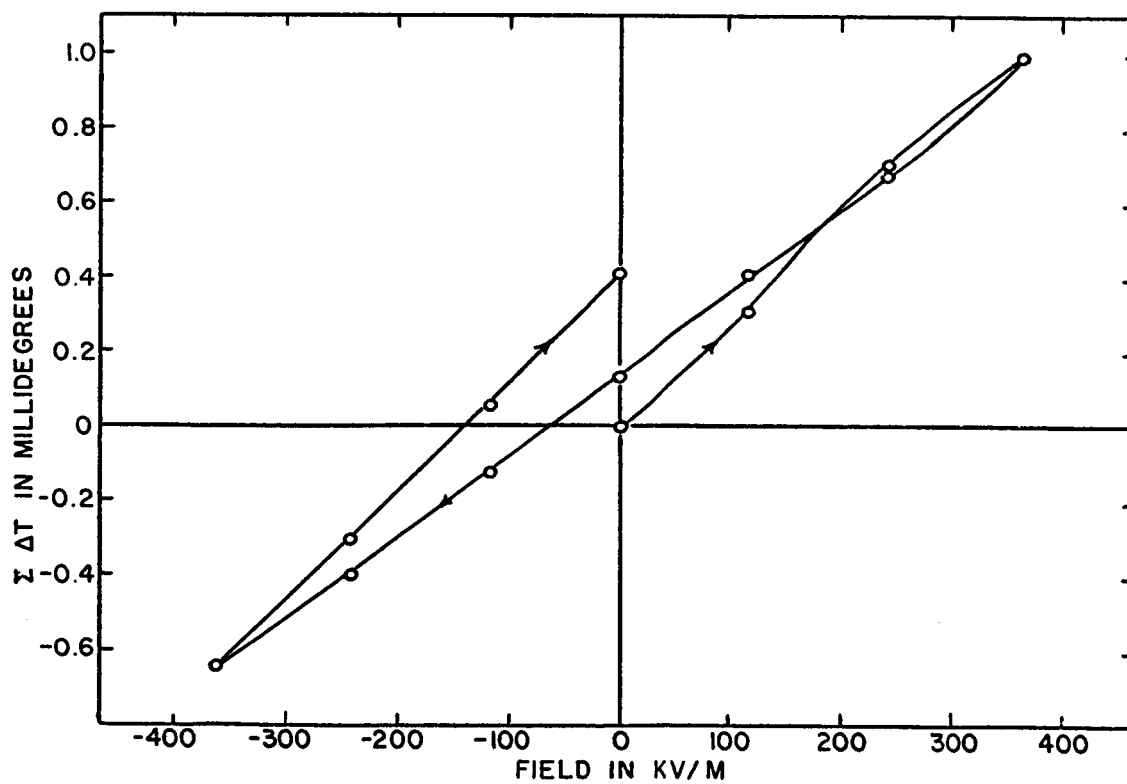
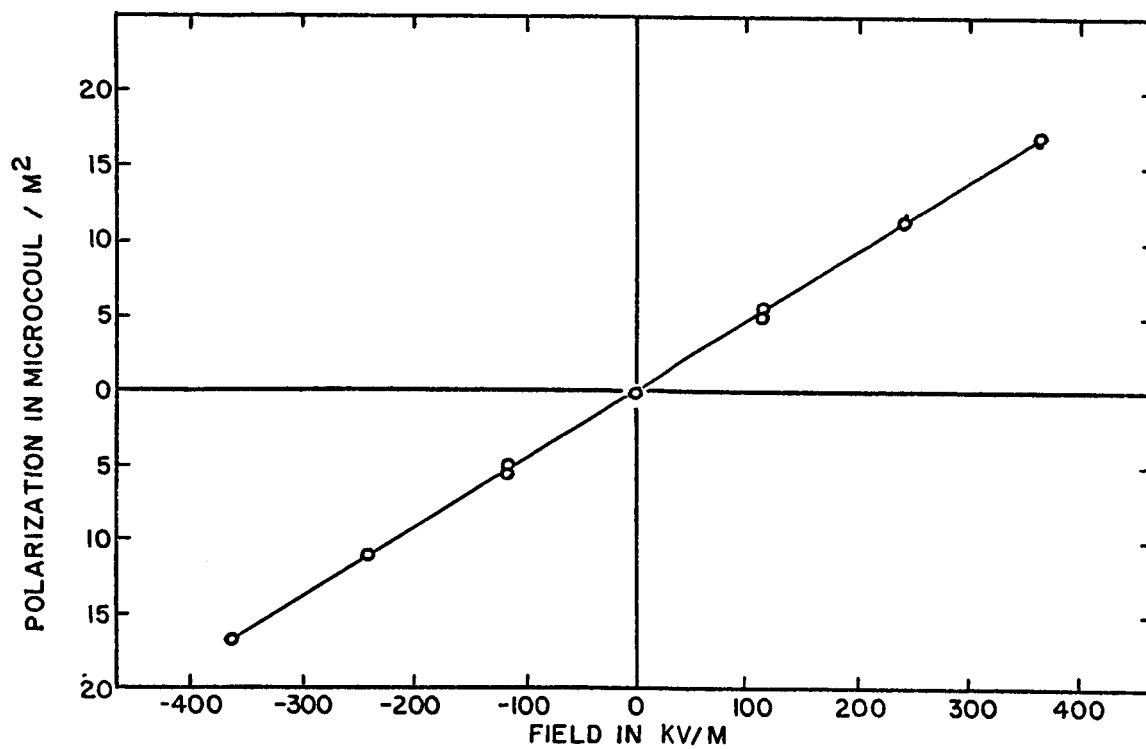


FIG.3I POLARIZATION AND ELECTROCALORIC EFFECTS IN TARTARIC ACID AT 218.85°K

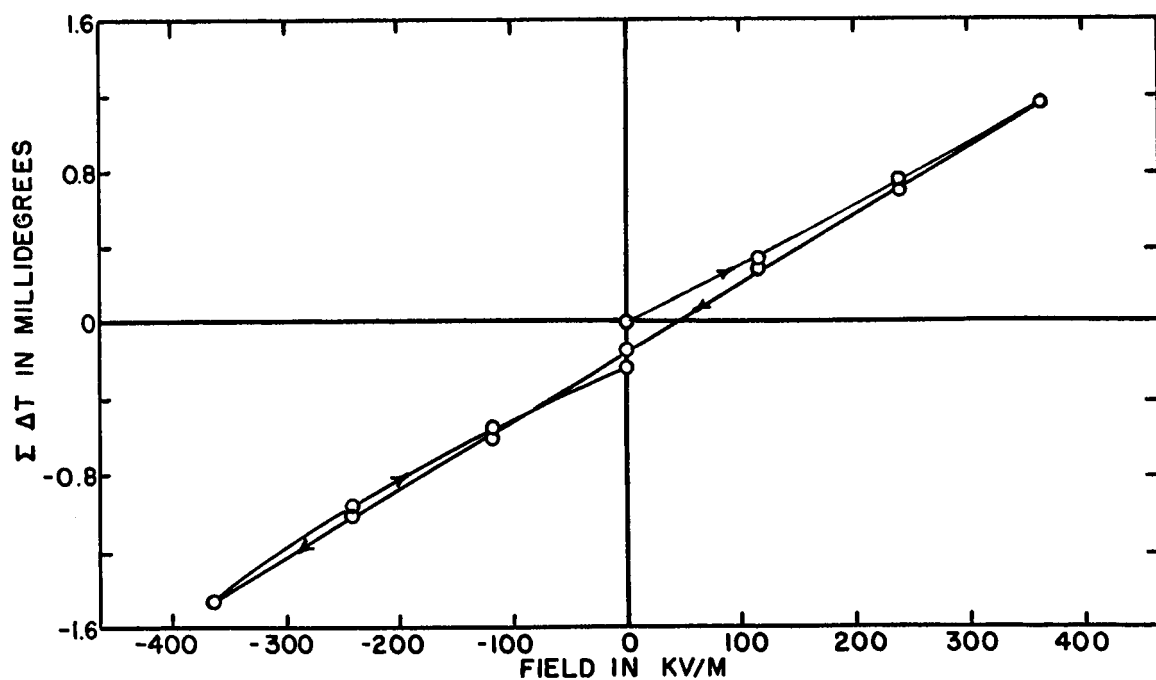
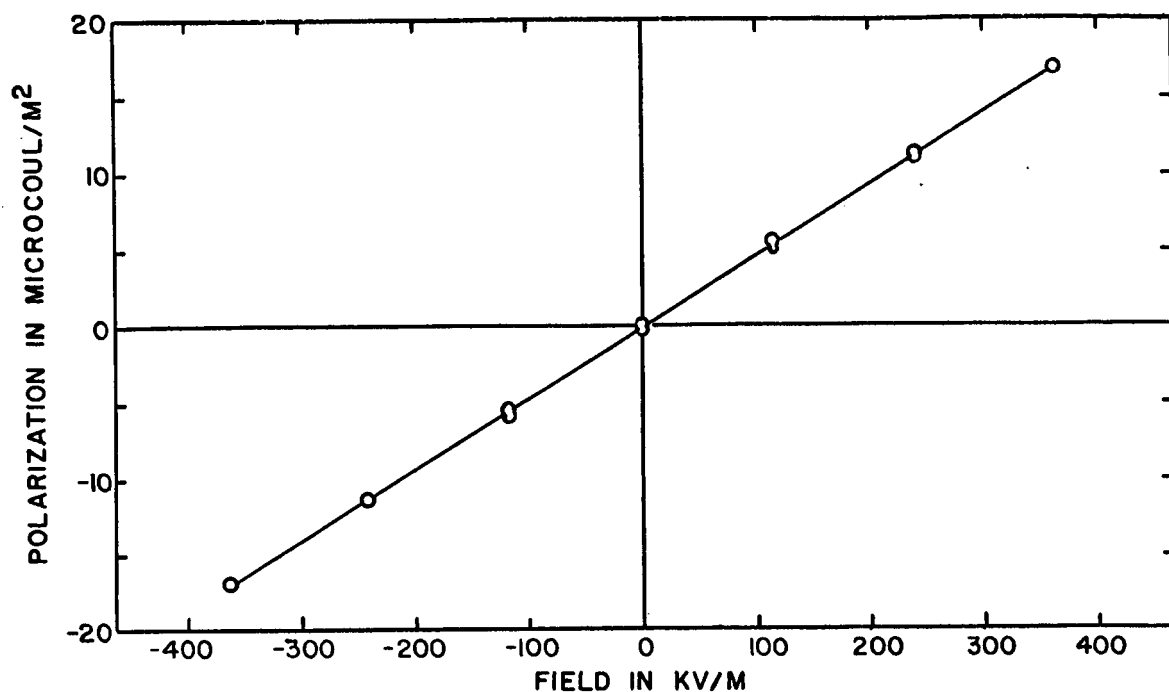


FIG. 32 POLARIZATION AND ELECTROCALORIC EFFECTS IN
TARTARIC ACID AT 320.62°K

value for the temperature coefficient of K is $1.9 \times 10^{-4}/^{\circ}\text{C}$ which is doubtfully perceptible in our measurements.

Because tartaric acid presumably does not break up into domains like ferroelectric substances do, there is a better chance to obtain valid measurements of P and then obtain an equation of state by fitting measured values to a physically reasonable analytic expression. In our case, a cue to obtaining such an analytical expression came from the well-known expression for the spontaneous polarization of a ferroelectric substance,

$$P_s^2 = -\omega/\xi, \quad (15)$$

where ω is a Curie-Weiss term, $(T - T_c)/\epsilon_0 C$, and ξ is a constant (for a substance which undergoes a second order transition). Accordingly, the measured values for P_s^2 that we previously obtained for tartaric acid by the method of thermal depolarization were plotted vs. T with the result shown in Fig. 33. Besides exhibiting a linear relationship between P^2 and T , a notable property of tartaric acid exhibited in Fig. 33 is the disappearance of the spontaneous polarization at a critical temperature T_c . We refrain from calling T_c a "Curie temperature" because we have no evidence that the crystal obeys a Curie-Weiss law above T_c ; in fact, the crystal rapidly becomes electrically conductive as it approaches T_c .

Except in the small region close to the critical temperature T_c , the spontaneous polarization of tartaric acid as a function of temperature is well represented by a linear expression in the temperature,

$$P_s^2 = 0.182 \times 10^{-6} (375 - T) \text{ Coul}^2/\text{m}^4.$$

An expression for the field-induced polarization of tartaric acid can be obtained directly from the experimental values presented in Fig. 32; it is

$$\Delta P = 37.3 \times 10^{-12} \Delta E.$$

At this point we assume that the values of $(\partial E/\partial P)$ at constant entropy and at constant temperature are practically the same, a result that can be verified later from the observation that the electrocaloric temperature changes are only about one millidegree; i.e., we presume that $(\partial P/\partial E)_T = 37.3 \times 10^{-12}$.

Integration of the above expression gives an equation of the form

$$P(T) = BE + \phi(T)$$

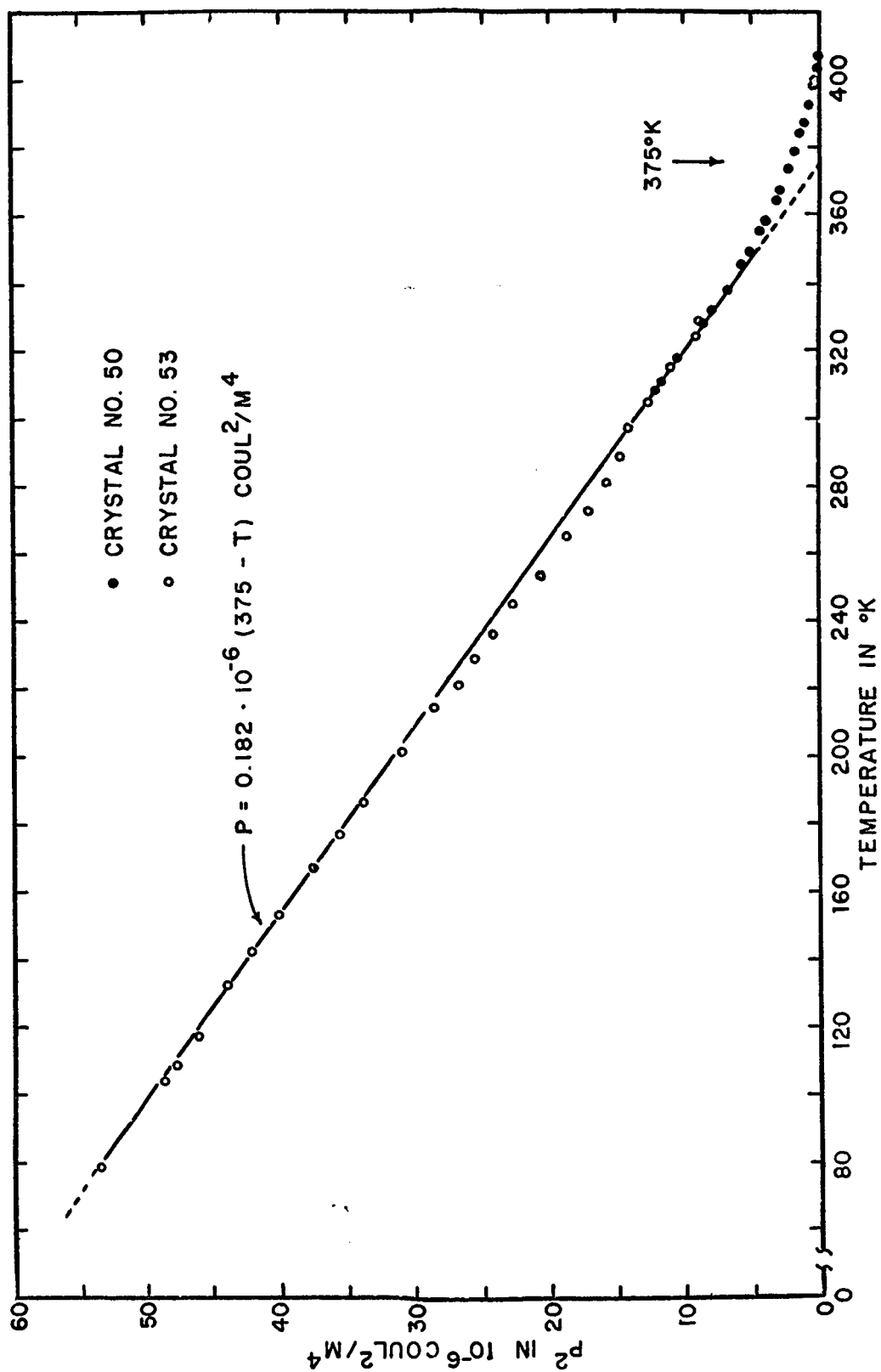


FIG. 33 SPONTANEOUS POLARIZATION OF TARTARIC ACID DETERMINED
 BY THERMAL DEPOLARIZATION

where B is the constant 37.3×10^{-12} , and $\phi(T)$ is an arbitrary function of temperature. Knowing that $P(T)$ approaches $P_S(T)$ as E approaches zero, and employing the experimental values for $P_S(T)$ shown in Fig. 33, we have

$$P(T) = BE + A(T_C - T)^{1/2} \quad (31)$$

where $A = (0.182 \times 10^{-6})^{1/2} = 0.426 \times 10^{-3} \text{ Coul/m}^2 \cdot \text{deg}^{1/2}$,

and $B = 37.3 \times 10^{-12} \text{ Coul}^2/\text{N} \cdot \text{m}^2$.

This is the equation of state for tartaric acid in the region of interest except for the small region close to the critical temperature.

It is instructive to see whether Eq. (31) leads to a physically reasonable expression for the Gibbs free energy.

Combining Eq. (10) and (31), we have

$$(\partial G / \partial P)_T = (P/B) - (A/B)(T_C - T)^{1/2}.$$

Integration of this expression gives

$$G_1 = G_{10} - (A/B)(T_C - T)^{1/2} P + P^2/2B \quad (32)$$

where G_{10} is the free energy of an unpolarized crystal at the temperature T .

The salient feature of the above expression is that it is an odd function of the polarization in contrast to the analogous expression for the Gibbs free energy of a ferroelectric crystal. This odd function for P might have been expected because the even function that is written for a ferroelectric crystal describes the symmetrical reversibility of the direction of its polarization whereas the polarization of a pyroelectric crystal does not reverse. The qualitative behaviors of the even and odd functions of polarization at temperatures near the critical temperature are shown below. In both the ferroelectric and pyroelectric crystals the magnitude of the lower-order (negative) term diminishes with increasing temperature until at some critical temperature the spontaneous polarization in the stable state (the state of minimum free energy) diminishes to zero. An important difference between these two free energy functions is that Eq. (11) for a ferroelectric crystal predicts correctly that the reciprocal isothermal susceptibility, $1/\chi^T = \epsilon_0(\partial^2 G_1 / \partial P^2)_T$ approaches zero at the critical temperature whereas Eq. (32) for a pyroelectric crystal predicts that the isothermal

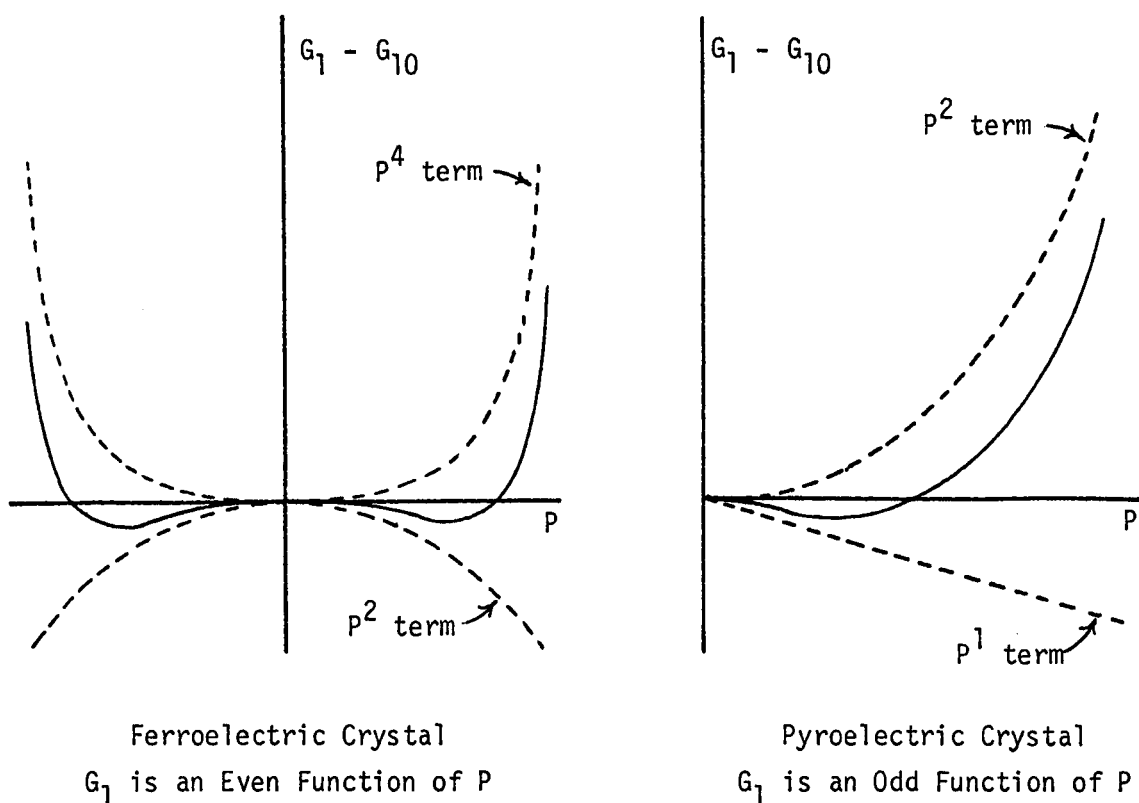


Fig. 34. A qualitative Comparison of the Even and Odd Functions of Polarization that Describe the Free Energy of Ferroelectric Pyroelectric Crystals.

susceptibility will be constant right up to the critical temperature. We have already pointed out that the susceptibility was found to be practically constant from 90°K to 320°K; we did not verify this prediction by extending our susceptibility measurements to the critical temperature (375°K) because of the low melting point of our Woods metal seals and because other measurements showed that the conductivity increases rapidly in this region.

The electrocaloric effect in crystalline tartaric acid was measured at fields up to 3,629 V/cm from 320.62°K down to 218.85°K and at fields up to 1,790 V/cm at temperatures down to 91.10°K. The typical results of these measurements, displayed in Figs. 30 and 31, show that the polarization is practically reversible in the thermodynamic sense and that the temperature changes were significantly smaller than those ordinarily obtained with ferroelectric substances.

If the general considerations already outlined are correct, in particular if Eq. (32) for the Gibbs free energy is correct, then measured values of the electro-

caloric effect should agree with the values that can be predicted from the general thermodynamic equation,

$$dT = - (T/\rho c_E)(\partial P/\partial T)_E dE. \quad (4)$$

But from Eq. (32) or from the equation of state we have

$$(\partial P/\partial T)_E = - (A/2)(T_C - T)^{-1/2}.$$

If this expression is substituted into Eq. (32) and if Eq. (4) is integrated while assuming that the electrocaloric temperature change is much smaller than T , the result is

$$\Delta T = (AT/\rho c_E)(T_C - T)^{-1/2} \Delta E. \quad (33)$$

Unfortunately, the published values of c_E for tartaric acid do not cover the full range of temperatures needed here and they are not in good agreement with each other.^{32,33,34} These values are shown in Fig. 35, the horizontal lines in the figure representing the temperature ranges over which the various authors made their measurements. A straight line was drawn to represent the values used for our calculations, extra weight being given to the values at 309.2°K and 323°K because of their consistency. The value at 301.5° was ignored because it is anomalously high. The resulting linear relationship that was used is

$$c_E = 120 + 3.50T \text{ Joules/kg}\cdot\text{deg.}$$

Fig. 36 was drawn to compare the measured values of the electrocaloric effect and the values calculated from Eq. (33). The agreement is better than we have a right to expect, especially near 300°K where the two published values of the heat capacity are in agreement, but the curvature of the patterns of the experimental and calculated values appear to be opposite to each other. Electrocaloric measurements at higher temperature (if they are possible) and better values for the specific heat would be required to verify this trend. Values at much lower temperatures would be difficult to measure because the measured thermal emf becomes smaller. Thermal emf's for 10^{-4} °K are shown for several temperatures in Fig. 36.

Our conclusion is that Eq. (32) is a reasonable quantitative representation of the Gibbs free energy of tartaric acid from 90°K to 320°K.

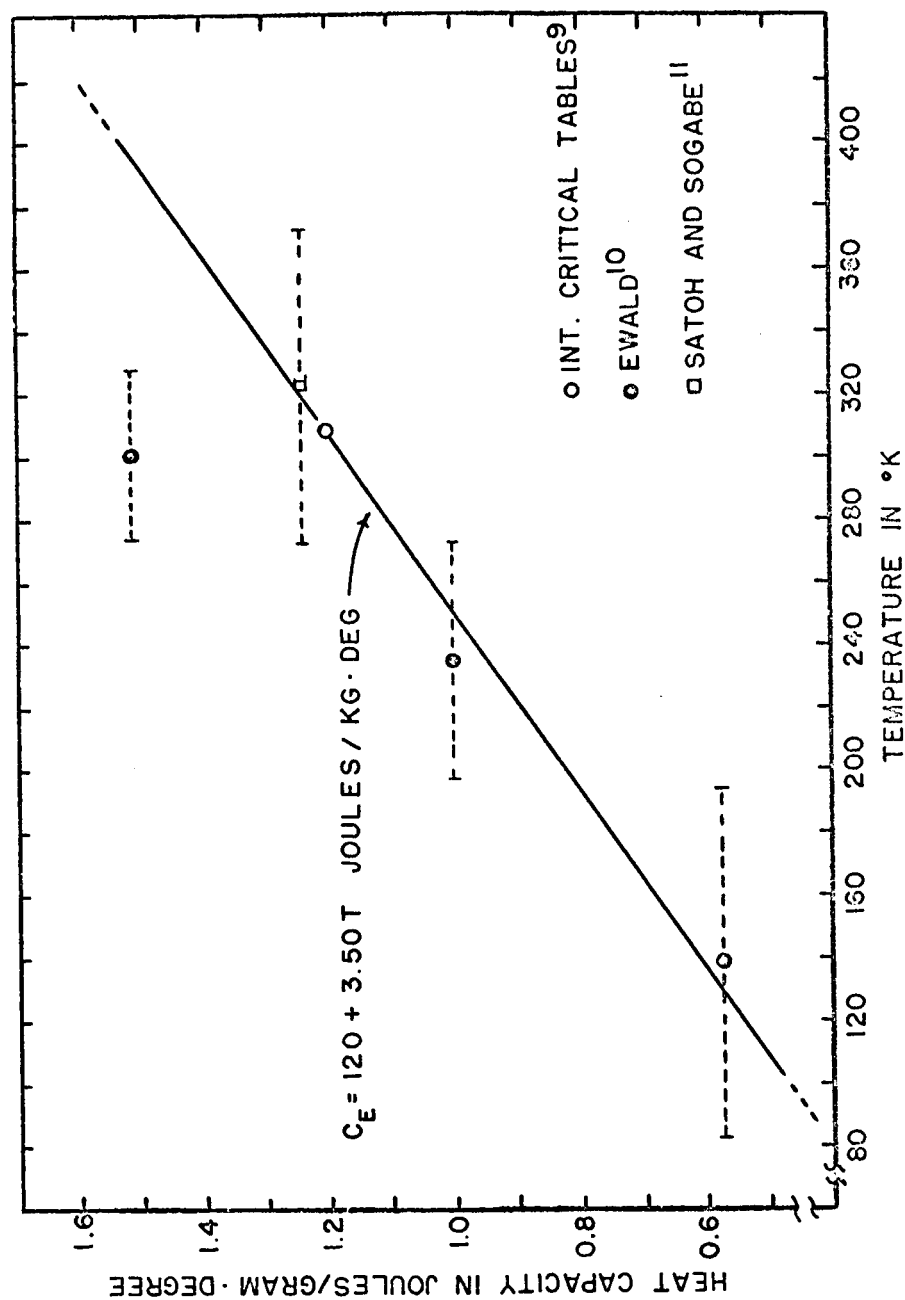


FIG. 35 PUBLISHED VALUES FOR THE HEAT CAPACITY OF
TARTARIC ACID

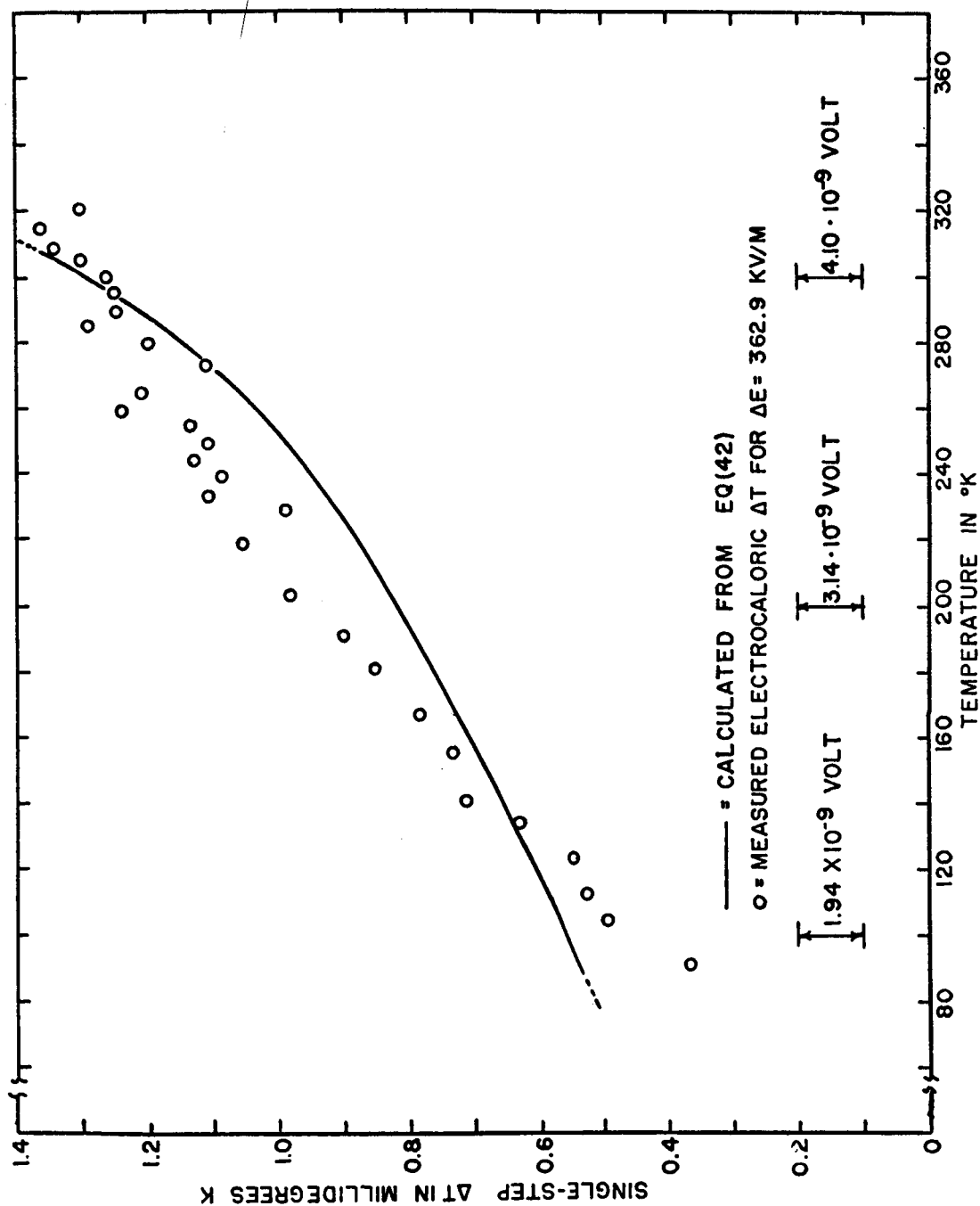


FIG.36 MEASURED VS. THEORETICAL ELECTROCALORIC EFFECTS
 IN TARTARIC ACID

We have not made electrocaloric measurements between 320°K and 375°K and are not able to explain the significance of the deviation of P_s^2 from linearity in T that is evident in Fig. 33. Part of the deviation could be due to a small error in determining P_s ; only changes in P_s can be measured by the method of thermal depolarization, and it is difficult to tell when the thermal depolarization currents actually become zero.

CONCLUSIONS

Quantitative measurements of the electrocaloric effect in ferroelectric and pyroelectric substances are feasible over a wide range of temperature. The information obtained from these measurements contributes to an understanding of the phase transition and the thermodynamic properties of ferroelectric and pyroelectric substances. The accuracy and validity of such measurements were established by observing the effect in a substance while it was in its paraelectric phase where the results are quantitatively predictable from the Curie-Weiss law.

Our measurements of the electrocaloric effect in the ferroelectric region further confirm the idea that the Langevin-type model which is based on long-range interactions between dipoles characterized by an inner field parameter γ is not sound.

We were unable to find an elastic Gibbs function G_1 for potassium dihydrogen phosphate and its isomorph, potassium dihydrogen arsenate, that was consistent with its dielectric and electrocaloric behavior both above and below the Curie temperature; in fact, not even the first Devonshire coefficient ω for these crystals was a smooth function of temperature through the transition region. Therefore, we suspect that KH_2PO_4 undergoes a first-order rather than a second-order transition at its Curie temperature, a suspicion that is in agreement with the recent calorimetric measurements of Reese and May.³⁵ Our studies of KH_2AsO_4 revealed a discontinuity in its spontaneous polarization at T_c , a value of T_p that is less than T_c , anomalous behavior of the Devonshire coefficients at T_c , and a "hook" in the cooling curve. All of these indicate that the ferroelectric transition in KH_2AsO_4 is of first rather than second order.

Triglycine sulfate which undergoes a well-confirmed second order transition behaved differently. Measurements of the electrocaloric effect in this substance are in accord with the Devonshire theory and are in reasonable agreement with dielectric measurements. The first Devonshire coefficient ω is continuous with no change in slope right through the Curie temperature, $\partial\omega/\partial T$ being constant down to about 312°K where it begins to diminish significantly.

Values for the intrinsic polarization of tartaric acid that are much larger and more reliable than previously reported were obtained. Between 91.1°K and 375°K we obtain

$$P_s(T) = 0.426 \times 10^{-3} (375 - T)^{1/2} \text{ coul/m}^2.$$

which is unlike the analagous expressions for a ferroelectric substance in that it is an odd function of P .

A useful characteristic of a material which is to be used as a radiation detector delivering its signal into a low-impedance detector is the pyroelectric coefficient p^E . Its value and its dependence on temperature were determined from measurements of the electrocaloric effect for each of the substances studied. Under certain conditions the sensitivity of a pyroelectric radiation detector can be changed by a change in the applied field whereas under others it can be made independent of applied field.

LIST OF REFERENCES

- 1 L. F. Bates, Modern Magnetism, Cambridge at the University Press, 3rd Ed., 1951.
- 2 P. Kobeko and J. Kurtschatov, "Dielectricische Eigenschaften der Seignettesalkristalle", Zeit. Phys. 66, 192-205 (1930).
- 3 J. F. Hautzenlaub, "Electric and Dielectric Behavior of Potassium Dihydrogen Phosphate", Ph.D. Thesis, Mass. Inst. of Technology (1943).
- 4 H. Baumgartner, "Electriche Sattigungsercheinungen und der elektrokalarische Effekt von Kaliumphosphat KH_2PO_4 ", Helv. Phys. Acta 23, 651-696 (1950).
- 5 S. Roberts, "Adiabatic Study of the 128° Transition in Barium Titanate", Phys. Rev. 85, 925L (1952).
- 6 R. W. Schmitt, "Adiabatic Thermal Changes in Barium Titanate Ceramic at Low Temperatures", Phys. Rev. 85, 1-4 (1956).
- 7 A. I. Karchevskii, "Electrocaloric Effect in Polycrystalline BaTiO_3 ", Soviet Phys. Solid State (Trans.) 3, 2249-2254 (1962).
- 8 G. G. Wiseman and J. K. Kuebler, "Electrocaloric Effect in Rochelle Salt," Phys. Rev. 131, 2023-2027 (1963).
- 9 A. G. Chynoweth, "Dynamic Method for Measuring the Pyroelectric Effect with Special Reference to Barium Titanate", J. App. Phys. 27, 78 (1956).
- 10 A. G. Chynoweth, "Spontaneous Polarization of Guanidine Aluminum Sulfate Hexahydrate at Low Temperatures", Phys. Rev. 102, 1021-1023 (1956).
- 11 A. G. Chynoweth, "Pyroelectricity, Internal Domains, and Interface Charges in Triglycine Sulfate", Phys. Rev. 117, 1235 - 1243 (1960).
- 12 Sperry Microwave Electronics Company, (Division of Sperry Rand Corporation), Clearwater, Florida, "Research Program on Pyroelectric Detection Techniques and Materials", Final Report, Contract NSw-711, November, 1963.
- 13 Microwave Electronics Company (Sperry Rand), "Research Program on Pyroelectric Detection Techniques and Materials, Phase II", First Quaterly Report, Contract No. NASw-974, October, 1964.
- 14 Microwave Electronics Company (Sperry Rand), "Research Program in Pyroelectric Detection Techniques and Materials; Phase II", Second Quaterly Report, Contract No. NASw-974, January, 1965.
- 15 W. P. Mason, "Piezoelectric Crystals and Their Application to Ultrasonics," D. Van Nostrand (1950).
- 16 E. T. Jaynes, Ferroelectricity, Princeton University Press (1953).

- 17 G. G. Wiseman, et. al., "Investigation of Electrocaloric Effects in Ferroelectric Substances", Status Reports No. 1 through No. 7, NASA Research Grant NsG-575 with the University of Kansas, March 1, 1964 to July 31, 1967.
- 18 A. F. Devonshire, "Theory of Ferroelectrics", Advances in Physics (Phil. Mag. Suppl.) 3, 85 - 130 (1954).
- 19 A. Brooks, "Analysis of Phase-Shift Controlled Thermoregulator Circuits", Rev. Sci. Inst. 27, 746-748 (1956).
- 20 G. Busch and P. Scherrer, "A New Seignette-electric Substance", Naturwiss. 23, 737 (1935).
- 21 H. Baumgartner, "Unterschied der Dielektrizitätskonstanten zwischen einem freien und einem geklemmten KH_2PO_4 -kristall", Helv. Phys. Acta 24, 326 (1951).
- 22 H. M. Barkla and D. M. Finlayson, "The Properties of KH_2PO_4 Below the Curie Point", Phil. Mag. (7) 44, 109-130 (1953).
- 23 C. C. Stephenson and J. G. Hooley, "The Heat Capacity of Potassium Dihydrogen Phosphate", J. Am. Chem. Soc. 66 1397-1401 (1944).
- 24 S. Hoshino, T. Mitsui, F. Jona, and R. Pepinsky, "Dielectric and Thermal Study of Tri-Glycine Sulfate and Tri-Glycine Fluoberyllate", Phys. Rev. 107, 1255-1258 (1957).
- 25 F. Jona and G. Shirane, Ferroelectric Crystals, The MacMillan Press, New York (1962).
- 26 J. A. Gonzalo, "Critical Behavior of Ferroelectric Triglycine Sulfate", Phys. Rev. 144, 662-665 (1966).
- 27 G. Busch, "Neue Seignette-Elektrika", Helv. Phys. Acta 11, 269-298 (1938).
- 28 W. Bantle, "Die Spezifische Wärme seignette-elektrischer Substanzen Dielektrische Messung an KD_2PO_4 -Kristallen", Helv. Phys. Acta 15, 373-404 (1942).
- 29 C. C. Stephenson and A. C. Zettlemoyer, "The Heat Capacity of KH_2AsO_4 from 15 to 300°K. The Anomaly at the Curie Temperature", Jour. Am. Chem. Soc. 66, 1402-1405 (1944).
- 30 W. G. Cady, Piezoelectricity, McGraw-Hill (1946).
- 31 Am. Inst. of Phys. Handbook (Second Ed. 1963), Sec. 9 - 102.
- 32 International Critical Tables 5: 102, McGraw-Hill (1933).
- 33 Rudolph Ewald, "Messung spezifischer Warmen und. Bietrage zur Molekulargewichtsbestimmung", Annalen der Physik 44, 1213-1237 (1914).
- 34 S. Satoh and T. Sogabe, "The Specific Heat of Some Solid Aliphatic Acids and Other Ammonium Salts at the Atomic Heat of Nitrogen", Scientific Papers of the Institute of Physical and Chemical Research (Tokyo) 36, 97-105 (1939).

- 35 W. Reese and L. F. May, "Critical Phenomena in Order-Disorder Ferroelectrics
I. Calorimetric Studies of KH_2PO_4 ", Phys. Rev. 162, 510-518 (1967).

POSTMASTER: If Undeliverable (Section 158
Postal Manual) Do Not Return

"The aeronautical and space activities of the United States shall be conducted so as to contribute . . . to the expansion of human knowledge of phenomena in the atmosphere and space. The Administration shall provide for the widest practicable and appropriate dissemination of information concerning its activities and the results thereof."

— NATIONAL AERONAUTICS AND SPACE ACT OF 1958

NASA SCIENTIFIC AND TECHNICAL PUBLICATIONS

TECHNICAL REPORTS: Scientific and technical information considered important, complete, and a lasting contribution to existing knowledge.

TECHNICAL NOTES. Information less broad in scope but nevertheless of importance as a contribution to existing knowledge.

TECHNICAL MEMORANDUMS: Information receiving limited distribution because of preliminary data, security classification, or other reasons.

CONTRACTOR REPORTS: Scientific and technical information generated under a NASA contract or grant and considered an important contribution to existing knowledge.

TECHNICAL TRANSLATIONS: Information published in a foreign language considered to merit NASA distribution in English.

SPECIAL PUBLICATIONS: Information derived from or of value to NASA activities. Publications include conference proceedings, monographs, data compilations, handbooks, sourcebooks, and special bibliographies.

TECHNOLOGY UTILIZATION PUBLICATIONS: Information on technology used by NASA that may be of particular interest in commercial and other non-aerospace applications. Publications include Tech Briefs, Technology Utilization Reports and Notes, and Technology Surveys.

Details on the availability of these publications may be obtained from:

SCIENTIFIC AND TECHNICAL INFORMATION DIVISION
NATIONAL AERONAUTICS AND SPACE ADMINISTRATION
Washington, D.C. 20546